Dissertation
submitted to the
Combined Faculties of the Natural Sciences and Mathematics
of the Ruperto-Carola-University of Heidelberg, Germany
for the degree of
Doctor of Natural Sciences

put forward by
M.Sc. Enderalp Yakaboylu
born in Eskisehir, Turkey
Oral examination: 6 th February 2014

To Özge

Relativistic features and time delay of laser-induced tunnel-ionization

Referees: **Hon. Prof. Dr. Christoph H. Keitel**

Prof. Dr. Georg Wolschin

Zusammenfassung

Die Tunnelionisierung wird im Rahmen der relativistischen Quantenmechanik untersucht. Dies geschieht, indem für ein beliebiges konstantes elektromagnetisches Feld ein Energieoperator eingeführt wird, mit dessen Hilfe sich der klassisch verbotene Bereich der Tunnelionisation identifizieren lässt. Außerdem werden die relativistischen Signaturen der Tunnelionisation erforscht. Ein eindimensionales, intuitives Bild sagt eine Verschiebung des Impulses entlang der Laserpropagationsrichtung für das Wellenpaket des ionisierten Elektrons voraus. Es zeigt sich, dass diese Beobachtung mit der etablierten Starkfeld-Näherung konsistent ist. Darüber hinaus wird die Spin-Dynamik während der Tunnelionisation sowohl in der Standard- als auch in einer modifizierten Starkfeld-Näherung diskutiert. Als Nächstes wird die Zeitverzgerung während der Tunnelionisation mithilfe einer erweiterten Definition der Wigner-Zeitverzgerung untersucht. Anschließend wird dieses Konzept unter Bezug auf die Phase des Propagators zu fester Energie umdefiniert. Der entwickelte Formalismus wird auf das tiefe Tunnelregime und den schwellennahen Bereich angewendet. Es wird gezeigt, dass auch in großer Entfernung in letzterem Fall Signaturen der durch den Tunnelprozess auftretenden Zeitverzgerung noch messbar sind. Schließlich wird eine pfadabhängige Formulierung der Eichtheorie diskutiert. Diese äquivalente Formulierung der Eichtheorie führt zu einer kanonischen Eichung, in welcher das Feynman'sche Pfadintegral besonders intuitiv erscheint und sich die Berechnung des quasiklassischen Propagators stark vereinfacht.

Abstract

Tunnel-ionization is investigated in the framework of relativistic quantum mechanics. For an arbitrary constant electromagnetic field a gauge invariant energy operator is introduced in order to identify the classically forbidden region for tunnel-ionization. Furthermore, relativistic features of tunnel-ionization are explored. A one-dimensional intuitive picture predicts that the ionized electron wave packet in the relativistic regime experiences a momentum shift along the laser's propagation direction. This is shown to be consistent with the well-known strong field approximation. Furthermore, spin dynamics in tunnel-ionization process is discussed in the standard as well as in the dressed strong field approximation. Next, the tunneling time delay is investigated for tunnel-ionization by extending the definition of the Wigner time delay. Later, this concept is redefined in terms of the phase of the fixed energy propagator. The developed formalism is applied to the deep-tunneling and the near-threshold-tunneling regimes. It is shown that in the latter case signatures of the tunneling time delay can be measurable at remote distance. Finally, the path-dependent formulation of gauge theory is discussed. It is demonstrated that this equivalent formulation of gauge theory leads to a canonical gauge fixing, in which the Feynman path integral becomes more intuitive and the calculation of the quasiclassical propagator is considerably simplified.

Within the scope of this thesis, the following articles were accepted/published in refereed journals:

- Enderalp Yakaboylu, Michael Klaiber, Heiko Bauke, Karen Z. Hatsagortsyan, and Christoph H. Keitel,
  "Relativistic features and time delay of laser-induced tunnel-ionization,"
  Phys. Rev. A. (arXiv:1309.0610)

- Michael Klaiber, Enderalp Yakaboylu, Heiko Bauke, Karen Z. Hatsagortsyan, and Christoph H. Keitel,
  "Under-the-Barrier Dynamics in Laser-Induced Relativistic Tunneling,"
  Phys. Rev. Lett. **110**, 053814 (2013)

- Michael Klaiber, Enderalp Yakaboylu, and Karen Z. Hatsagortsyan,
  "Above-threshold ionization with highly charged ions in superstrong laser fields. I. Coulomb-corrected strong-field approximation,"
  Phys. Rev. A **87**, 023417 (2013)

- Michael Klaiber, Enderalp Yakaboylu, and Karen Z. Hatsagortsyan,
  "Above-threshold ionization with highly charged ions in superstrong laser fields. II. Relativistic Coulomb-corrected strong-field approximation,"
  Phys. Rev. A **87**, 023418 (2013)

Within the scope of this thesis, the following preprint was submitted:

- Enderalp Yakaboylu, Karen Z. Hatsagortsyan, and Christoph H. Keitel,
  "The propagator of a relativistic particle via the path-dependent vector potential,"
  arXiv:1311.6343

- Enderalp Yakaboylu and Karen Z. Hatsagortsyan,
  "On the quantization of the nonintegrable phase in electrodynamics,"
  arXiv:1309.0715

- Michael Klaiber, Enderalp Yakaboylu, Carsten Müller, Heiko Bauke, Gerhard G. Paulus, and Karen Z. Hatsagortsyan,
  "Spin dynamics in relativistic ionization with highly charged ions in superstrong laser fields,"
  arXiv:1305.5379

Contents

1. Introduction

On the visible side of the universe, all known phenomena can be well described with four fundamental interactions. These are the strong, the weak, the electromagnetic and the gravitational forces. As human beings, obviously we are familiar with and aware of phenomena mediated via the latter two forces in our daily experiences, even just right now while reading the current sentences and comprehending them in our brains. The weak and the strong interactions, on the other hand, might seem not to be empiric and heuristic due to the fact that they are short range forces, which are responsible for certain decay processes, and binding neutrons and protons together in the cores of atoms, respectively.

The present work is dedicated to the study of the electromagnetic interaction: the interaction of light and matter. In the chronology of science, electricity and magnetism were first considered as two unrelated physical phenomena [1]. They were studied and formulated separately as a theory of static electric and magnetic fields until the remarkable step taken by Michael Faraday in 1831 [2]. He observed the role of the dynamics, i.e., the time dependency, by demonstrating that a changing of magnetic field generates an electric field, which was the first step towards the unification of electromagnetism. However, this led to inconsistencies in the existing equations at that time and it was James Clerk Maxwell who did manage to remove these inconsistencies in 1865 [3]. He wrote down a consistent set of equations which are now called Maxwell's equations. Then, the two theories had been unified in a single elegant theory, as electromagnetism (or electrodynamics), the first victorious unified scientific theory of fundamental forces. The unification was so elegant that it was already consistent with the special theory of relativity formulated by Albert Einstein 40 years later [4].

The elegance of the unification of electricity and magnetism expressed by Maxwell's equations allows to express the electric and magnetic field in terms of potentials such that any other potential related by a so-called gauge transformation describes the same electric and magnetic fields. This property is known as gauge invariance of electromagnetism [5].

Historically, the introduction of potentials may seem to be just a mathematical convention in order to calculate the electromagnetic fields and hence the gauge invariance may be interpreted as an artifact of the theory. However, in terms of the paradigm of modern physics, gauge invariance is not a consequence of electromagnetism, it is the reason for the existence of electromagnetism. More fundamentally, gauge invariance can be viewed as a consequence of the conservation of the electric charge under a global symmetry transformation via Noether's theorem [6–8]. Furthermore,

demanding a local symmetry transformation imposes an interaction between the associated conserved quantity and the gauge field. Electromagnetism is such a type of interaction. In general, a gauge theory can be patterned as follows [9]: First, for every conservation law there is an associated symmetry via Noether's theorem: Second, the local symmetries lead to the existence of gauge fields: And third, the resulting gauge theory imposes interactions between the gauge field and the conserved quantity. Such a generalization of the local gauge invariance, for instance, leads to the existence of non-abelian gauge fields, also called Yang-Mills fields [10].

In order to describe all phenomena related to electrodynamics on the experimentally feasible scale of the universe, a quantum theory of electromagnetism is imperative. After many milestone contributions to its development, the complete quantum theory of the electromagnetic field was finally formulated by Sin-Itiro Tomonaga [11], Julian Schwinger [12, 13], Richard Feynman [14–16] and Freeman Dyson [17, 18], which resulted in the most accurate theory (see, for instance, [19]) that is available today: Quantum electrodynamics (QED).

QED provides a framework to investigate both light and matter in terms of their quantum nature, i.e., in terms of the quanta of their fields: Photons and electrons. However, for a large number of photons in a given volume, as in the case of lasers, a coherent state of light can be treated as a classical electromagnetic field [2, 20]. In this case, the interaction of an electron with a classical field can be well described within the framework of quantum mechanics. In this sense, the present thesis is based on the relativistic quantum mechanical formulation of the interaction of classical light, specifically lasers, with a quantized matter field representing electrons.

The investigation of the regime of the relativistic laser-electron interaction is feasible with current laser technology [21, 22], particularly in the strong field ionization of highly charged ions [23–30]. The main aspect of this work is to investigate the relativistic strong field ionization, specifically the relativistic features of tunnel-ionization. Fig. 1.1 illustrates how in such a process the bound electron of a H-like ion leaks out to the continuum and is ionized [31].

In fact, quantum tunneling, on its own, is a novel phenomenon of quantum mechanics. It has been in the focus of both theoretical and experimental attention since the formulation of quantum mechanics (see for instance [32] for a comprehensive review). In particular the issue of whether the motion of a particle under a barrier is instantaneous or not is a long standing and controversial problem in physics since MacColl's first attempt to consider it in 1932 [33]. The main reason for the controversy is due to the fact that there cannot exist a well-defined time operator in standard quantum mechanics, time is just a parameter and it cannot be translated in an observable [34, 35]. Nonetheless, it is possible to infer information about the time via different proposals [36–43].

Furthermore, it is often argued in the literature that the description of ionization with the mechanism of tunneling is just an intuitive picture and it does not have to reflect the "physical reality" (for instance see [44]). The main argument of this assertion is based on the gauge dependency of the potential barrier. Nevertheless, a

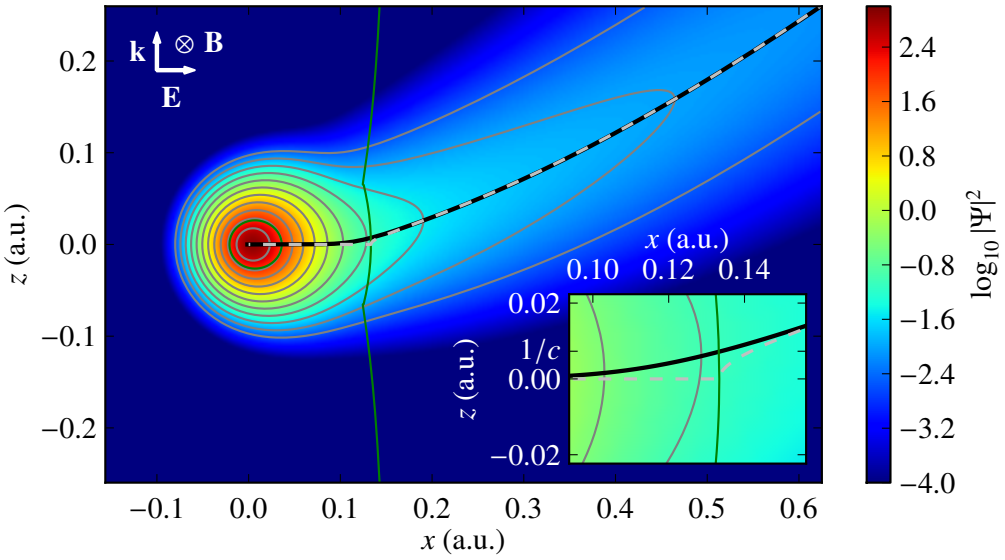

Figure 1.1. – Numerical simulation of the electron wave function in a soft-core potential via the Dirac equation. The density plot shows the electron density at the moment when maximal laser field strength is attained. The solid black line indicates the maximum of the density in laser propagation direction while the dashed line corresponds to the most probable trajectory resulting from the quasi-classical description. Solid green lines correspond to the border of the classical forbidden region. White arrows and the cross indicate the directions of the laser's electromagnetic fields and its propagation direction. The inset shows a scale-up of the region close to the tunnel exit, see chapter 6. The applied parameters are $I_p/c^2 = 0.25$, and $E_0/E_a = 1/30$. The figure is taken from [31].

careful investigation of gauge theory indicates that it is always possible to identify a gauge invariant tunneling barrier for the ionization process [45].

After all, in a nutshell, the theoretical ingredients of this thesis are the relativistic properties of quantum tunneling and gauge theory. In this direction, we begin the thesis by discussing gauge theory in chapter 2 in order to establish a tunneling barrier without any ambiguity. We introduce a gauge invariant energy operator for an arbitrary constant electromagnetic field. Thereby, the classically forbidden region can be identified both in the nonrelativisitic as well as in the relativistic regime of tunnel-ionization. Besides, in that chapter, the path-dependent formulation of gauge theory is discussed. The formulation is developed by DeWitt and Mandelstam in order to discuss quantum theory without electromagnetic potentials [46, 47]. Basically, the formalism replaces the gauge freedom with the path freedom, i. e., the vector potentials are defined via certain paths such that each path corresponds to an associated gauge function [48, 49]. Based on this geometrical picture of gauge theory we propose a canonical gauge fixing which makes the Feynman path integral formulation of quantum mechanics more intuitive and simplifies the calculation of the quasiclassical propagator.

Then, we consider the relativistic features of tunnel-ionization in two separate chapters. In chapter 3, we have discussed the one dimensional intuitive picture of tunnel-ionization at the presence of a magnetic field and it is shown that the ionized electron wave packet in the relativistic regime experiences a momentum shift along the laser's propagation direction in contrast to the well-known nonrelativisitic regime. We confirm the momentum shift by comparing it to the result of the strong field approximation (SFA) [50–53]. Since the SFA neglects the influence of the binding potential on the continuum state, we have modeled the binding potential with a zero-range potential.

Later, in chapter 4, the spin effects in the tunneling regime are investigated via the SFA. Accordingly, the SFA is explicitly driven for different partitions of the Hamiltonian as in [54, 55]. It is demonstrated that the SFA predicts an asymmetry in the tunneling probabilities of different spin states. This asymmetry is suppressed in the nonrelativisitic regime taking into account the influence of the laser field on the bound state.

In chapter 5, we unite two powerful methods, the proper time formalism and the path dependent formulation of gauge theory, for the calculation of the propagator of a relativistic charged particle interacting with an external electromagnetic field. Specifically, the developed formalism is applied to the calculation of the quasiclassical propagator for a spinless charged particle interacting with the following external fields: an arbitrary constant and uniform electromagnetic field, an arbitrary plane wave and an arbitrary plane wave combined with an arbitrary constant and uniform electromagnetic field. The result will later be used for the analysis of tunneling time delay in chapter 6.

In chapter 6, the tunneling time delay is investigated via Wigner's time delay concept. This concept is based on the time difference between the quasiclassical and the Wigner trajectory, which is the trajectory of the peak of the wave packet, at the remote distance. First, Wigner's time delay is applied to various model problems. Then, we extend the Wigner's time delay definition to tunnel-ionization problems. It is shown that there exist signatures of the tunneling time delay that may be measurable at remote distances. Finally, we propose the phase of the fixed energy propagator as a measure of the tunneling time delay, which is much more compatible than Wigner's original definition for the relativistic problems.

Finally, chapter 7 is devoted to the discussion on one of the most important long standing unresolved problems in theoretical physics [56]: charge quantization. Although this chapter seems to be a little far away from the main line of the thesis, the connection emerges from the path-dependent formulation of gauge theory that we introduced in chapter 2. In fact, it is shown that the path-dependent formalism can provide a compact description for the flux quantization. Moreover, the path-dependent formalism gives suggestions for searching quantized fluxes in different configurations and other possible reasons for charge quantization. As an example of charge quantization, the developed formalism is employed in a (1+1) dimensional spacetime, predicting the fundamental unit of charge.

In addition to the main chapters, we present two issues connected with the main

aspect of the thesis as appendices which can also be read as independent works. Firstly, we calculate the causal electric field, Liénard - Wiechert potential, for a (1+1) dimensional spacetime in appendix A. Secondly, we discuss the relativistic spin operator in appendix B on the base of the inhomogeneous Lorentz group and we derive a spin operator which commutes with the free Dirac Hamiltonian and satisfies the corresponding $SU(2)$ algebra.

1.1. Notation, system of units and presentation of the thesis

The metric signature is $g = (+,-,-,-)$ and unless otherwise stated Einstein summation convention is used in the entire work. The Lorentz scalar product $A^\mu B_\mu$ for two vectors A and B appears as $A\,B$ as well as $A \cdot B$ and the three vectors are represented via bold characters as $\boldsymbol{A}$.

The totally anti-symmetric tensor $\epsilon^{\mu\nu\rho\sigma}$ has $\epsilon^{0123} = 1$ and the usual Levi-Civita symbol is defined as $\epsilon^{0ijk} = \epsilon^{ijk}$.

Feynman slash notation $\not{A}$ for a vector A indicates $\gamma^\mu A_\mu$. In the standard representation [57] the Dirac matrices γ^μ are

$$\gamma^0 = \beta = \begin{pmatrix} I & 0 \\ 0 & -I \end{pmatrix}, \quad \gamma^i = \beta\,\alpha^i = \begin{pmatrix} 0 & \sigma^i \\ -\sigma^i & 0 \end{pmatrix} \tag{1.1}$$

with the 2×2 identity matrix I and the Pauli matrices

$$\sigma^1 = \begin{pmatrix} 0 & 1 \\ 1 & 0 \end{pmatrix}, \quad \sigma^2 = \begin{pmatrix} 0 & -i \\ i & 0 \end{pmatrix}, \quad \sigma^3 = \begin{pmatrix} 1 & 0 \\ 0 & -1 \end{pmatrix}. \tag{1.2}$$

The notation for electromagnetism is adapted from [2]: Electric charge is negative, $e < 0$, the four-vector potential is defined as $A^\mu = (\phi, \boldsymbol{A})$ and the Maxwell equations are written in the CGS (Gaussian) units as

$$\partial_\mu F^{\mu\nu} = \frac{4\pi}{c} J^\nu, \tag{1.3}$$

$$\epsilon^{\alpha\beta\mu\nu}\partial_\mu F_{\alpha\beta} = 0 \tag{1.4}$$

with the field strength tensor

$$F_{\mu\nu} = \partial_\mu A_\nu - \partial_\nu A_\mu\,. \tag{1.5}$$

In chapters 3, 4, and 6, where we present numerical results, atomic units (a.u.) are used for convenience. In these units we have

$$\hbar = 1\,, \quad m_e = 1\,, \quad e = -1 \quad \frac{1}{4\pi\epsilon_0} = 1 \tag{1.6}$$

with Planck's constant $\hbar$, the electron mass m_e, the electron charge e, and the Coulomb force constant $(4\pi\epsilon_0)^{-1}$. Other physical quantities can be expressed in terms of the constants (1.6) in a reduced way, for instance the dimensionless fine structure constant

$$\alpha = \frac{e^2}{(4\pi\epsilon_0)\hbar c} \approx 1/137 \tag{1.7}$$

identifies the speed of light as $c \approx 137$. Other physical quantities can be found in a similar way in atomic units, see Table 1.1.

Physical Quantity	atomic units (a.u.)	SI units
length (Bohr radius)	$a_0 = 4\pi\epsilon_0\hbar^2/(m_e e^2) = 1$	$0.526\,\mathring{A}$
time	$t = (4\pi\epsilon_0)^2\hbar^3/(m_e e^4) = 1$	2.42×10^{-17} s
energy (Hartree)	$\varepsilon_h = -m_e e^3/(4\pi\epsilon_0\hbar)^2 = 1$	27.2 eV
electric field	$E = -\varepsilon_h/(ea_0) = 1$	5.14×10^{11} V/m

Table 1.1. – A brief summary of some fundamental quantities. Here time is the required quasiclassical time for an electron to fly one period in the first Bohr orbit, the Hartree energy is twice the ionization energy of the ground state of Hydrogen atom, and intensity is given in units of $I = \epsilon_0 c E^2/2 = 3.5 \times 10^{16}\,\mathrm{W/cm^2}$, further information can be found in [58].

The presentation of the thesis is the following. Each chapter has its own introduction and conclusion sections, where we give a motivation, statement of the problem and the summary of the chapter, respectively. At the end of the introduction of every chapter we clearly indicate the system of units that is used throughout the chapter and cite the relevant articles that partly include the results and figures.

2. On gauge theory

2.1. Introduction

The homogeneous Maxwell equations, Gauss' law for magnetism and Faraday's law of induction, identify the electromagnetic field strength tensor in terms of gauge dependent vector potentials. Moreover, any other vector potential, related by a gauge transformation, describes the same physical reality which is known as the gauge invariance of electromagnetism.

The gauge invariance is, in fact, deeply connected with the charge conservation. This connection was made first by Herman Weyl when he attempted to unify electromagnetism and general relativity [5]. In this connection, the gauge invariance is equivalent to the phase invariance of a wave function. More fundamentally, the electric charge conservation appears as a consequence of the invariance of the theory under a global internal continuous symmetry transformation via Noether's theorem [59]. Furthermore, extending the global symmetry transformation to the local one requires the introduction of a vector potential (gauge field), which ends up with the interaction. In a sense, a global internal continuous symmetry implies a conserved quantity, while demanding the associated local symmetry induces the interaction between the conserved quantity and the gauge field [6–8].

Moreover, as elegantly described by Aharanov and Bohm, the vector potential has a significant role in quantum mechanics [60]. The vector potential does not only provide a compact mathematical formulation of the associated field strength tensor but also it explains predictions such as the Aharanov-Bohm effect [60–62], flux quantization [63–66] and Dirac's charge quantization condition when the existence of a magnetic monopole is assumed [67, 68].

In this chapter, we first briefly summarize the conventional gauge theory in Sec. 2.2 where we introduce the gauge invariant physical energy operator via discussing the gauge covariant operators in quantum mechanics. It is shown that for a constant electromagnetic field there exists a well-defined potential barrier which later indicates the gauge invariance of the tunneling barrier in the tunnel-ionization process.

After that, we will present the path-dependent formulation of gauge theory in the next Sec. 2.3. The formalism is developed by DeWitt and Mandelstam in order to discuss quantum theory without electromagnetic potentials [46, 47]. Indeed, as discussed in [69], it can be shown that the formalism emerged from the nonintegrable (path-dependent) phase factor. In this equivalent formulation of gauge theory the vector potentials are defined via certain paths such that each path corresponds to an

associated gauge function [48, 49]. The formalism further represents a geometric picture of the path transformation, i.e., gauge transformation, via the electromagnetic flux.

The CGS units are used throughout this chapter and the results can be partly found in [45, 69].

2.2. Conventional gauge theory

The conventional gauge theory (the reason of why we call it conventional will be clear in the following sections when we introduce the path-dependent formulation of gauge theory) can be summarized in the light of [9, 70]. Here we focus on the abelian case.

In classical electrodynamics the Maxwell equations in (3+1) spacetime dimensions read

$$\partial_\mu F^{\mu\nu} = \frac{4\pi}{c} J^\nu \,, \tag{2.1}$$

$$\epsilon^{\alpha\beta\mu\nu}\partial_\mu F_{\alpha\beta} = 0 \,, \tag{2.2}$$

where the components of the electromagnetic field strength tensor $F^{\mu\nu}$ are the electric field $F^{i0} = E^i$ and the magnetic field $F^{jk} = \epsilon^{ijk}B_k$ such that

$$F^{\mu\nu} = \begin{pmatrix} 0 & -E_x & -E_y & -E_z \\ E_x & 0 & -B_z & B_y \\ E_y & B_z & 0 & -B_x \\ E_z & -B_y & B_x & 0 \end{pmatrix} . \tag{2.3}$$

Further, the four-vector current is defined as $J^\mu = (c\rho, \boldsymbol{J})$. The homogeneous Maxwell equations (2.2) allow to express the electric and magnetic fields in terms of a four-vector potential $A^\mu = (\phi, \boldsymbol{A})$ as

$$F_{\mu\nu} = \partial_\mu A_\nu - \partial_\nu A_\mu \,. \tag{2.4}$$

In other words, the electric field and the magnetic field can be written as

$$\boldsymbol{E} = -\nabla\phi - \frac{1}{c}\partial_t \boldsymbol{A} \,, \tag{2.5}$$

$$\boldsymbol{B} = \nabla \times \boldsymbol{A} \,. \tag{2.6}$$

Furthermore, any other four-vector potential, related by a so-called gauge transformation, describes the same electric and magnetic field. The transformation

$$A^\mu \to A'^\mu = A^\mu + \partial^\mu \chi \,, \tag{2.7}$$

$$\phi \to \phi' = \phi + \frac{1}{c}\partial_t \chi \,, \tag{2.8}$$

$$\boldsymbol{A} \to \boldsymbol{A}' = \boldsymbol{A} - \nabla\chi \tag{2.9}$$

leaves the electromagnetic field strength tensor invariant and, consequently, all the physically measurable phenomena related to electrodynamics such as Maxwell equations, the Lorentz force law become gauge invariant. Furthermore, the Schrödinger equation which governs the time evolution of the wave function

$$i\hbar\frac{\partial\psi(\boldsymbol{x},t)}{\partial t}=\frac{1}{2}\left(-i\hbar\nabla-\frac{e}{c}\boldsymbol{A}(\boldsymbol{x},t)\right)^2\psi(\boldsymbol{x},t)+e\phi(\boldsymbol{x},t)\,\psi(\boldsymbol{x},t) \tag{2.10}$$

becomes invariant under the gauge-transformation ([70]) as long as the wave function transforms as

$$\psi(x)\rightarrow\exp\left(\frac{ie\chi}{\hbar c}\right)\psi(x)\,. \tag{2.11}$$

More generally, as we underlined in the introduction Sec.(2.1), the gauge invariance is not a consequence of electromagnetism, rather it leads to the existence of the interaction of electromagnetism. This perspective of understanding of gauge theory makes the weak interaction and the strong interaction more clear. Explicitly, gauge theory follows from the steps [9]. First, for every conservation law there is an associated symmetry via Noether's theorem; second, the local ones among them lead to the existence of gauge fields; and third, the gauge field theory imposes interactions between the gauge field and the conserved quantity. Such a generalization of the local gauge invariance leads to the existence of non-abelian gauge fields, i.e., Yang-Mills theory which is the generalization of electromagnetism [10].

2.2.1. Gauge invariant energy operator

Besides the elegance of gauge theory, all the physical quantities, i. e., the experimental observables cannot depend on the choice of the gauge function. For example, the canonical momentum operator $\boldsymbol{p}$ transforms under the gauge transformation $U=\exp\left(\frac{ie\chi}{\hbar c}\right)$ as

$$\boldsymbol{p}\rightarrow U^{\dagger}\boldsymbol{p}U=\boldsymbol{p}+\frac{e}{c}\nabla\chi\neq\boldsymbol{p}\,. \tag{2.12}$$

The kinetic momentum $\boldsymbol{q}(\boldsymbol{A})=\boldsymbol{p}-e\boldsymbol{A}/c$, however, obeys

$$\boldsymbol{q}(\boldsymbol{A})\rightarrow U^{\dagger}\boldsymbol{q}U=\boldsymbol{p}-e\boldsymbol{A}'/c=\boldsymbol{q}(\boldsymbol{A}')\,. \tag{2.13}$$

Here, the canonical momentum $\boldsymbol{p}$ which generates the space translation and satisfies the canonical commutation relation is not a physical measurable quantity, it is the kinetic momentum $\boldsymbol{q}(\boldsymbol{A})$ that is measured in an experiment. In general, any operator that satisfies the transformation

$$O(\boldsymbol{p},\boldsymbol{x},\boldsymbol{A},\phi)\rightarrow U^{\dagger}O(\boldsymbol{p},\boldsymbol{x},\boldsymbol{A},\phi)U=O(\boldsymbol{p},\boldsymbol{x},\boldsymbol{A}',\phi') \tag{2.14}$$

is called a physical operator. For instance, the Hamiltonian for a charge particle interacting with an arbitrary electromagnetic field in the nonrelativisitic regime

$$H=\frac{(\boldsymbol{p}-e\boldsymbol{A}/c)^2}{2}+e\phi \tag{2.15}$$

transforms under the gauge transformation as

$$H \to \frac{(\boldsymbol{p} - e\boldsymbol{A}'/c)^2}{2} + e\phi\,. \tag{2.16}$$

Hence, it cannot be a physical operator (because ϕ is not equally transformed to ϕ'), while $H - i\hbar\,\partial/\partial t$ is the physical operator which guarantees the invariance of the Schrödinger equation under a gauge transformation.

In contrast to the Hamiltonian H, the total energy of a system has to be a gauge invariant physical quantity. Therefore, we have to distinguish two concepts: the Hamiltonian and the total energy. The Hamiltonian is the generator of the time translation and the Legendre transformation of the associated Lagrangian, while the total energy is defined as a conserved quantity of the dynamical system under a time translation symmetry of the Lagrangian. As a consequence, if the Hamiltonian is explicitly time independent, then the Hamiltonian coincides with the total energy operator.

For a time independent electromagnetic field there exists a certain gauge where the Hamiltonian is explicitly time independent. The identification of the Hamiltonian as a total energy operator implies that both the vector potential $\boldsymbol{A}$ and the scalar potential ϕ associated to the constant electromagnetic field have to be time independent. This leads to the fact that

$$\phi = -\int^{\boldsymbol{x}} \boldsymbol{E}(\boldsymbol{x}') \cdot d\boldsymbol{x}'\,, \tag{2.17}$$

where we have used Eq. (2.5). In this gauge, the Hamiltonian which coincides with the total energy operator $\hat{\varepsilon}$ in the presence of any external potential $V(\boldsymbol{x})$ reads

$$H = \hat{\varepsilon} = \frac{1}{2}\left(\boldsymbol{p} - \frac{e}{c}\boldsymbol{A}(\boldsymbol{x})\right)^2 - e\int^{\boldsymbol{x}} \boldsymbol{E}(\boldsymbol{x}') \cdot d\boldsymbol{x}' + V(\boldsymbol{x})\,, \tag{2.18}$$

where the time independent vector potential $\boldsymbol{A}(\boldsymbol{x})$ generates the associated magnetic field via Eq. (2.6).

Accordingly, if we identify Eq. (2.18) as a definition of the gauge independent total energy operator, it reads in an arbitrary gauge

$$\hat{\varepsilon} = \frac{1}{2}\left(\boldsymbol{p} - \frac{e}{c}\boldsymbol{A}'(\boldsymbol{x}, t)\right)^2 - e\int^{\boldsymbol{x}} \boldsymbol{E}(\boldsymbol{x}') \cdot d\boldsymbol{x}' + V(\boldsymbol{x})\,, \tag{2.19}$$

where we have used the transformation (2.14). The first term on the right hand side of Eq. (2.19) is the kinetic energy for an arbitrary vector potential $\boldsymbol{A}'(\boldsymbol{x}, t)$ that appears in the corresponding Hamiltonian. The second term should not be regarded as a scalar potential, but defines the potential energy.

The energy operator (2.19) has to fulfill the conservation law for time independent fields

$$\frac{d\hat{\varepsilon}}{dt} = \frac{i}{\hbar}\,[H,\, \hat{\varepsilon}] + \frac{\partial\hat{\varepsilon}}{\partial t} = 0 \tag{2.20}$$

for the corresponding Hamiltonian

$$H = \frac{1}{2}\left(\boldsymbol{p} - \frac{e}{c}\boldsymbol{A}'(\boldsymbol{x}, t)\right)^2 + e\,\phi(\boldsymbol{x}) + V(\boldsymbol{x})\,. \tag{2.21}$$

The validity of the requirement (2.20) can be proven in a straightforward calculation. We find

$$\frac{\partial \hat{\varepsilon}}{\partial t} = -\frac{e}{2}\left((\boldsymbol{p} - e\boldsymbol{A}'/c)\cdot\frac{\partial \boldsymbol{A}'}{c\,\partial t} + \frac{\partial \boldsymbol{A}'}{c\,\partial t}\cdot(\boldsymbol{p} - e\boldsymbol{A}'/c)\right), \tag{2.22}$$

$$\begin{aligned}[H,\,\hat{\varepsilon}] = -\frac{e}{2}\Bigg((\boldsymbol{p} - e\boldsymbol{A}'/c)\cdot\left[\boldsymbol{p},\,\int^{\boldsymbol{x}}\boldsymbol{E}\cdot d\boldsymbol{x}' + \phi\right] \\ + \left[\boldsymbol{p},\,\int^{\boldsymbol{x}}\boldsymbol{E}\cdot d\boldsymbol{x}' + \phi\right]\cdot(\boldsymbol{p} - e\boldsymbol{A}'/c)\Bigg)\end{aligned} \tag{2.23}$$

and hence

$$\frac{d\hat{\varepsilon}}{dt} = -\frac{e}{2}\left(\left(\boldsymbol{p} - \frac{e}{c}\boldsymbol{A}'\right)\cdot\left(\boldsymbol{E} + \nabla\phi + \frac{\partial \boldsymbol{A}'}{c\,\partial t}\right) + \left(\boldsymbol{E} + \nabla\phi + \frac{\partial \boldsymbol{A}'}{c\,\partial t}\right)\cdot\left(\boldsymbol{p} - \frac{e}{c}\boldsymbol{A}'\right)\right) = 0 \tag{2.24}$$

is obtained.

As a consequence, for an arbitrary constant electromagnetic field, there exists a well-defined gauge invariant energy operator which fulfills the conservation law (2.20). The definition (2.19), then, suggests to introduce the gauge independent effective potential energy as

$$V_{\text{eff}}(\boldsymbol{x}) = -e\int^{\boldsymbol{x}}\boldsymbol{E}(\boldsymbol{x}')\cdot d\boldsymbol{x}' + V(\boldsymbol{x})\,. \tag{2.25}$$

The physical energy operator for an arbitrary constant electromagnetic field can be generalized to the relativistic regime straightforwardly by using the Dirac Hamiltonian

$$H = c\,\boldsymbol{\alpha}\cdot\left(\boldsymbol{p} - \frac{e}{c}\boldsymbol{A}(\boldsymbol{x},t)\right) + e\,\phi(\boldsymbol{x}) + V(\boldsymbol{x}) + \beta c^2 \tag{2.26}$$

with the Dirac matrices $\boldsymbol{\alpha}$ and β [57]. From Eq. (2.19) we deduce the physical energy operator in the relativistic case as

$$\hat{\varepsilon} = c\,\boldsymbol{\alpha}\cdot(\boldsymbol{p} - e\boldsymbol{A}(\boldsymbol{x},t)/c) - e\int^{\boldsymbol{x}}\boldsymbol{E}(\boldsymbol{x}')\cdot d\boldsymbol{x}' + V(\boldsymbol{x}) + \beta c^2\,. \tag{2.27}$$

It is also straightforward to show that the relativistic energy operator (2.27) fulfills the conservation law (2.20) as

$$\frac{d\hat{\varepsilon}}{dt} = \frac{i}{\hbar}\left(-ec\,\boldsymbol{\alpha}\left[\boldsymbol{p},\,\int^{\boldsymbol{x}}\boldsymbol{E}(\boldsymbol{x}')\cdot d\boldsymbol{x}'\right] + ec\,\boldsymbol{\alpha}\,[\phi,\boldsymbol{p}]\right) - e\boldsymbol{\alpha}\,\partial_t\boldsymbol{A} = 0\,. \tag{2.28}$$

2.3. The path-dependent formulation of gauge theory

In their celebrated paper [71], Wu and Yang pointed out that the field strength tensor underdescribes the complete electromagnetic phenomena, in other words, a different

physical realization of electromagnetic phenomena may have the same field strength tensor $F_{\mu\nu}$. Further, they gave a complete description of electromagnetism based on the concept of the nonintegrable (path-dependent) phase factor (or it may be called Wilson line [72])

$$\exp\left(-\frac{ie}{\hbar c}\int_{\mathcal{P}}^{x} A_\nu dy^\nu\right). \tag{2.29}$$

The integration path $\mathcal{P}$ starts at a point where the fields are zero and runs up to the point of interest x. Historically, such kind of line integrals of the potentials were previously suggested in [46, 47, 73, 74]. Moreover, it was shown by DeWitt [46] and Mandelstam [47] that the nonintegrable phase factor Eq. (2.29) can eliminate the vector potential from the formalism. However, the expense is that the "unique" vector potentials, which depend on the field strength tensor, become path dependent. Every gauge function in the conventional gauge theory has a corresponding path in this equivalent formulation [48, 49].

Electromagnetism is a consequence of the local phase transformation of the wave function. In fact, we can impose this transformation via the nonintegrable phase factor as

$$\psi(x) \to \Psi(x) = \exp\left(-\frac{ie}{\hbar c}\int_{\mathcal{P}}^{x} A_\nu(y) dy^\nu\right)\psi(x)\,, \tag{2.30}$$

which corresponds to identifying the gauge function χ via the path integral

$$\chi(x) = -\int_{\mathcal{P}}^{x} A_\nu(y) dy^\nu\,. \tag{2.31}$$

Then the associated Schrödinger equation becomes invariant under the following gauge transformation

$$A_\mu(x) \to \mathcal{A}_\mu(x) \equiv A_\mu(x) - \frac{\partial}{\partial x^\mu}\int_{\mathcal{P}}^{x} A_\nu dy^\nu\,. \tag{2.32}$$

The latter yields to the gauge invariant vector potential $\mathcal{A}_\mu(x)$. Explicitly, let us first parametrize the path $y = y(s, x)$ as

$$y(1, x) = x\,, \quad y(0, x) = x'\,, \tag{2.33}$$

where the electromagnetic field vanishes at x', at which A_μ may, without loss of generality, be set equal to zero. Then, Eq. (2.32) becomes

$$\begin{aligned}
\mathcal{A}_\mu(x) &= A_\mu(x) - \frac{\partial}{\partial x^\mu}\int_0^1 A_\nu(y)\frac{\partial y^\nu}{\partial s} ds \\
&= A_\mu(x) - \int_0^1 \left(\frac{A_\nu(y)}{\partial y^\lambda}\frac{\partial y^\lambda}{\partial x^\mu}\frac{\partial y^\nu}{\partial s} + A_\nu(y)\frac{\partial}{\partial s}\frac{\partial y^\nu}{\partial x^\mu}\right) ds\,, \\
&= A_\mu(x) - \int_0^1 \left(\frac{A_\lambda(y)}{\partial y^\nu}\frac{\partial y^\nu}{\partial s}\frac{\partial y^\lambda}{\partial x^\mu} + A_\nu(y)\frac{\partial}{\partial s}\frac{\partial y^\nu}{\partial x^\mu} - F_{\nu\lambda}(y)\frac{\partial y^\lambda}{\partial x^\mu}\frac{\partial y^\nu}{\partial s}\right) ds\,,
\end{aligned} \tag{2.34}$$

where in last line we have used $A_{\nu,\lambda}(y) = A_{\lambda,\nu}(y) - F_{\nu\lambda}(y)$. Further, the first two integrand terms in Eq. (2.34) can be written as $\frac{\partial}{\partial s}\left(A_\lambda(y)\frac{\partial y^\lambda}{\partial x^\mu}\right)$ and using the boundary conditions (2.33),

$$\mathcal{A}_\mu(x) = \int_0^1 F_{\nu\lambda}(y)\frac{\partial y^\nu}{\partial s}\frac{\partial y^\lambda}{\partial x^\mu} ds \tag{2.35a}$$

is obtained. Furthermore, since the field strength tensor $F_{\mu\nu}$ is antisymmetric, Eq. (2.35a) can be written as

$$\mathcal{A}_\mu(x) = \frac{1}{2}\int_0^1 F_{\nu\lambda}(y)\left(\frac{\partial y^\nu}{\partial s}\frac{\partial y^\lambda}{\partial x^\mu} - \frac{\partial y^\lambda}{\partial s}\frac{\partial y^\nu}{\partial x^\mu}\right)ds\,. \tag{2.35b}$$

At this point it worths to verify that Eq. (2.35) satisfies the natural relation

$$F_{\mu\nu} = \frac{\partial \mathcal{A}_\nu(x)}{\partial x^\mu} - \frac{\partial \mathcal{A}_\mu(x)}{\partial x^\nu}\,, \tag{2.36}$$

as follows :

$$\frac{\partial \mathcal{A}_\nu(x)}{\partial x^\mu} - \frac{\partial \mathcal{A}_\mu(x)}{\partial x^\nu} = \frac{\partial}{\partial x^\mu}\int_0^1 F_{\alpha\beta}(y)\frac{\partial y^\alpha}{\partial s}\frac{\partial y^\beta}{\partial x^\nu}ds - \frac{\partial}{\partial x^\nu}\int_0^1 F_{\alpha\beta}(y)\frac{\partial y^\alpha}{\partial s}\frac{\partial y^\beta}{\partial x^\mu}ds, \tag{2.37}$$

$$= \int_0^1 \left[\frac{\partial F_{\alpha\beta}}{\partial y^\lambda}\frac{\partial y^\lambda}{\partial x^\mu}\frac{\partial y^\alpha}{\partial s}\frac{\partial y^\beta}{\partial x^\nu} + F_{\alpha\beta}\frac{\partial}{\partial s}\left(\frac{\partial y^\alpha}{\partial x^\mu}\right)\frac{\partial y^\beta}{\partial x^\nu}\right. \tag{2.38}$$

$$\left. - \underbrace{\frac{\partial F_{\alpha\beta}}{\partial y^\lambda}\frac{\partial y^\lambda}{\partial x^\nu}\frac{\partial y^\alpha}{\partial s}\frac{\partial y^\beta}{\partial x^\mu}}_{\lambda\leftrightarrow\beta} - \underbrace{F_{\alpha\beta}\frac{\partial}{\partial s}\left(\frac{\partial y^\alpha}{\partial x^\nu}\right)\frac{\partial y^\beta}{\partial x^\mu}}_{\beta\leftrightarrow\alpha}\right]ds\,,$$

$$= \int_0^1 \left[\underbrace{\left(\partial_\lambda F_{\alpha\beta} - \partial_\beta F_{\alpha\lambda}\right)}_{\partial_\alpha F_{\lambda\beta}}\frac{\partial y^\alpha}{\partial s}\frac{\partial y^\lambda}{\partial x^\mu}\frac{\partial y^\beta}{\partial x^\nu} + F_{\alpha\beta}\frac{\partial}{\partial s}\left(\frac{\partial y^\alpha}{\partial x^\mu}\frac{\partial y^\beta}{\partial x^\nu}\right)\right]ds\,, \tag{2.39}$$

$$= \int_0^1 \frac{\partial}{\partial s}\left(F_{\alpha\beta}\frac{\partial y^\alpha}{\partial x^\mu}\frac{\partial y^\beta}{\partial x^\nu}\right)ds = F_{\alpha\beta}\frac{\partial y^\alpha}{\partial x^\mu}\frac{\partial y^\beta}{\partial x^\nu}\bigg|_0^1 = F_{\mu\nu}\,. \tag{2.40}$$

Here, in the second line we interchange the dummy indexes λ and β, and β and α in the third and forth integrands, respectively. Further, in the third line we have used the Bianchi identity

$$\partial_\lambda F_{\mu\nu} + \partial_\mu F_{\nu\lambda} + \partial_\nu F_{\lambda\mu} = 0\,. \tag{2.41}$$

Finally, in the last line, the corresponding boundary conditions (2.33) are used such that

$$\frac{\partial y^\alpha(s=1)}{\partial x^\mu} = g^\alpha{}_\mu\,, \tag{2.42}$$

$$F_{\alpha\beta}(s=0) = 0\,. \tag{2.43}$$

The expression (2.35) is gauge independent because it is written solely in terms of the gauge invariant field strength tensor $F_{\mu\nu}$. However, the expense is that the vector potential is path dependent and every gauge function in the conventional gauge theory has a counterpart in the path-dependent formalism [48, 49]. As a consequence, we will label both the vector potential $\mathcal{A}_\mu$ and the wave function Ψ with the path index $\mathcal{P}$ which refers to a certain path as

$$\left[i\hbar\gamma^\mu\left(\partial_\mu - \frac{ie}{\hbar c}\mathcal{A}_\mu(\mathcal{P},x)\right) - mc\right]\Psi(\mathcal{P},x) = 0\,. \tag{2.44}$$

Moreover, the Dirac equation (2.44) is invariant under the following path transformation

$$\mathcal{A}_\mu(\mathcal{P}', x) = \mathcal{A}_\mu(\mathcal{P}, x) + \partial_\mu \oint_{\partial\Sigma}^{x} A_\nu dy^\nu \,, \tag{2.45}$$

as long as the wave function satisfies

$$\Psi[\mathcal{P}', x] = \exp\left(\frac{ie}{\hbar c} \oint_{\partial\Sigma}^{x} A_\mu dy^\mu\right) \Psi[\mathcal{P}, x] \,, \tag{2.46}$$

with the closed loop $\partial\Sigma = \mathcal{P} - \mathcal{P}'$.

Furthermore, using the four-dimensional Stokes' law, the loop integral can be converted to surface integral

$$\oint_{\partial\Sigma}^{x} A^\mu dy_\mu = \frac{1}{2} \int_{\Sigma}^{x} F^{\mu\nu} d\sigma_{\mu\nu} = \Phi_{EM}(x) \tag{2.47}$$

with the electromagnetic flux Φ_{EM} [75]. In addition to that, using the definition of the path dependent vector potential (2.32), the electromagnetic flux for a nonconfined field can also be identified as

$$\int_{\mathcal{P}}^{x} \mathcal{A}_\mu(\mathcal{P}') dy^\mu = \Phi_{EM}(x) \,, \tag{2.48}$$

which implies that for any path $\mathcal{P}$

$$\int_{\mathcal{P}}^{x} \mathcal{A}_\mu(\mathcal{P}) dy^\mu = 0 \tag{2.49}$$

always holds[1]. In conclusion, true electromagnetism can be described by path invariance of the so-called nonintegrable phase factor which is known as Wilson line when the gauge group is nonabelian [72].

In order to illustrate the equivalence between the conventional gauge theory and the path-dependent formalism, let us specify some certain paths which have a well-known counterpart in the conventional gauge theory. For the sake of simplicity, assume that there is only a constant and uniform electric field $\boldsymbol{E}_0$ and further, without loss of generality, let the initial point be $x'^\mu = (0, \mathbf{0})$. If one chooses the path $\mathcal{P} = \mathcal{P}_1 + \mathcal{P}_2$ with the segments

$$\mathcal{P}_1 : \qquad y^\mu(s, x) = (0, s\,\boldsymbol{x}) \,, \quad 0 \le s \le 1 \,, \tag{2.50}$$

$$\mathcal{P}_2 : \qquad y^\mu(s, x) = (s\,ct, \boldsymbol{x}) \,, \quad 0 \le s \le 1 \,, \tag{2.51}$$

then the path dependent vector potential becomes

$$\begin{aligned} \mathcal{A}^\mu(x) &= F_{0i} \int_0^1 \frac{\partial y^0}{\partial s} \frac{\partial y^i}{\partial x_\mu} ds, \\ &= (0, -ct\,\boldsymbol{E}_0) \,. \end{aligned} \tag{2.52}$$

[1]For confined fields, the electromagnetic flux is always given by Eq. (2.47), and further $\int_{\mathcal{P}}^{x} \mathcal{A}_\mu(\mathcal{P}) dy^\mu$ may not be equal to zero, see Sec. 7.3.

This gauge is called velocity gauge. On the other hand, if we choose the segments of the path as

$$\mathcal{P}'_1 : \qquad y^\mu(s,x) = (s\,ct, \mathbf{0})\,, \quad 0 \le s \le 1\,, \tag{2.53}$$

$$\mathcal{P}'_2 : \qquad y^\mu(s,x) = (ct, s\,\boldsymbol{x})\,, \quad 0 \le s \le 1, \tag{2.54}$$

then the vector potential yields

$$\begin{aligned} \mathcal{A}^\mu(x) &= F_{i0}\int_0^1 \frac{\partial y^i}{\partial s}\frac{\partial y^0}{\partial x_\mu} ds\,, \\ &= (-\boldsymbol{x}\cdot\boldsymbol{E}_0, \mathbf{0})\,, \end{aligned} \tag{2.55}$$

which is known as length gauge. Furthermore, if we trace a straight line as

$$\mathcal{P}'' : \quad y^\mu(s,x) = (s\,ct, s\,\boldsymbol{x})\,, \quad 0 \le s \le 1\,, \tag{2.56}$$

then, the vector potential is given by

$$\begin{aligned} \mathcal{A}_\mu(x) &= F_{i0}\int_0^1 \left(\frac{\partial y^i}{\partial s}\frac{\partial y^0}{\partial x^\mu} - \frac{\partial y^0}{\partial s}\frac{\partial y^i}{\partial x^\mu}\right) ds\,, \\ \mathcal{A}^\mu(x) &= \left(-\frac{1}{2}\boldsymbol{x}\cdot\boldsymbol{E}_0, -\frac{1}{2}ct\,\boldsymbol{E}_0\right), \end{aligned} \tag{2.57}$$

which is known as Fock-Schwinger gauge $x_\mu\mathcal{A}^\mu = 0$. Following the path transformation (2.45), relations between different gauges is given by the electromagnetic flux. For instance, the gauge transformation between velocity and length gauge is given by

$$\Phi_{EM}(x) = -ct\,\boldsymbol{x}\cdot\boldsymbol{E}_0 \tag{2.58}$$

with $\partial\Sigma = \mathcal{P} - \mathcal{P}'$. Similarly, the transformation between the length gauge and the Fock-Schwinger gauge can be accomplished by

$$\Phi_{EM}(x) = -\frac{1}{2}ct\,\boldsymbol{x}\cdot\boldsymbol{E}_0 \tag{2.59}$$

with $\partial\Sigma = \mathcal{P}' - \mathcal{P}''$.

In the previous section, we have introduced the gauge invariant energy operators (2.19) and (2.27) for the nonrelativistic and relativistic regimes. The condition (2.14), which identifies a physical operator, can be written in terms of the path-dependent formulation of gauge theory as

$$O(\mathcal{P}) \to \exp\left(-\frac{ie}{\hbar c}\Phi_{EM}\right) O(\mathcal{P}) \exp\left(\frac{ie}{\hbar c}\Phi_{EM}\right) = O(\mathcal{P}')\,. \tag{2.60}$$

For the scalar potential the transformation (2.60) indicates

$$\mathcal{A}_0(\mathcal{P}) = \mathcal{A}_0(\mathcal{P}')\,. \tag{2.61}$$

In general, for an arbitrary electromagnetic field this condition, naturally, cannot be fulfilled. The condition (2.61) can be satisfied if and only if the electromagnetic flux Φ_{EM} through the area bounded by the loop $\partial\Sigma = \mathcal{P} - \mathcal{P}'$ is time independent, i.e.,

$$\mathcal{A}_0(\mathcal{P}) - \mathcal{A}_0(\mathcal{P}') = \partial_t \int_\Sigma F^{\mu\nu} d\sigma_{\mu\nu} = 0 \tag{2.62}$$

which imposes the following two necessary constraints; first the electromagnetic field has to be time independent, second the two paths $\mathcal{P}$ and $\mathcal{P}'$ can only deviates from each other on a hypersurface of the constant time. In fact, these constraints identify the corresponding Hamiltonian as an energy operator, which is consistent with the result of the previous section.

The full machinery of the path-dependent formalism of gauge theory provides some fundamental simplifications for the path integral formulation of quantum mechanics. Namely, let us consider the propagator in terms of the Feynman path integral which is defined by

$$K_F^E(\boldsymbol{x}, \boldsymbol{x}'; t) = \int D(\mathcal{P}_F) \exp\left(\frac{i}{\hbar} S(\mathcal{P}_F)\right), \tag{2.63}$$

where $D(\mathcal{P}_F)$ and $S(\mathcal{P}_F)$ represent the sum over all paths and the action evaluated along the path $\mathcal{P}_F$, respectively. For the sake of simplicity, we consider the action of a spinless charged particle interacting with an electromagnetic field

$$S(\mathcal{P}_F) = -mc^2 \int_{\mathcal{P}_F} d\tau - \frac{e}{c} \int_{\mathcal{P}_F} \mathcal{A}_\mu(\mathcal{P}_G, y) dy^\mu \tag{2.64}$$

with the particle's infinitesimal proper time $c\,d\tau = \sqrt{dy^\mu dy_\mu}$. Here we should emphasize that paths appearing in the Feynman path integrals $\mathcal{P}_F$ are real paths in the sense that the transition amplitude of a particle from spacetime point x' to x depends on these paths. Paths used for the vector potential $\mathcal{P}_G$ are just the gauge paths. Moreover, the action (2.64) can be defined via the electromagnetic flux (2.48) as

$$S(\mathcal{P}_F) = -mc^2 \int_{\mathcal{P}_F} d\tau - \frac{e}{c} \Phi_{EM}(\Sigma, x) \tag{2.65}$$

with $\partial\Sigma = \mathcal{P}_F - \mathcal{P}_G$.

The compact form of the action (2.65) provides us a further simplification for the quasiclassical propagators. The quasiclassical propagator can be defined via the classical action S_c which is the action evaluated along the classical trajectory (world line) $\mathcal{P}_c$. Furthermore, using the VanVleck-Pauli-Morette formula [76–79], it reads

$$K_F(\boldsymbol{x}, \boldsymbol{x}'; t) = \sqrt{\left(\frac{1}{2\pi i\hbar}\right)^3 \det\left(\frac{-\partial^2 S_c}{\partial \boldsymbol{x} \partial \boldsymbol{x}'}\right)} \exp\left(-\frac{i}{\hbar} mc^2 \int_{\mathcal{P}_c} d\tau - \frac{i}{\hbar}\frac{e}{c} \Phi_{EM}(\mathcal{P}_c - \mathcal{P}_G, x)\right). \tag{2.66}$$

Now, if we choose a gauge such that the corresponding gauge path becomes the classical path, the flux term in the above expression vanishes and then the quasiclassical propagator reduces to

$$K_F(\boldsymbol{x}, \boldsymbol{x}'; t) = \sqrt{\left(\frac{1}{2\pi i\hbar}\right)^3 \det\left(\frac{-\partial^2 S_c}{\partial \boldsymbol{x} \partial \boldsymbol{x}'}\right)} \exp\left(-\frac{i}{\hbar} mc^2 \int_{\mathcal{P}_c} d\tau\right) \tag{2.67}$$

where the classical path $\mathcal{P}_c$ satisfies the Lorentz force law

$$m\frac{\partial^2 y_c^\mu}{\partial \tau^2} = \frac{e}{c} F^{\mu\nu}(y_c) \frac{\partial y_{c\nu}}{\partial \tau} \tag{2.68}$$

with the particle's proper time τ. Here we should underline that Eq. (2.68) is not a parametrization independent equation (see for example [1]).

The latter defines the path dependent vector potential (2.35) as

$$\mathcal{A}_\mu(\mathcal{P}_c, x) = -\frac{mc}{e}\int_{\tau_i}^{\tau_f} \frac{\partial^2 y_{c\nu}}{\partial\tau^2}\frac{\partial y_c^\nu}{\partial x^\mu}d\tau\,, \tag{2.69}$$

with the boundary conditions $y^\mu(\tau_f) = x^\mu$ and $y^\mu(\tau_i) = x'^\mu$, where the dependence on the electromagnetic fields contains only in the definition of the classical path via Eq. (2.68). Furthermore, in terms of the reparametrization invariant form of the equations of motion

$$\frac{\partial p^\mu}{\partial s} = \frac{e}{c}F^{\mu\nu}(y_c)\frac{\partial y_{c\nu}}{\partial s} \tag{2.70}$$

with the particle's four momentum p^μ, the vector potential for the classical path reads

$$\mathcal{A}_\mu(\mathcal{P}_c, x) = -\frac{c}{e}\int_0^1 \frac{\partial p_\nu}{\partial s}\frac{\partial y_c^\nu}{\partial x^\mu}\,ds\,. \tag{2.71}$$

For a nonrelativistic particle, on the other hand, the classical trajectory can be parametrized with the physical time t'. Then, the path dependent vector potential for the nonrelativistic classical path $\boldsymbol{y}(t')$ with the boundary conditions $\boldsymbol{y}(0) = \boldsymbol{x}'$ and $\boldsymbol{y}(t) = \boldsymbol{x}$ can be written as

$$\mathcal{A}_\mu(\mathcal{P}_c, x) = \frac{mc}{e}\int_0^t \frac{\partial^2\boldsymbol{y}}{\partial t'^2}\cdot\frac{\partial\boldsymbol{y}_c}{\partial x^\mu}\,dt' = \frac{c}{e}\int_0^t \frac{\partial\boldsymbol{p}}{\partial t'}\cdot\frac{\partial\boldsymbol{y}_c}{\partial x^\mu}\,dt'\,, \tag{2.72}$$

where we have used $\partial t'/\partial x^\mu = 0$. This form of the vector potential (2.72) provides great convenience for the quasiclassical propagator for a nonrelativistic particle. Since the integral of the corresponding potential terms in the action vanishes, i.e.,

$$\int_0^t dt'\left(\frac{e}{c}\mathcal{A}\cdot\dot{\boldsymbol{y}}(t') - e\mathcal{A}^0\right) = 0\,, \tag{2.73}$$

the quasiclassical propagator for a nonrelativistic particle in the classical path gauge yields

$$K_F(\boldsymbol{x}, \boldsymbol{x}'; t) = \sqrt{\left(\frac{1}{2\pi i\hbar}\right)^3 \det\left(\frac{-\partial^2 S_c}{\partial\boldsymbol{x}\partial\boldsymbol{x}'}\right)}\exp\left(\frac{i}{\hbar}\int_{\mathcal{P}_c}^t \frac{m\,\dot{\boldsymbol{y}}_{\boldsymbol{c}}{}^2}{2}dt'\right). \tag{2.74}$$

In fact, this result can also be obtained directly via replacing the particle's infinitesimal proper time with the usual nonrelativistic kinetic term of the Lagrangian in Eq. (2.67).

In summary, since the equations of motion are gauge invariant, they are first found in any convenient gauge, then the propagator for a nonrelativistic particle as well as for a relativistic particle can be calculated in the corresponding classical path gauge via Eq. (2.74) and Eq.(2.67), respectively. The compact form of the quasiclassical propagator can be applied to any type of potential, when the classical equations of motion are known. The developed convenience for the quasiclassical propagator will be used for the calculation in later chapters in order to discuss the tunneling time delay of the tunnel-ionization process.

2.4. Conclusion

In this chapter, after briefly reviewing the conventional gauge theory, we have introduced the gauge invariant physical energy operator for an arbitrary constant electromagnetic field. This result will be used later to identify the tunneling barrier without any ambiguity in the tunnel-ionization process. Then, the path-dependent formulation of gauge theory was developed explicitly via the nonintegrable phase factor. There we have imposed the local phase invariance of the wave function via the path-dependent gauge function. In this equivalent formulation of gauge theory we have replaced the gauge functions with a path such that it reveals the new set of gauge choices which makes the Feynman path integral formulation of quantum mechanics more convenient. This leads to the fact that for the quasiclassical analysis these gauges let the interaction part of the classical action vanish. These results will later be used to calculate the quasiclassical propagators in chapter 5.

3. Relativistic features of laser-induced tunnel-ionization

3.1. Introduction

The investigation of the relativistic regime of laser-atom interactions, in particular the strong field ionization of highly charged ions [23–30], is feasible with current laser technology [21,22]. Strong field multiphoton atomic processes in the relativistic domain are governed by three parameters [80] which can be chosen to be the Keldysh parameter $\gamma = \omega\sqrt{2I_p}/E_0$ [50], the barrier suppression parameter E_0/E_a, and the relativistic laser field parameter $\xi = E_0/(c\omega)$, with the ionization potential I_p, the atomic field $E_a = (2I_p)^{3/2}$, the laser's electric field amplitude E_0, the angular frequency ω, and the speed of light c. At small Keldysh parameters ($\gamma \ll 1$) the laser field can be treated as quasistatic and the ionization is in the so-called tunneling regime up to intensities with $E_0/E_a \lesssim 1/10$, while for higher intensities over-the-barrier ionization dominates [81]. In the nonrelativistic case, quasistatic tunnel-ionization is a well-established mechanism, which is incorporated as a first step in the well-known simple-man three-step model of strong field multiphoton ionization [82]. In the first step of this intuitive picture the bound electron tunnels out through the effective potential barrier governed by the atomic potential $V(\boldsymbol{x})$ and the scalar potential of the quasistatic laser field as $V_{\text{barrier}}(\boldsymbol{x}) = \boldsymbol{x} \cdot \boldsymbol{E}(t_0) + V(\boldsymbol{x})$, where t_0 indicates the moment of quasistatic tunneling. In nonrelativistic settings, the effect of the magnetic field component of the laser field can be neglected and the quasistatic laser field is described solely in terms of the scalar potential $\boldsymbol{x} \cdot \boldsymbol{E}(t_0)$. In the second step the ionized electron propagates in the continuum according to the quasiclassical theory and the third step is a potential recollision of the laser driven electron with the ionic core that will not be considered in this work.

When entering the relativistic regime at $\xi^2 \gtrsim 1$, the laser's magnetic field modifies the second step via an induced drift motion of the continuum electron into the laser's propagation direction. For even stronger laser fields, that is when $I_p/c^2 \sim \gamma^2\xi^2 \sim 1$, the laser's magnetic field can also not be neglected anymore during the first step. Here, the description by a sole scalar potential $V_{\text{barrier}}(\boldsymbol{x})$ is not valid anymore and the intuitive picture of tunneling fails. The presence of a vector potential which generates the associated magnetic field led to a controversy over the effective potential barrier [44]. Hence we ask, can the tunneling picture be remedied for the application in the relativistic regime and can it be formulated in a gauge-independent form? These questions are addressed in this chapter. It is shown that for a quasistatic

electromagnetic wave, it is possible to define the tunneling barrier without ambiguity in any gauge via the energy operator [45] that we identified in chapter 2.

One of the theoretical tools applied in this chapter is the strong field approximation (SFA) [83, 84], see Sec. 4.2. Neglecting the atomic potential for the continuum electron and approximating its dynamics with a Volkov state is the main approximation of the SFA [50–52]. Consequently, the prediction of the SFA is much more accurate for a zero-range potential than for a more realistic long-range potential as the Coulomb potential. SFA calculations for tunnel-ionization modeled with a zero-range potential show that there is a momentum shift along the laser's propagation direction due to the tunneling step. We find that this shift can also be estimated via a WKB analysis when a Coulomb potential is used and that it is measurable in a detector after the laser field has been turned off [45].

The structure of the chapter is the following: In Sec. 3.2 the parameter domain of the relativistic tunneling dynamics is estimated. In Sec. 3.3 gauge independence of the tunneling barrier is established in nonrelativistic as well as in relativistic setting. The intuitive picture for tunnel-ionization is discussed in Sec. 3.4 reducing the full problem to a one-dimensional one. In Sec. 3.5 the SFA formalism is presented and the momentum distribution at the tunnel exit is calculated.

Atomic units (a. u.) are used throughout this chapter. The chaper is based on [31, 45] and all the figures are taken from [45].

3.2. Relativistic parameters

Let us estimate the role of relativistic effects in the tunnel-ionization regime which is valid for $\gamma \ll 1$ and for the intensities up to $E_0/E_a < 1/10$. The typical velocity of the electron during the under-the-barrier dynamics can be estimated from the bound state energy I_p as $\kappa \equiv \sqrt{2I_p}$ (for a hydrogenlike ion with charge Z and $I_p = c^2 - \sqrt{c^4 - Z^2c^2}$ in the ground state it follows $\kappa \sim Z$). The nonrelativistic regime of tunneling is defined via $\kappa \ll c$. This relation is valid for hydrogenlike ions with nuclear charge up to $Z \sim 20$ where $\kappa/c \sim 0.14$. For ions with charge $Z > 20$ the relativistic regime is entered because the velocity during tunneling is not negligible anymore with respect to the speed of light. However, even for an extreme case of U^{91+} with $Z = 92$ it is $\kappa/c \sim 0.6$, i. e., the dynamics is still weakly-relativistic and a Foldy-Wouthuysen expansion of the relativistic Hamiltonian up to order $(\kappa/c)^2$ is justified. The expansion yields

$$H = \frac{1}{2}\left(\boldsymbol{p} + \frac{\boldsymbol{A}(\eta)}{c}\right)^2 - \phi(\eta) + V(\boldsymbol{x}) - \frac{\boldsymbol{p}^4}{8c^2} + \frac{\boldsymbol{\sigma}\cdot\boldsymbol{B}(\eta)}{2c} + i\frac{\boldsymbol{\sigma}\cdot(\nabla\times\boldsymbol{E}(\eta))}{8c^2} + \frac{\boldsymbol{\sigma}\cdot(\boldsymbol{E}(\eta)\times\boldsymbol{p})}{4c^2} + \frac{\nabla\cdot\boldsymbol{E}(\eta)}{8c^2}, \tag{3.1}$$

where $V(\boldsymbol{x})$ is the binding potential, the four-vector potential is given by $A^\mu = (\phi(\eta), \boldsymbol{A}(\eta))$ and the phase of the electromagnetic wave is $\eta = x^\mu k_\mu = \omega(t - \hat{\boldsymbol{k}}\cdot\boldsymbol{x}/c)$, with $x^\mu = (c\,t, \boldsymbol{x})$, $k^\mu = \omega/c(1, \hat{\boldsymbol{k}})$ and the lasers propagation direction $\hat{\boldsymbol{k}}$.

In the tunneling regime, the typical displacement along the laser's propagation direction can be estimated as $\hat{\boldsymbol{k}} \cdot \boldsymbol{x} \sim \hat{\boldsymbol{k}} \cdot \boldsymbol{F}_L \tau_K^2$ with the Lorentz force $\boldsymbol{F}_L$ and the typical ionization time (Keldysh time) $\tau_K = \gamma/\omega = \kappa/E_0$. Identifying the Lorentz force along the laser's propagation direction as $\hat{\boldsymbol{k}} \cdot \boldsymbol{F}_L \sim \kappa B_0/c$ ($E_0 = B_0$), the typical distance reads $\hat{\boldsymbol{k}} \cdot \boldsymbol{x} \sim \gamma\kappa^2/(\omega c)$. Hence, electric as well as magnetic non-dipole terms are negligible since $\omega\ \hat{\boldsymbol{k}} \cdot \boldsymbol{x}\ /\ c\ \sim\ \gamma\,(\kappa/c)^2\ \ll\ 1$, i. e., the typical width of the electron's wave packet is small compared to the laser's wavelength.

Furthermore, the leading spin term in Eq. (3.1) is the spin-magnetic field coupling Hamiltonian $H_P = \boldsymbol{\sigma} \cdot \boldsymbol{B}/(2c)$. Its order of magnitude can be estimated as $H_P/\kappa^2 \sim E_0/(c\kappa^2) = \kappa/c(E_0/E_a)$. Therefore, in the tunneling regime the spin related terms and the Darwin term $\nabla \cdot \boldsymbol{E}(\eta)/(8c^2)$ in Eq. (3.1) can be neglected because $E_0/E_a \ll 1$. In summary, the electron's under-the-barrier dynamics is governed in the Göppert-Mayer gauge, see Sec. III, by the Hamiltonian

$$\begin{aligned} H &= H_0 + H_{ED} + H_{MD} + H_{RK} + H_I\,, \\ &= \frac{1}{2}\left(\boldsymbol{p} + \boldsymbol{x} \cdot \boldsymbol{E}(\omega t)\frac{\hat{\boldsymbol{k}}}{c}\right)^2 - \frac{\boldsymbol{p}^4}{8c^2} + \boldsymbol{x} \cdot \boldsymbol{E}(\omega t) + V(\boldsymbol{x}) \end{aligned} \tag{3.2}$$

with the free atomic Hamiltonian $H_0 = \boldsymbol{p}^2/2 + V(\boldsymbol{x})$, the electric-dipole $H_{ED} = \boldsymbol{x} \cdot \boldsymbol{E}(\omega t)$, the magnetic-dipole $H_{MD} = \boldsymbol{x} \cdot \boldsymbol{E}(\omega t)\boldsymbol{p} \cdot \hat{\boldsymbol{k}}/c$, the relativistic kinetic energy correction $H_{RK} = -\boldsymbol{p}^4/(8c^2)$, and finally $H_I = (\boldsymbol{x} \cdot \boldsymbol{E}(\omega t))^2/(2c^2)$. For the electron's under-the-barrier dynamics the relative strengths of the various terms of the Hamiltonian (3.2) are $H_{ED}/H_0 \sim 1$, $H_{MD}/H_0 \sim (\kappa/c)^2$, $H_{RK}/H_0 \sim (\kappa/c)^2$, and $H_I/H_0 \sim (\kappa/c)^2$ for typical displacements $\boldsymbol{x} \cdot \boldsymbol{E} \sim \kappa^2$ along the polarization direction.

3.3. Gauge invariance of the tunneling barrier

Tunneling is, by definition, the penetration of a potential barrier by a particle which is classically forbidden. The classical forbidden region is the domain where the potential barrier exceeds the energy of the incoming particle. Hence, the electron dynamics during ionization can be described as tunneling through a potential barrier if the total energy of the electron is conserved. In other words, the tunneling picture of any process becomes legitimate for constant fields only. Then there exists a well-defined gauge invariant energy operator which can reveal the tunneling barrier unambiguously as we have introduced in the previous chapter (2.2.1). Thus, for ionization in a laser field we have to identify the quasistatic limit such that the tunneling picture becomes applicable.

The tunnel-ionization regime in a laser field is determined by the Keldysh parameter $\gamma \ll 1$. It defines the so-called tunneling formation time $\tau_K = \gamma/\omega$, which may be interpreted as the time that a classical free electron would need to cover the length $l \sim I_p/E_0$ of the tunneling barrier at the characteristic velocity of the bound electron κ. The tunneling regime $\gamma \ll 1$ corresponds to situations when the formation time of the ionization process is much smaller than the laser period. Consequently, the electromagnetic field can be treated as quasistatic during the tunneling ionization

process and the electron energy is approximately conserved. Therefore, the gauge-independent operator for the total energy $\hat{\varepsilon}$ in a quasistatic electromagnetic field can be defined and from the latter the gauge-independent potential energy can be deduced, which in the case of tunnel-ionization constitutes the gauge-independent tunneling barrier. Therefore, Eq. (2.25) defines the gauge independent tunneling barrier in the tunnel-ionization regime. In the long wavelength approximation it yields

$$V_{\text{barrier}} = \boldsymbol{x} \cdot \boldsymbol{E}(t_0) + V(\boldsymbol{x}) \,, \tag{3.3}$$

where t_0 is the moment of ionization and $V(\boldsymbol{x})$ is the binding potential.

As an illustration of the gauge independence of the tunneling barrier, let us compare two fundamental gauges used in strong field physics to describe nonrelativistic ionization. In the length gauge where $\phi = -\boldsymbol{x} \cdot \boldsymbol{E}_0$, $\boldsymbol{A} = 0$, the nonrelativistic Hamiltonian for a constant uniform electric field is given by

$$H = \frac{\boldsymbol{p}^2}{2} + \boldsymbol{x} \cdot \boldsymbol{E}_0 + V(\boldsymbol{x}) \,. \tag{3.4}$$

Here, the Hamiltonian coincides with the physical energy operator. In the velocity gauge, however, where $\boldsymbol{A} = -c\boldsymbol{E}_0 t$, $\phi = 0$, the same dynamics is governed by the Hamiltonian

$$H = \frac{(\boldsymbol{p} - \boldsymbol{E}_0 t)^2}{2} + V(\boldsymbol{x}) \,. \tag{3.5}$$

In Eq. (3.5) it seems as if there is no potential barrier. However, the energy operator

$$\hat{\varepsilon} = \frac{(\boldsymbol{p} - \boldsymbol{E}_0 t)^2}{2} + \boldsymbol{x} \cdot \boldsymbol{E}_0 + V(\boldsymbol{x}) \tag{3.6}$$

reveals the tunneling barrier $\boldsymbol{x} \cdot \boldsymbol{E}_0 + V(\boldsymbol{x})$. Thus, for arbitrary time independent (quasistatic) electromagnetic fields, the gauge-independent tunneling barrier can be defined without any ambiguity. The tunneling barrier can be generalized into the relativistic regime straightforwardly by Eq. (2.27).

In the nonrelativistic regime, the Hamiltonian which coincides with the total energy operator is the length gauge. One possible generalization of the length gauge into the relativistic regime is the Göppert-Mayer gauge

$$A^\mu = -\boldsymbol{x} \cdot \boldsymbol{E}(\eta)(1, \hat{\boldsymbol{k}}), \tag{3.7}$$

Taking into account that the dipole approximation for the laser field can be applied inside the tunneling barrier, the Hamiltonian which coincides with the total relativistic energy operator in the Göppert-Mayer gauge reads

$$H = \hat{\varepsilon} = c\boldsymbol{\alpha} \cdot \left(\boldsymbol{p} - \hat{\boldsymbol{k}} \frac{\boldsymbol{x} \cdot \boldsymbol{E}(\eta_0)}{c} \right) + \boldsymbol{x} \cdot \boldsymbol{E}(\eta_0) + V(\boldsymbol{x}), \tag{3.8}$$

where η_0 is the laser phase at the moment of ionization.

The tunneling barrier results from an interpretation of the individual mathematical terms of the quasistatic energy operator (3.8). It has, however, also a physical

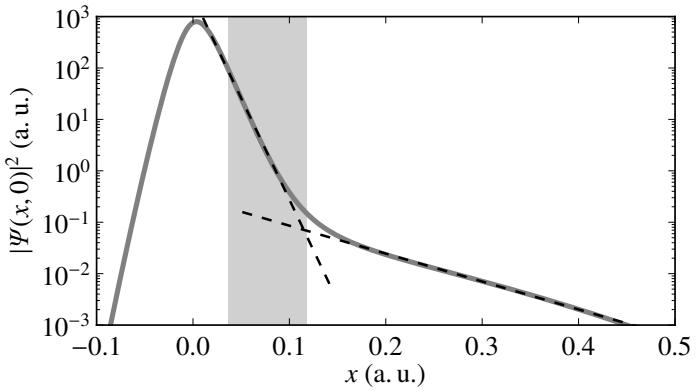

Figure 3.1. – The electron density (solid line) along the laser polarization direction at the instant of maximal field strength at the atomic core. The shaded area represents the classical forbidden area, gray dashed lines are exponential fits on the wave function density. The electron's wave function $\psi(x, z)$ is obtained by solving the two-dimensional Dirac equation for an electron in a soft-core potential interacting with an external laser pulse and the laser parameters are the same as in [31].

significance as it can be also confirmed by an ab initio numerical simulation of the tunneling process in a highly charged ion in a laser field of relativistic intensities based on the Dirac equation [31, 45, 85]. Fig. 3.1 shows the gauge-independent electron density along the laser's polarization direction at the instant of maximal field strength at the atomic core. The electron density can be divided in two parts that are characterized by two different decay rates. The switchover region includes the tunneling exit that is defined by the tunneling barrier. The decay of the density under the barrier is related to damping due to tunneling, i. e., approximately $\exp(-\kappa x)$, whereas outside the barrier it is dominated by transversal spreading. As the change of slopes occurs close to the tunneling exit the tunneling barrier is real and physical and not just a result of an interpretation in a particular gauge.

3.4. Intuitive picture for the tunnel-ionization process

Having identified the gauge invariant tunneling barrier, we elaborate in this section on the intuitive picture for the tunnel-ionization process in the relativistic regime. For the reminder of the section we choose our coordinate system such that the laser's electric field component $\boldsymbol{E}_0$ is along the x direction, the laser's magnetic component $\boldsymbol{B}_0$ is along the y direction and the laser propagates along the z direction. Since we work in the quasistatic regime, the Hamiltonian in the Göppert-Mayer gauge is used, as it coincides with the energy operator. In the nonrelativistic limit the latter is equal to the length gauge Schrödinger Hamiltonian.

3.4.1. Nonrelativistic case

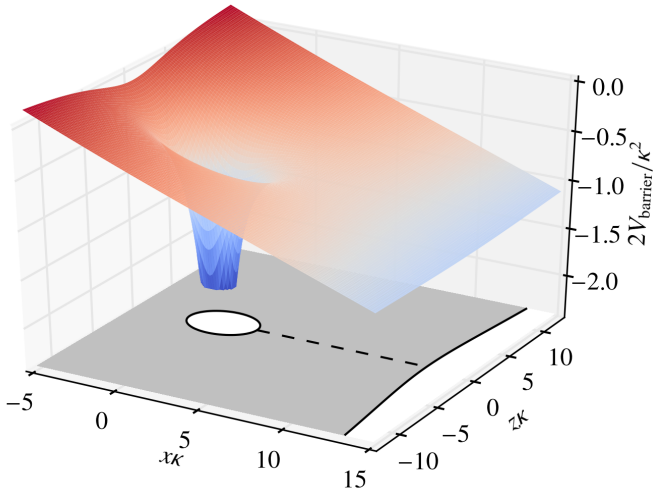

Figure 3.2. – The potential barrier V_{barrier} for quasistatic tunnel-ionization. The electric field $E(t_0) = -\kappa^3/30$ is along the x direction. The most probable tunneling path is indicated by the black dashed line.

In the nonrelativistic limit the intuitive picture for tunnel-ionization is well-known. In this picture the magnetic field and nondipole effects can be neglected, and the Hamiltonian reads

$$H = \frac{\boldsymbol{p}^2}{2} + x\,E(t_0) - \frac{\kappa}{r}, \tag{3.9}$$

with $r = \sqrt{x^2 + y^2 + z^2}$. Introducing the potential

$$V_{\text{barrier}}(\boldsymbol{x}) = x\,E(t_0) - \frac{\kappa}{r}, \tag{3.10}$$

one can define the classical forbidden region. The tunneling probability increases with decreasing width of the barrier. Thus, the most probable tunneling path is concentrated along the electric field direction as indicated by the dashed line in Fig. 3.2. Therefore, it is justified to restrict the analysis of the tunneling dynamics along the laser's polarization direction[1].

[1] The one-dimensional motion along the laser's electric field during tunnel-ionization can also be justified from the following estimation. The role of different forces can be evaluated by their contribution to the action, which can be estimated by an order of magnitude as $S \sim \varepsilon\tau$, where ε is the typical energy and τ is the typical time of an acting force. The contribution from the laser's electric field is $S_L \sim \tau_K x_e E_0 \sim \kappa^3/E_0 = E_a/E_0$, with the typical distance on which the laser's electric field acts on the tunneling electron $x_e \sim \kappa^2/E_0$ (the barrier length) and the Keldysh time τ_K. The contribution from the Coulomb potential can be separated into two parts. The longitudinal Coulomb force contribution is of the order of $S_c^{\parallel} \sim (\kappa/x_c)\tau_c \sim 1$, with the typical time τ_c and coordinate $x_c \sim \kappa\tau_c$, where the Coulomb force makes the main contribution on the electron. The transverse Coulomb force contribution can be estimated via $S_c^{\perp} \sim F_c^{\perp} z_c \tau_c \sim z_c^2/x_c^2 \sim \sqrt{E_0/E_a}$, where the transverse Coulomb force is $F_c^{\perp} \sim \kappa z_c/x_c^3$, the typical longitudinal coordinate is derived equating the laser and Coulomb forces $\kappa/x_c^2 = E_0$, and the typical transverse coordinate is estimated from $\kappa z_c^2 \sim x_c$. Therefore, the longitudinal contribution of the Coulomb potential into the dynamics represents the leading order correction to the zero-range potential case, while the transversal effect of the Coulomb potential is an higher order correction in the tunneling regime where E_0/κ^3 is small and will be neglected.

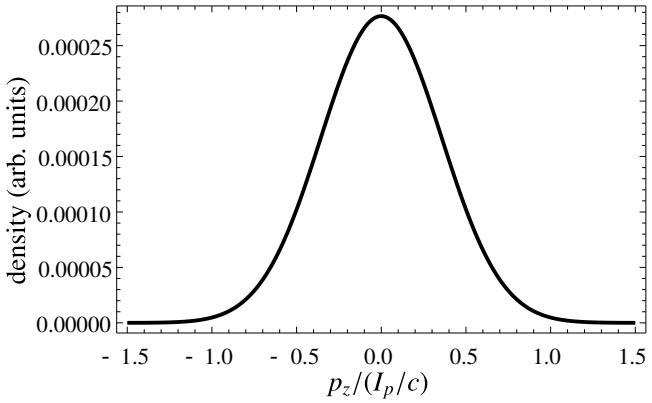

Figure 3.3. – The nonrelativistic tunneling probability versus the momentum along z direction. The maximum tunneling probability occurs at $p_z = 0$. The applied parameters are $E(t_0) = -\kappa^3/30$ and $\kappa = 90$. Without loss of generality, $p_y = 0$ was chosen.

In this one-dimensional picture the barrier for tunnel-ionization is

$$V_{\text{barrier}} = xE(t_0) - \frac{\kappa}{|x|}\,. \tag{3.11}$$

The momentum components p_y and p_z along the y and the z direction are conserved and tunneling along the x direction is governed by the energy

$$\varepsilon_x = -I_p - \frac{p_y^2}{2} - \frac{p_z^2}{2}\,. \tag{3.12}$$

The wave function of the electron and the corresponding transition probability can be derived within the Wentzel-Kramers-Brillouin (WKB) approximation [70, 86]. The zeroth order WKB wave function is given by

$$\psi \propto \exp\left(iS_{\text{cl}}\right) \tag{3.13}$$

with the classical action (Hamilton's principle function [87])

$$S_{\text{cl}} = -\varepsilon_x t + \int^x p_x(x')\,dx' \tag{3.14}$$

and the momentum's x component

$$p_x(x) = \sqrt{2(\varepsilon_x - V_{\text{barrier}})}\,. \tag{3.15}$$

The WKB tunneling probability follows as

$$|T|^2 \propto \exp\left(-2\int_{x_0}^{x_e} dx\,|p_x(x)|\right), \tag{3.16}$$

where x_0 and x_e are the entry point and exit point of the barrier such that $p(x_0) = p(x_e) = 0$, respectively. The dependence of the tunneling probability on the momentum p_z is shown in Fig. 3.3. The tunneling probability is maximal for $p_z = 0$, because

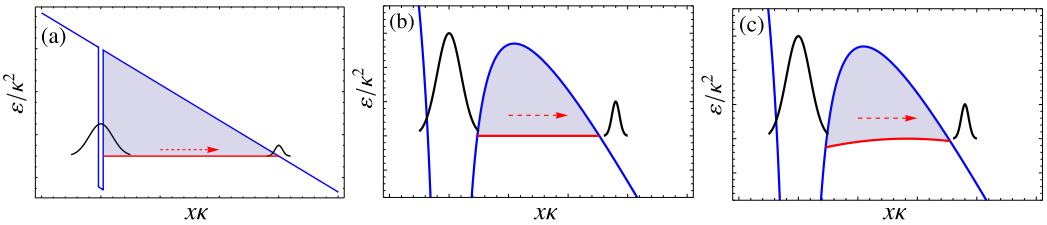

Figure 3.4. – Schematic picture of nonrelativistic (a) and (b) and relativistic (c) tunneling from a bound state into the continuum: (a) the atomic potential is aproximated by a zero-range potential; (b) and (c) the Coulomb potential case. The potential barrier (solid, blue) and the energy levels (dashed, red) for $p_z = 0$ (in the nonrelativistic cases) and for the most probable transversal momentum p_z (relativistic case) are plotted against the longitudinal tunneling coordinate x. The shaded area can be interpreted as a measure for the tunneling probability. The electron wave packet is indicated in black.

the energy level (3.12) decreases with increasing p_z^2. From this it follows that the exit coordinate increases with increasing p_z.

In summary, nonrelativistic tunneling from an atomic potential can be visualized by a one-dimensional picture given in Fig. 3.4(a) and (b). The area between the barrier and the energy level represents a measure for the probability of the process: The larger the area the less likely the ionization.

3.4.2. Relativistic case

In the relativistic regime, the largest correction to the nonrelativistic Hamiltonian comes from the magnetic dipole term. Let us consider the role of the magnetic dipole interaction in the laser field for the tunneling picture. The corresponding Hamiltonian which coincides with the energy operator reads

$$H = \frac{1}{2}(\boldsymbol{p} - xE(t_0)\hat{\boldsymbol{z}}/c)^2 + xE(t_0) - \frac{\kappa}{r}\,. \tag{3.17}$$

Similar to the nonrelativistic case, an approximate one-dimensional description is valid for the most probable tunneling path along the electric field direction. Restricting the dynamics along the electric field direction and neglecting the dependence of the ionic core's potential on the transverse coordinate, we have $p_{y,z} = \text{const}$ and the momentum along the polarization direction is given by Eq. (3.15) with the barrier (3.11), which is the same as in the nonrelativistic case. The energy, however, is modified by the magnetic dipole term

$$\varepsilon_x = -I_p - \frac{p_y^2}{2} - \frac{(p_z - xE(t_0)/c)^2}{2}\,. \tag{3.18}$$

The energy level (3.18) depends on the x coordinate. This is because the electron's kinetic momentum along the laser's propagation direction $q_z(x) \equiv p_z - xE(t_0)/c$

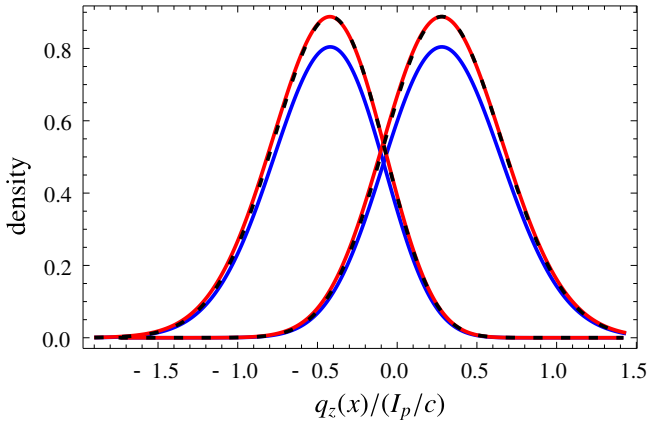

Figure 3.5. – Tunneling probability vs. the kinetic momentum along the laser's propagation direction at the tunnel entry (lines with peak on the left) and tunnel exit (lines with peak on the right). Results for calculations including magnetic dipole correction are indicated in blue while for the red lines also the leading relativistic correction to the kinetic energy are taken into account. The dashed-black lines correspond to a fully relativistic calculation, which are very close to the ones including leading relativistic corrections to the kinetic energy. The densities are normalized to the maximum density in the nonrelativistic case. A similar comparison was made in [31] for the case of a zero-range potential via SFA.

changes during tunneling due to the presence of the vector potential (magnetic field). As a consequence, the tunneling probability in the relativistic regime is maximal at some non-zero canonical momentum p_z in the laser's propagation direction. For instance, the kinetic momentum $q_z(x)$ with maximal tunneling probability at the tunneling entry is $q_z(x_0) \approx -0.42 I_p/c$, whereas at the exit it is $q_z(x_e) \approx 0.28 I_p/c$ for the Coulomb potential, see Fig. 3.5. During the under-the-barrier motion the electron acquires a momentum kick into the laser's propagation direction due to the Lorentz force, which can be estimated as

$$\Delta p_z \sim x_e E_0/c \sim I_p/c, \tag{3.19}$$

with the barrier length $x_e \sim I_p/E_0$. Thus, the tunneling can be visualized by a one-dimensional picture given in Fig. 3.4(c) when we take into account the magnetic dipole term. The area between the barrier and the position dependent energy level is larger than in the nonrelativistic case due to the non-vanishing transversal kinetic energy, indicating the reduced tunneling probability in the description of the leading relativistic effect.

The WKB analysis can be carried out also in a fully relativistic way. Taking into account the relativistic energy-momentum dispersion relation, one obtains for the momentum and the ionization energy along the polarization direction

$$\varepsilon_x = \sqrt{p_x^2 c^2 + c^4} + V_{\text{barrier}} - c^2\,, \tag{3.20}$$

$$p_x(x) = \sqrt{\left(\frac{c^2 - I_p - V_{\text{barrier}}}{c}\right)^2 - c^2 - p_y^2 - \left(p_z - \frac{xE(t_0)}{c}\right)^2} \tag{3.21}$$

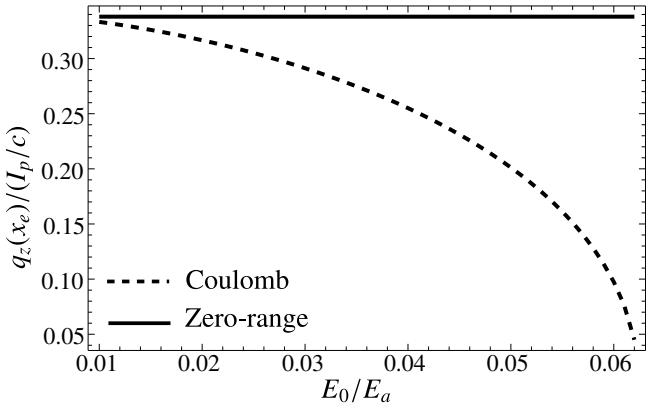

Figure 3.6. – The kinetic momentum shift at the tunnel exit $q_z(x_e)$ versus the barrier suppression parameter E_0/E_a for an electron bound by a Coulomb potential (dashed) and a zero-range atomic potential (solid).

which determines the fully relativistic tunneling probability via Eq. (3.16). The latter is shown in Fig. 3.5. For comparison it shows the calculation using the magnetic dipole correction, and the calculation with the leading relativistic kinetic energy correction $-\hat{p}_x^4/8c^2$[2].

As demonstrated in Fig. 3.5 the shift of the kinetic momentum along the laser's propagation direction that maximizes the WKB tunneling probability is determined mainly by the magnetic dipole correction to the Hamiltonian. This correction also decreases the tunneling probability, since the Lorentz force due to the laser's transversal magnetic field transfers energy from the tunneling direction into the perpendicular direction hindering tunneling. Taking into account further relativistic effects does not change the behavior qualitatively but increases the tunneling probability. This can be understood intuitively by noticing that in the reference frame of the relativistic electron the length of the barrier is contracted and in this way enhancing the tunneling probability. The mass correction term is more important in the zero-range-potential case than in the Coulomb-potential one, since the typical longitudinal velocities are smaller in the latter case. Furthermore, Fig. 3.5 indicates that the calculation including only the leading relativistic kinetic energy correction $O(1/c^2)$ reproduces the fully-relativistic approach satisfactorily. Thus, the magnetic dipole and the leading order mass shift are the only relevant relativistic corrections.

The value of the kinetic momentum shift at tunnel exit $q_z(x_e)$ varies significantly with respect to the barrier suppression parameter E_0/E_a in the case of a Coulomb potential of the ionic core, as shown in Fig. 3.6, while it does not depend on the laser field in the case of zero-range atomic potential. The main reason for the decreased momentum shift in the Coulomb potential case is that the length of the Coulomb-potential barrier is reduced approximately by a factor $(1 - 8E_0/E_a)$ compared to the barrier length of the zero-range potential. According to Eq. (3.19), this barrier length reduction leads to smaller momentum kick due to the magnetic field.

In order to verify the above results, we compare the prediction of the WKB

[2]The typical value of p_z is already of order of $1/c$ and the $-\hat{p}_z^4/8c^2$ term is neglected as an higher order term in the $1/c$ expansion.

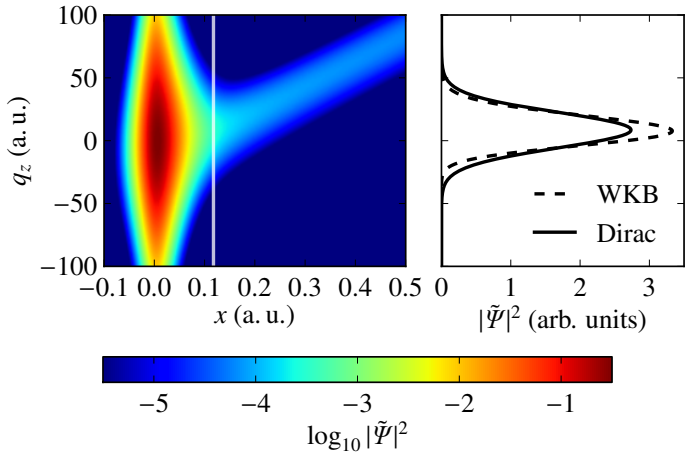

Figure 3.7. – Electronic density in the mixed space of position x and kinetic momentum q_z at the moment of maximal field strength at the atomic core (left panel). The electron's wave function has been obtained by simulating tunnel-ionization from a two-dimensional soft-core potential by solving the time-dependent Dirac equation with all numerical parameters as in Fig. 3.1. The right panel shows the normalized kinetic momentum distribution of the tunneled electron at the tunnel exit (indicated by the white line in the left panel) as obtained by solving the Dirac equation and by using the WKB approximation.

approximation with the results obtained by an *ab initio* numerical calculation solving the time-dependent Dirac equation [45, 85]. For this purpose tunnel-ionization from a two-dimensional soft-core potential was simulated yielding the time-dependent real space wave function $\psi(x, z, t)$. A transformation into a mixed representation of position x and kinetic momentum q_z via

$$\tilde{\psi}(x, q_z, t) = \frac{1}{\sqrt{2\pi}} \int \psi(x, z, t) e^{-iz(q_z - A_z/c)}\, dz \tag{3.22}$$

allows us to determine the kinetic momentum in z direction as a function of the x coordinate and in this way at the tunnel exit $x = x_e$, see Fig. 3.7. Both, the solution of the fully relativistic Dirac equation and the WKB approximation predict a momentum distribution with a maximum shifted away from zero. The momentum shifts are in a good agreement.

3.5. Tunnel-ionization with a zero-range potential model

The intuitive considerations of the previous section about relativistic under-the-barrier motion during tunnel-ionization led us to the conclusion that relativistic tunneling induces a momentum kick along the laser's propagation direction. The aim of this section is to prove this conclusion by a rigorous calculation based on SFA, to show

how this momentum shift arises during the under-the-barrier motion, and to find out how this relativistic signature is reflected in the electron momentum distribution in far distance at the detector.

The SFA is based on an S-matrix formalism, see Sec. 4.2. The ionization is described by the Hamiltonian

$$H = H_0 + H_I(t)\,, \tag{3.23}$$

where H_0 is the field-free atomic Hamiltonian including the atomic potential $V(\boldsymbol{x})$ and $H_I(t)$ denotes the Hamiltonian of the laser-atom interaction. Initially, at time $t \to -\infty$, the electron is in the bound state $|\psi(-\infty)\rangle = |\phi_0\rangle$. In SFA the influence of the atomic core potential on the free electron and the influence of the laser field on the bound state are neglected. This allows us to express the time evolution of the state vector in the form [80]

$$|\psi(t)\rangle = -i \int_{-\infty}^{t} dt'\; U_V(t,t') H_I(t')\,|\phi_0(t')\rangle\;, \tag{3.24}$$

where $U_V(t,t')$ is the Volkov propagator which satisfies

$$i\frac{\partial U_V(t,t')}{\partial t} = H_V(t) U_V(t,t') \tag{3.25}$$

with the Volkov Hamiltonian $H_V = H - V(\boldsymbol{x})$. The SFA wave function in momentum space of the final state reads

$$\langle \boldsymbol{p}|\psi\rangle = -i \int_{-\infty}^{\infty} dt'\; \langle \psi_V(t')|H_I(t')|\phi_0(t')\rangle\;, \tag{3.26}$$

where $|\psi_V(t)\rangle$ denotes a Volkov state [88]. The ionized part of the wave function in momentum space in Eq. (3.26) can be expressed also in the form [80]

$$\langle \boldsymbol{p}|\psi\rangle = -i \int_{-\infty}^{\infty} dt'\; \langle \psi_V(t')|\,V(\boldsymbol{x})\,|\phi_0(t')\rangle\;. \tag{3.27}$$

As the SFA neglects the effect of the atomic potential on the final state, the SFA gives an accurate prediction when the atomic potential is short ranged. For this reason, we will model tunnel-ionization with a zero-range potential in the following. The nonrelativistic tunneling scheme for this case is visulized in Fig. 3.4(a). The barrier has a triangular shape which simplifies the analytical treatment of the tunneling dynamics.

3.5.1. Nonrelativistic case

Let us start our analysis with the nonrelativistic consideration when the Hamiltonian for an atom in a laser field is given by Eq. (3.23) with

$$H_0 = \frac{p^2}{2} + V^{(0)}(\boldsymbol{x})\,, \tag{3.28}$$

$$H_I = \boldsymbol{x}\cdot\boldsymbol{E}(t)\,, \tag{3.29}$$

where $V^{(0)}(\boldsymbol{x})$ is the zero-range atomic potential. In SFA the ionized part of the wave function far away after the laser field has been turned off reads [89]

$$\langle \boldsymbol{p}|\psi\rangle = -i\mathcal{N}\int_{-\infty}^{\infty} dt\, e^{-i\tilde{S}(\boldsymbol{p},t)}\,, \tag{3.30}$$

where

$$\tilde{S}(\boldsymbol{p},t) = -\kappa^2 t/2 - \int^t dt'\, \boldsymbol{q}^2/2 \tag{3.31}$$

is the contracted action, $\boldsymbol{q} = \boldsymbol{p} + \boldsymbol{A}/c$ is the kinetic momentum, $\boldsymbol{A} = -c\int^t \boldsymbol{E}\, dt'$, $\mathcal{N} \equiv \langle \boldsymbol{q}|\, V^{(0)}\, |\phi^{(0)}\rangle = \text{const}$, and $|\phi^{(0)}\rangle\, e^{i\kappa^2 t/2}$ is the bound state of the zero-range potential. The time integral in Eq. (3.30) can be calculated via the saddle point approximation (SPA). The saddle point equation

$$\dot{\tilde{S}}(\boldsymbol{p},t_s) = q(t_s)^2 + \kappa^2 = 0 \tag{3.32}$$

yields the kinetic momentum $q(t_s) = i\kappa$ at the saddle point time t_s. Then, the wave function in momentum space reads in the quasi-static limit

$$\langle \boldsymbol{p}|\psi\rangle = -i\mathcal{N}\sqrt{\frac{2\pi}{|E(t_s)|\sqrt{p_\perp^2+\kappa^2}}}\exp\left[-\frac{(p_\perp^2+\kappa^2)^{3/2}}{3|E(t_s)|}\right] \tag{3.33}$$

for the vector potential $\boldsymbol{A} = cE_0\sin(\omega t)/\omega\hat{\boldsymbol{x}}$ and with $|E(t_s)| = E_0\sqrt{1-(p_x/(E_0/\omega))^2}$ and $p_\perp = \sqrt{p_y^2+p_z^2}$. From expression (3.33) it follows that the density of the ionized wave function is maximal at $p_\perp = 0$ for any value of p_x. The coordinate space wave function

$$\langle \boldsymbol{x}|\psi\rangle = -i\frac{\mathcal{N}}{(2\pi)^{3/2}}\int_{-\infty}^{\infty} dt \int d^3p\, \exp\left[i\boldsymbol{x}\cdot\boldsymbol{p} - i\tilde{S}(\boldsymbol{p},t)\right] \tag{3.34}$$

is obtained by a Fourier transform of Eq. (3.30). From the SPA it follows that the main contribution to the integral over $\boldsymbol{p}$ in Eq. (3.34) originates from momenta near the momentum which fulfills the saddle point condition $\boldsymbol{x} - \partial_{\boldsymbol{p}}\tilde{S}(\boldsymbol{p},t) = 0$. The latter defines the trajectories $\boldsymbol{x} = \boldsymbol{x}(\boldsymbol{p},t)$ which contribute to the transition probability with amplitudes depending on $\boldsymbol{p}$. For the most probable final momentum $\boldsymbol{p}_0 = 0$, the trajectory which starts at the tunneling entry at time t_s is given by

$$\boldsymbol{x}(t) = \partial_{\boldsymbol{p}}\tilde{S}(\boldsymbol{p}_0,t) = \int_{t_s}^{t} dt'\,\frac{\boldsymbol{A}(t')}{c}\,. \tag{3.35}$$

The line integral in Eq. (3.35) is along a path connecting the complex time t_s with the real time t. The complex saddle point time t_s can be determined by solving $q(t_s) = i\kappa$ for t_s. The corresponding kinetic momentum is

$$\boldsymbol{q}(t) = \frac{\boldsymbol{A}(t)}{c}\,. \tag{3.36}$$

In Fig. 3.8 the complex trajectory (3.35) and the complex kinetic momentum (3.36) along the tunneling direction are shown. The spatial coordinate is real under the barrier as well as behind the barrier, whereas the kinetic momentum is imaginary during tunneling and becomes real when leaving the barrier, which corresponds to the time $\mathrm{Re}[t_s]$. The tunneling exit coordinate is $x_e = x_e(\mathrm{Re}[t_s]) = I_p/E_0$ which is consistent with the intuitive tunneling picture. The momentum in the tunneling direction is $q(t_s) = i\kappa$ when tunneling starts, whereas it is $q(\mathrm{Re}[t_s]) = 0$ at the tunnel exit.

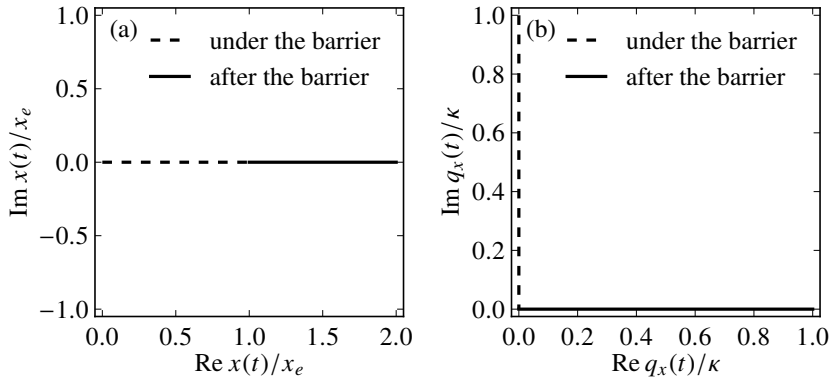

Figure 3.8. – Coordinate (a) and momentum (b) along the electric field direction of the complex SFA trajectory for tunnel-ionization from a zero-range potential. During the under-the-barrier motion the momentum is imaginary whereas the coordinate is real. Tunneling finishes when the kinetic momentum becomes real.

3.5.2. Relativistic case

Our fully relativistic consideration is based on the Dirac Hamiltonian with a zero-range atomic potential

$$H = c\boldsymbol{\alpha}\cdot(\boldsymbol{p}+\boldsymbol{A}/c) - \phi + \beta c^2 + V^{(0)}(\boldsymbol{x}) \tag{3.37}$$

where $\boldsymbol{\alpha}$ and β are standard Dirac matrices [90] and the Göppert-Mayer gauge (3.7) is employed. The ionized part of the momentum wave function in SFA yields

$$\langle \boldsymbol{p}|\psi\rangle = -i\int_{-\infty}^{\infty} dt \int d^3x\, \overline{\psi}_V(\boldsymbol{x},t)\gamma^0 V^{(0)}(\boldsymbol{x})\,\phi^{(0)}(\boldsymbol{x},t)\,. \tag{3.38}$$

Here $\phi^{(0)}(\boldsymbol{x},t) = e^{-i\varepsilon_0 t}\varphi^{(0)}(\boldsymbol{x})v^{(0)}{}_{\pm}$ is the ground state of the zero-range potential with the ground state spinor $v^{(0)}{}_{\pm}$ and $\varepsilon_0 = c^2 - I_p$; $\psi_V(\boldsymbol{x},t) = N_V u_{\pm} e^{iS}$ is the relativistic Volkov wave function in the Göppert-Mayer gauge for a free electron in a laser field, which is obtained from the Volkov wave function in the velocity gauge [88] with further gauge transformation via the gauge function $\chi = -\boldsymbol{x}\cdot\boldsymbol{A}/c$, $\boldsymbol{A}(\eta) \equiv -\dfrac{c}{\omega}\int^{\eta}\boldsymbol{E}(\eta')d\eta'$. Furthermore, N_V is the normalization constant,

$$S = -\varepsilon t + \left(\boldsymbol{p}+\frac{\boldsymbol{A}}{c}\right)\cdot\boldsymbol{x} - \frac{1}{c\Lambda}\int^{\eta}\left(\boldsymbol{p}\cdot\boldsymbol{A}+\frac{\boldsymbol{A}^2}{2c}\right)d\eta' \tag{3.39}$$

is the quasiclassical action and

$$u_{\pm} = \left(1+\frac{\omega}{2c^2\Lambda}(1+\boldsymbol{\alpha}\cdot\hat{\boldsymbol{k}})\boldsymbol{\alpha}\cdot\boldsymbol{A}\right)u_{0\pm} \tag{3.40}$$

with $\Lambda = p^\mu k_\mu = \omega(\varepsilon/c^2 - \boldsymbol{p}\cdot\hat{\boldsymbol{k}}/c)$, $p^\mu = (\varepsilon/c, \boldsymbol{p})$, and the free particle spinor $u_{0\pm}$. After averaging over the spin of the initial electron as well as over the spin of the ionized electron the wave function of the ionized electron reads

$$\langle \boldsymbol{p}|\psi\rangle = -i\frac{N_V(2\pi)^{3/2}}{2\omega}\int_{-\infty}^{\infty} d\eta\, e^{-i\bar{S}}\sum_{s,s'}\langle \boldsymbol{q_d}, s'|\, V^{(0)}(\boldsymbol{x})\,|\varphi_0, s\rangle\ . \tag{3.41}$$

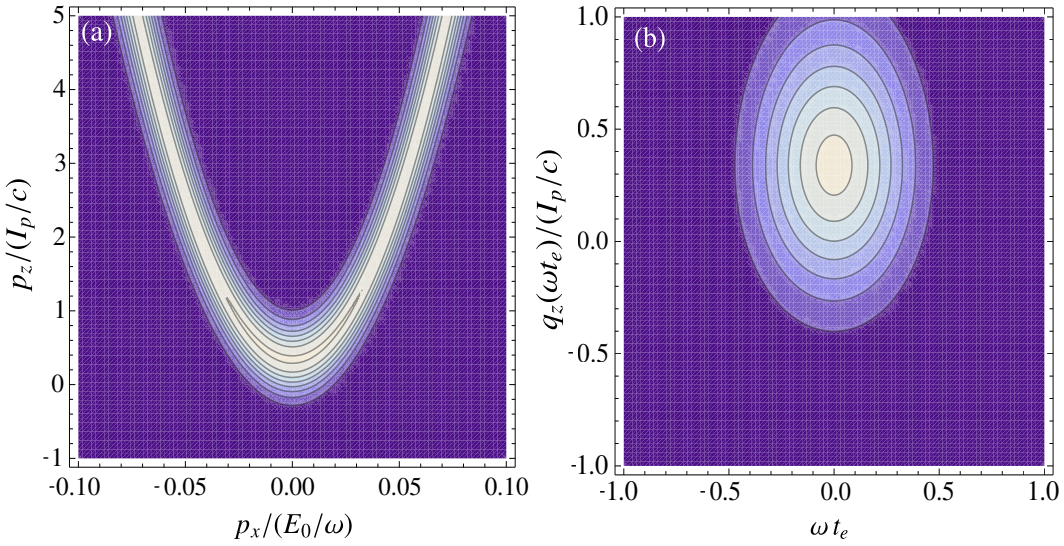

Figure 3.9. – The momentum distribution of the ionized electron: (a) in infinity at the detector; (b) at the tunnel exit, depending on the tunnel exit time t_e. The maximum tunneling probability occurs at $p_z = I_p/(3c)$. The applied parameters are $\kappa = 90$, $E_0/E_a = 1/30$ and $\omega = 10$.

Here, a coordinate transformation $(t, \boldsymbol{x}) \rightarrow (\eta, \boldsymbol{x})$ is employed and

$$\tilde{S} = \frac{1}{2\Lambda}\left(-\kappa^2\eta - \int^{\eta} \boldsymbol{q_d}^2 d\eta'\right) \tag{3.42}$$

is the contracted action with the field-dressed electron momentum in the laser field

$$\boldsymbol{q_d} = \boldsymbol{p} + \frac{\boldsymbol{A}}{c} - \frac{\hat{\boldsymbol{k}}(\varepsilon - \varepsilon_0)}{c}\,. \tag{3.43}$$

For a zero-range potential the inner product $\langle \boldsymbol{q_d}, s'| V^{(0)}(\boldsymbol{x}) |\varphi_0, s\rangle$ is only η dependent. Further, the η-integral in Eq. (3.41) can be calculated using SPA and the saddle point equation yields $\boldsymbol{q_d}^2(\eta_s) = -\kappa^2$ as in the nonrelativistic regime [45, 91]. Then, the wave function of the ionized electron in momentum space yields

$$\langle \boldsymbol{p}|\psi\rangle = -i\mathcal{N}(\eta_s)\sqrt{\frac{2\pi\Lambda}{\omega\,|E(\eta_s)|\,\sqrt{q_{d\perp}^2 + \kappa^2}}}\exp\left[-\frac{\omega(q_{d\perp}^2 + \kappa^2)^{3/2}}{3\Lambda\,|E(\eta_s)|}\right] \tag{3.44}$$

for the vector potential $\boldsymbol{A} = cE_0\sin(\eta)/\omega\hat{\boldsymbol{x}}$ with the laser's propagation vector $\hat{\boldsymbol{k}} = \hat{\boldsymbol{z}}$, where

$$|E(\eta_s)| = E_0\sqrt{1 - (p_x/(E_0/\omega))^2}\,, \tag{3.45}$$

$$q_{d\perp} = \sqrt{p_y^2 + \left(p_z - \frac{\varepsilon - \varepsilon_0}{c}\right)^2}\,, \tag{3.46}$$

$$\mathcal{N}(\eta_s) = \frac{N_V(2\pi)^{3/2}}{2\omega}\sum_{s,s'}\langle \boldsymbol{q_d}, s'| V^{(0)}(\boldsymbol{x}) |\varphi_0, s\rangle\,. \tag{3.47}$$

The relativistic momentum distribution of the ionized electron of Eq. (3.44) differs qualitatively from the nonrelativistic one. In the nonrelativistic case the maximum of

the distribution is at $p_\perp = 0$ for any p_x. In the relativistic case, however, the momentum distribution has a local maxima along the parabola which can be approximated as

$$p_z \approx \frac{I_p}{3c}\left(1 + \frac{I_p}{18c^2}\right) + \frac{p_x^2}{2c}\left(1 + \frac{I_p}{3c^2} + \frac{2I_p^2}{27c^4}\right) + O\left(\frac{I_p^2}{c^4}\right), \tag{3.48}$$

see Fig. 3.9(a). The global maximum of the tunneling probability is located at $p_z = I_p/(3c)$, while in the nonrelativistic case it is at $p_z = 0$. This shift of the maximum is connected with the first step of the ionization, the tunneling, whereas the parabolic wings are shaped in the second step, they are connected with the continuum dynamics. These wings are located around $p_z = U_p/c$ with ponderomotive potential $U_p = E_0^2/(4\omega^2)$.

The momentum distribution at the tunnel exit can be calculated via back propagation of the final momentum space wave function (3.44). Thus, the wave function at the tunnel exit is given by

$$\langle \boldsymbol{p}|\psi(t_e)\rangle = \int d^3p' \,\langle \boldsymbol{p}|\, U(t_e,t_f)\,|\boldsymbol{p}'\rangle\,\langle \boldsymbol{p}'|\psi(t_f)\rangle \approx \int d^3p' \,\langle \boldsymbol{p}|\, U_V(t_e,t_f)\,|\boldsymbol{p}'\rangle\,\langle \boldsymbol{p}'|\psi(t_f)\rangle \tag{3.49}$$

with the tunnel exit time $t_e = \mathrm{Re}[t_s]$ and final time t_f where the interaction is turned off, hence the Volkov wave function reduces to the free particle wave function. Because $\omega\,\hat{\boldsymbol{k}}\cdot\boldsymbol{x} \ll c$ holds at the tunnel exit, the exact Volkov propagator

$$\langle \boldsymbol{x}|\, U_V(t,t')\,|\boldsymbol{x}'\rangle = \int d^3p\; \psi_V(t,\boldsymbol{x})\psi_V^\dagger(t',\boldsymbol{x}') \tag{3.50}$$

can be simplified by expanding the phase dependent functions around ωt_e, which yields

$$U_V(t_e,t_f) = \int d^3p\, \exp\Big(i\varphi(t_e,t_f)\Big)\,|\boldsymbol{p_e}\rangle\,\langle \boldsymbol{p}| \tag{3.51}$$

with the exit momentum and the phase

$$\boldsymbol{p_e} = \boldsymbol{p} + \frac{\boldsymbol{A}(\omega t_e)}{c} + \hat{\boldsymbol{k}}\frac{\omega}{c^2\Lambda}(\boldsymbol{p} + \frac{\boldsymbol{A}(\omega t_e)}{2c})\cdot\boldsymbol{A}(\omega t_e)\,, \tag{3.52}$$

$$\varphi(t_e,t_f) = \varepsilon(t_f - t_e) + \frac{1}{c\Lambda}\int^{\omega t_e} d\eta\,\left(\boldsymbol{p} + \frac{\boldsymbol{A}(\eta)}{2c}\right)\cdot\boldsymbol{A}(\eta)\,, \tag{3.53}$$

respectively. As a result, the momentum space wave function at the tunnel exit t_e reads in terms of the final wave function $\langle \boldsymbol{p}'|\psi(t_f)\rangle$

$$\langle \boldsymbol{p}|\psi(t_e)\rangle = e^{i\varphi(t_e,t_f)}\,\langle \boldsymbol{p}'|\psi(t_f)\rangle \tag{3.54}$$

with

$$\boldsymbol{p}' = \left(-\frac{A_x(\omega t_e)}{c}, p_y, p_z + \frac{A_x(\omega t_e)^2\omega}{2c^3\Lambda}\right). \tag{3.55}$$

The transversal momentum distribution at the tunnel exit can be calculated via replacing the momentum in the wave function Eq. (3.44) with Eq. (3.55), which can be seen in Fig. 3.9(b). The comparison of Figs. 3.9(a) and (b) indicates that the relativistic shift of the peak of the transverse momentum distribution at the tunnel

exit $p_z = I_p/(3c)$ is maintained in the final momentum distribution. The parabola can for example be calculated from classical trajectories. The kinetic momentum at the exit is connected with the final momenta via

$$\begin{aligned} q_x(\eta_s) &= p_x + \frac{A(\eta_s)}{c} = 0\,, \\ q_z(\eta_s) &= p_z + \frac{\omega}{c^2\Lambda}\left(p_x A(\eta_s) + \frac{A(\eta_s)^2}{2c}\right) = \frac{I_p}{3c} \end{aligned} \tag{3.56}$$

and the relation

$$p_z = \frac{I_p}{3c} + \frac{\omega p_x^2}{2c\Lambda} \tag{3.57}$$

follows.

We investigate the trajectory of the electron and its momentum during the tunneling in the relativistic regime. The coordinate wave function can be obtained via a Fourier transform of momentum space wave function (3.41). Then, the stationary phase condition gives the quasiclassical trajectories at the most probable momentum given by Eq. (3.48). The results are plotted in Fig. 3.10. It shows that in the relativistic regime the most probable trajectory is the trajectory where the electron enters the barrier with the transversal momentum $-2I_p/(3c)$ and reaches the exit with $I_p/(3c)$. This is in accordance with our intuitive discussion in Sec. 3.4. For the most probable momentum, the trajectory starts at the real axis, obtains complex values during tunneling and has to return to the real axis after tunneling as shown in Fig. 3.10(a).

The shift of the electron's momentum distribution along the laser's propagation direction in the relativistic regime could be measurable by detecting the final momentum distribution of the ion [92]. The ionized electron acquires momentum along the laser's propagation direction in the laser field because of the absorbed momentum of laser photons. However, part of the momentum of laser photons is transferred to the ion. The energy conservation law provides a relationship between the number of absorbed photons n and the electron momentum p_e

$$n\omega - I_p + c^2 \approx \varepsilon_e\,, \tag{3.58}$$

where ω is the laser frequency, I_p the ionization potential and $\varepsilon_e = c\sqrt{p_e^2 + c^2}$ the energy of the electron. The kinetic energy of the ionic core can be neglected due to the large mass of the ion. Additionally, the momentum conservation law gives information on the sharing of the absorbed photon momentum between the ion and the photoelectron

$$\begin{pmatrix} n\omega/c \\ 0 \\ 0 \end{pmatrix} = \begin{pmatrix} p_{ez} + p_{0z} \\ p_{ex} + p_{0x} \\ p_{ey} + p_{0y} \end{pmatrix}. \tag{3.59}$$

In the nonrelativistic tunneling regime of ionization in the linearly polarized laser field, the photoelectron's most probable momentum is $p_e = 0$, when $n\omega = I_p$ and the ion carries out a momentum $p_{0z} = I_p/c$. In the relativistic regime of interaction the most probable value of the photoelectron's momentum is not vanishing but equals to

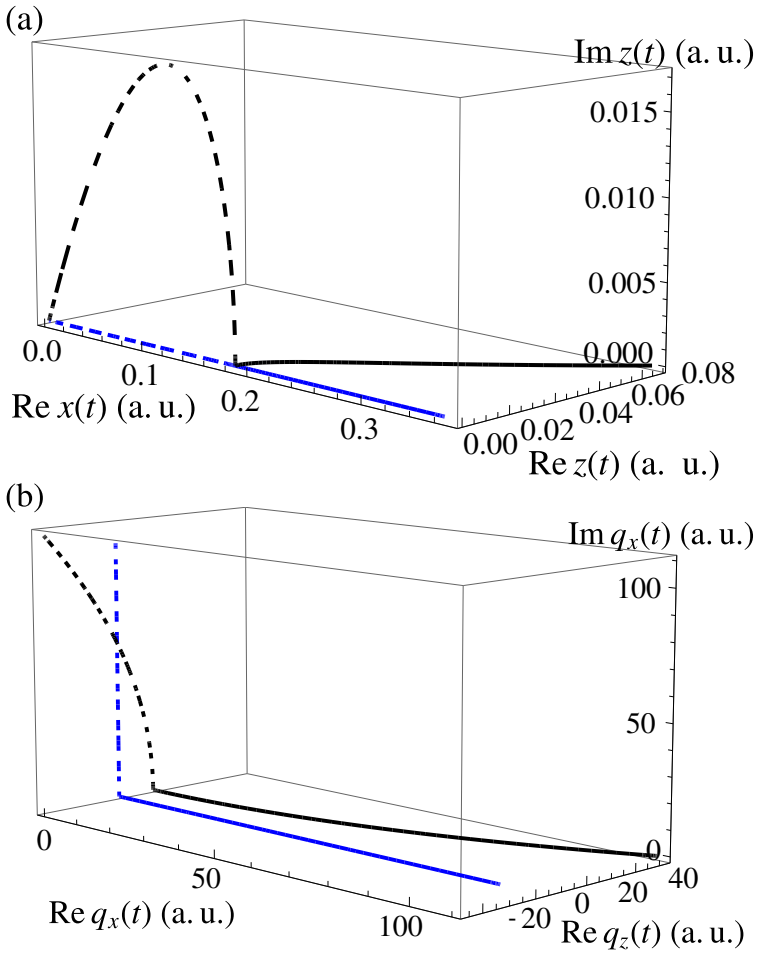

Figure 3.10. – Comparison of the nonrelativistic (blue) and relativistic (black) complex SFA trajectories: (a) coordinates and (b) momentum components. The dashed and the solid lines correspond to the under-the-barrier motion and the motion after the tunneling, respectively. In the relativistic regime, the trajectory enters the tunneling barrier at $(0, 0)$, it is complex under the barrier and becomes real again when it leaves the tunneling barrier. The trajectory enters the barrier with the transversal momentum $-2I_p/(3c)$ and leaves the barrier with $I_p/(3c)$. The applied parameters are $\kappa = 90$, $E_0/E_a = 1/30$.

$p_{ez} \approx I_p/3c$ in the case of linear polarization. In this case the momentum conservation will provide the ion momentum $p_{0z} \approx 2I_p/3c$. In [92, 93] the momentum sharing between ion and electron during tunnel-ionization in a strong circularly polarized laser field is investigated. Their result supports the simple-man model prediction. It is shown that the total momentum of the absorbed photons, that is I_p/c, is transferred to the ion and not to the ionized electron. The difference with respect to our result may be explained by the focal averaging as well as by the fact that our parameters are situated in the pure tunneling regime whereas the references deal with ionization at the transition to over-the-barrier ionization. The momentum shift of the ionized electrons at the detector that we describe is a genuine feature of the relativistic tunneling dynamics.

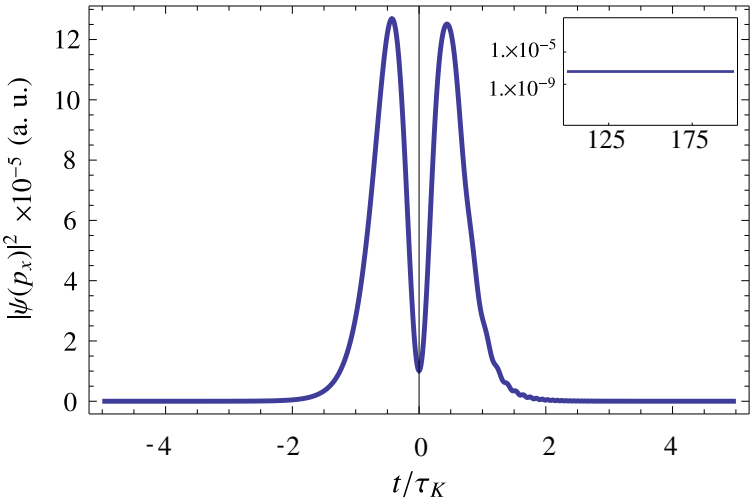

Figure 3.11. – The ionization momentum amplitude for $p_x = 0$ vs. the observation time t. The inset shows the momentum amplitude for large times, which coincides with the ionization amplitude. The applied parameters are $E_0/E_a = 1/30$ and $\kappa = 1$.

3.5.3. Tunneling formation time

The physical interpretation of the Keldysh time as the ionization formation time given in Sec. III B can be readily clarified within the SFA formalism. In the SFA, the momentum wave function in the case of a zero-range atomic potential at some intermediate time is given by

$$\langle p_x|\psi(t)\rangle = -i\int_{-\infty}^{t} dt' \exp[-i\tilde{S}(t,t')]\,\langle \boldsymbol{q}(t')|H_I(t')|\phi_0\rangle \ , \tag{3.60}$$

where $\langle \boldsymbol{q}(t')|H_I(t')|\phi_0\rangle$ is the pre-exponential factor that slowly varies with time and the quasiclassical action $\tilde{S}(t,t')$ is given either by Eq. (3.31) for the nonrelativistic case, or by Eq. (3.42) for the relativistic case.

A numerical integration of Eq. (3.60) for a monochromatic laser field in the nonrelativistic regime is shown on Fig. 3.11. The value of the momentum amplitude starts with zero at early times and then varies on a time scale that is of the order of the Keldysh time. Thus, the Keldysh time is the typical time scale for the formation of the moment components of the ionized wave function, or in short, the formation time of the ionization. For large times, the momentum amplitude stabilizes on some positive value, which can be identified as the ionization amplitude of the specific momentum component, see inset in Fig. 3.11. Considering nonrelativistic or relativistic ionization from a Coulomb potential will not change the qualitative behaviour of the time evolution of the ionization amplitude shown in Fig. 3.11.

3.6. Conclusion

We have carried out an investigation of the relativistic regime of tunnel-ionization with an emphasis on the role of the under-the-barrier dynamics. In the quasistatic limit, the potential barrier of relativistic tunneling can be defined in a gauge invariant manner by means of an analysis of the physical energy operator. In contrast to the nonrelativistic case, relativistic tunnel-ionization in the quasistatic limit is modeled as tunneling through a potential barrier in an additional magnetic field. Moreover, the latter problem is shown to reduce to one-dimensional tunneling with a coordinate dependent energy.

Later on, we have calculated the momentum distribution of the ionized electron wave packet at the tunnel exit using the SFA. We showed that the Lorentz force due to the magnetic field during the under-the-barrier motion induces a momentum shift of the electron in the laser's propagation direction.

4. Spin dynamics in tunnel-ionization

4.1. Introduction

In the previous chapter we have discussed the relativistic features of tunnel-ionization. However, we have neglected the spin dynamics and hence the spin features of tunnel-ionization. In the present chapter we investigate the spin effects in the tunneling regime as a further relativistic feature of tunnel-ionization. Thus, this chapter can be considered as a continuing chapter of the previous one. Although we have already used the techniques of strong field approximation (SFA) in the previous chapter, its formal development will be discussed in the present chapter.

The spin dynamics in electromagnetic waves and the spin resolved calculations of light matter interactions have attracted great interest in theoretical physics for a long time. Particularly, there are considerable works on laser assisted Mott [94–96] and Møller scattering [97], free electron motion in a strong laser field [98, 99] and the Kapitza-Dirac effect [100]. The spin resolved production rates have been calculated for the process of electron-position pair production in strong laser fields [101–103]. Spin effects have been shown in the relativistic laser-driven bound electron dynamics [104–107]. The spin dynamics in nonsequential double ionization of helium has been considered in [108, 109].

In the nonrelativistic as well as in the relativistic regimes, an analytical treatment of strong field ionization and hence of tunnel-ionization can be employed by using the SFA [50–53]. As a pioneering work on the spin effect of ionization, the spin asymmetries have been investigated in [110] using the standard technique of SFA. However, the standard SFA approximates the final state with the Volkov state via neglecting the Coulomb potential on the continuum state and it further neglects the laser field on the bound state dynamics. Although the former seems to be legitimate, the latter approximation may fail for the spin resolved calculation of ionization rates [111]. This standard method can be modified and improved via employing a different partition of the Hamiltonian within the SFA formalism [54, 55], which enables us to take into account the effect of the laser field on the bound state dynamics [111].

For the generic problem of spin dynamics in tunnel-ionization we investigate the spin asymmetries in relativistic tunneling ionization with standard SFA in different gauges. Furthermore, we compare the results of the standard SFA with the results

that we obtained within the framework of improved SFA. On this purposes, we first develop the SFA in terms of a different partitions of the Hamiltonian in Sec. 4.2. Later, in Sec. 4.3, the spin asymmetries for a circularly polarized laser field are investigated in the velocity gauge as well as in the length gauge with standard SFA. The results are obtained for the most interesting case where the quantization axis is aligned with the laser's propagation direction. Finally, in Sec. 4.4, the same calculations are repeated in the improved SFA which we call it dressed SFA.

Atomic units (a. u.) are used throughout this chapter and the results can be partly found in [89, 91, 111].

4.2. Strong field approximation (SFA)

The S-Matrix treatment for strong field ionization can be calculated using the strong field approximation (SFA). The S-Matrix element for transition from the initial state $|\psi_i(t_i)\rangle$ to the final state $|\psi_f(t_f)\rangle$ can be written as

$$S_{i\to f} = \lim_{\substack{t_f\to\infty \\ t_i\to-\infty}} \langle\psi_f(t_f)|\, U(t_f,t_i)\, |\psi_i(t_i)\rangle \tag{4.1}$$

where the evolution operator $U(t,t')$ is given by the differential equation

$$i\partial_t U(t,t') = H(t)U(t,t') \tag{4.2}$$

with the Hamiltonian $H(t)$ which governs the corresponding dynamics.

The Hamiltonian can be split up as

$$H = H_i(t) + V_i(t)\,, \tag{4.3}$$
$$= H_f(t) + V_f(t) \tag{4.4}$$

with certain initial and final partitions [54, 55], where the associated time evolution operators satisfy

$$i\partial_t U_{i,f}(t,t') = H_{i,f}(t)U_{i,f}(t,t')\,. \tag{4.5}$$

The time evolution operator (4.2), then, can be written for the initial partitions (4.3) as

$$U(t_f,t_i) = U_i(t_f,t_i) - i\int_{t_i}^{t_f} dt\, U(t_f,t)V_i(t)U_i(t,t_i)\,. \tag{4.6}$$

If the integral equation is solved iteratively as

$$U(t_f,t_i) = U_i(t_f,t_i) - i\int_{t_i}^{t_f} dt\, U_i(t_f,t)V_i(t)U_i(t,t_i) + \cdots \tag{4.7}$$

one ends up with the usual perturbation theory. Moreover, the time evolution operator can also be solved via the final partitions (4.4) as

$$U(t_f,t_i) = U_f(t_f,t_i) - i\int_{t_i}^{t_f} dt\, U(t_f,t)V_f(t)U_f(t,t_i) \tag{4.8}$$

whose iterative solution yields

$$U(t_f, t_i) = U_f(t_f, t_i) - i \int_{t_i}^{t_f} dt\, U_f(t_f, t) V_f(t) U_f(t, t_i) + \cdots . \tag{4.9}$$

In fact, one can further combine two different expansions via replacing the integrand $U(t_f, t)$ in Eq. (4.6) with the iterative solution (4.9). The result reads

$$\begin{aligned} U(t_f, t_i) = U_i(t_f, t_i) - i \int_{t_i}^{t_f} dt\, U_f(t_f, t) V_i(t) U_i(t, t_i) \\ + (-i)^2 \int_{t_i}^{t_f} dt \int_{t}^{t_f} dt'\, U_f(t_f, t') V_f(t') U_f(t', t) V_i(t) U_i(t, t_i) + \cdots \end{aligned} \tag{4.10}$$

The first integral in Eq. (4.10) is known as the strong field approximation for the time evolution operator. Then, the transition matrix in the SFA reads

$$M_{i\to f} = (S - 1)_{i\to f} = -i \int_{-\infty}^{\infty} dt\, \langle \psi_f(t)|\, V_i(t)\, |\psi_i(t)\rangle \tag{4.11}$$

where we have used

$$|\psi_i(t)\rangle = U_i(t, t_i)\, |\psi_i(t_i)\rangle\ , \tag{4.12}$$

$$|\psi_f(t)\rangle = U_f(t, t_f)\, |\psi_f(t_f)\rangle\ . \tag{4.13}$$

If we compare the result of the SFA (4.11) with the exact expression (4.6), it is seen that the main approximation of the SFA is to neglect the influence of the final potential $V_f(t)$ on the exact final state.

The transition matrix (4.11) can further be written as

$$M_{i\to f} = -i \int_{-\infty}^{\infty} dt\, \langle \psi_f(t)|\, H - H + V_i(t)\, |\psi_i(t)\rangle\ , \tag{4.14}$$

$$= -\int_{-\infty}^{\infty} dt\, \partial_t \langle \psi_f(t)|\psi_i(t)\rangle - i \int_{-\infty}^{\infty} dt\, \langle \psi_f(t)|\, V_f(t)\, |\psi_i(t)\rangle\ , \tag{4.15}$$

$$= -i \int_{-\infty}^{\infty} dt\, \langle \psi_f(t)|\, V_f(t)\, |\psi_i(t)\rangle\ , \tag{4.16}$$

where in the second line we have used

$$i\partial_t\, |\psi_{i,f}(t)\rangle = H_{i,f}(t)\, |\psi_{i,f}(t)\rangle \tag{4.17}$$

and in the last line we used the fact that the interaction vanishes at $t \to \pm\infty$. The result (4.16) can also be obtained via first plugging the iterative solution (4.7) into Eq. (4.8) and then taking the hermitian conjugate of the outcome.

In this chapter we investigate the spin dynamics in the tunneling regime $\gamma \ll 1$ in the standard SFA as well as in the modified SFA. The relativistic strong field ionization can be governed by the relativistic Hamiltonian

$$H = c\boldsymbol{\alpha} \cdot \boldsymbol{p} + c^2\beta + V_a(r) + \boldsymbol{\alpha} \cdot \boldsymbol{A} - \phi \tag{4.18}$$

with the binding Coulomb potential $V_a(r) = -\kappa/r$. The spin dynamics in the tunneling regime can be investigated via the probabilities of the spin-flip SF, the spin-flip asymmetry A and the ensemble averaged asymmetry parameter $\langle A \rangle$, which can be defined in terms of the differential ionization rate $|M_{i\to f}|^2$ as

$$SF = \frac{2|M_{+\to-}|^2}{T}, \tag{4.19}$$

$$A = \frac{|M_{+\to-}|^2 - |M_{-\to+}|^2}{T}, \tag{4.20}$$

$$\langle A \rangle = \frac{|M_{+\to+}|^2 + |M_{-\to+}|^2 - |M_{+\to-}|^2 - |M_{-\to-}|^2}{T} \tag{4.21}$$

with the total rate $T = |M_{+\to+}|^2 + |M_{-\to+}|^2 + |M_{+\to-}|^2 + |M_{-\to-}|^2$ [110], where $+(-)$ represents the spin-up (down) state.

Before concluding the derivation of the SFA, we should underline that the SFA cannot yield gauge invariant results. Although the perturbative expansion of the time evolution operator obeys the gauge invariance at each order, the strong field expansion breaks down the gauge symmetry in general.

4.3. Standard SFA

In the standard SFA which is also known as the Keldysh-Faisal-Reiss (KFR) theory [50–53], the full Hamiltonian (4.18) is partitioned as

$$H_i = c\boldsymbol{\alpha}\cdot\boldsymbol{p} + c^2\beta - \frac{\kappa}{r}, \quad V_i = \boldsymbol{\alpha}\cdot\boldsymbol{A} - \phi, \tag{4.22}$$

$$H_f = c\boldsymbol{\alpha}\cdot\boldsymbol{p} + c^2\beta + \boldsymbol{\alpha}\cdot\boldsymbol{A} - \phi, \quad V_f = -\frac{\kappa}{r}. \tag{4.23}$$

Here H_f and H_i correspond to the Volkov Hamiltonian and the usual Coulomb potential Hamiltonian, respectively. As a consequence, the SFA transition matrix becomes

$$M_{s\to s'} = -i\int_{-\infty}^{\infty} dt\ \langle \psi_V^{s'}(t)|\,\boldsymbol{\alpha}\cdot\boldsymbol{A}(t) - \phi(t)\,|\phi_0^s(t)\rangle \tag{4.24}$$

where $|\psi_V^{s'}(t)\rangle$ and $|\phi_0^s(t)\rangle$ are the Volkov state and the bound state, respectively. Inserting the resolution of identity, the above transition matrix in the position space reads

$$M_{s\to s'} = -i\int_{-\infty}^{\infty} dt \int d^3x\, \overline{\psi}_V^{s'}(\boldsymbol{x},t)\gamma^\mu A_\mu(t)\phi_0^s(\boldsymbol{x},t)\,. \tag{4.25}$$

Equivalently, using Eq. (4.16), the transition matrix could also be written as

$$M_{s\to s'} = i\kappa\int_{-\infty}^{\infty} dt \int d^3x\, \overline{\psi}_V^{s'}(\boldsymbol{x},t)\gamma^0\frac{1}{r}\phi_0^s(\boldsymbol{x},t)\,. \tag{4.26}$$

At this stage, it should be noted that the result is clearly gauge dependent because both the Volkov state and the interaction Hamiltonian depend on the choice of the

gauge. In the strong field literature, there are two common gauges that are used for the calculation of the transition amplitude; the length gauge (the Göppert-Mayer gauge in the existence of a magnetic field) and the velocity gauge. Hence, we will obtain the corresponding results in both gauges and we will compare them. It should be noted here that although the SFA generates gauge dependent results, the difference between the qualitative behavior of the results is not significant.

Furthermore, the standard SFA does not take into account the effect of the electromagnetic field on the bound state, which has a drastic consequence for the spin dynamics in tunnel-ionization as we will discuss now.

The Volkov wave function in the velocity gauge $A^\mu = (0, \boldsymbol{A}(\eta))$ with $\eta = k \cdot x$ can be written as

$$\psi_V^s(\boldsymbol{x}, t) = \sqrt{\frac{c^2}{\varepsilon}} \exp(iS) \left(1 - \frac{1}{2c\, k \cdot p} \not{k} \not{A}\right) v_s \,. \tag{4.27}$$

Here the classical action of a charge particle interacting with a plane wave reads

$$S = -p \cdot x + \frac{1}{c\, k \cdot p} \int^{\eta} d\eta' \left(p \cdot A + \frac{1}{2c} A^2\right) \tag{4.28}$$

and the free particle spinor is

$$v_\pm = \sqrt{\frac{\varepsilon + c^2}{2c^2}} \begin{pmatrix} \varsigma_\pm \\ \dfrac{c}{\varepsilon + c^2} \boldsymbol{p} \cdot \boldsymbol{\sigma}\, \varsigma_\pm \end{pmatrix} \tag{4.29}$$

with the two component nonrelativistic spinors $\varsigma_\pm$ [90]. The Volkov solution in the Göppert-Mayer gauge

$$A^\mu = -\frac{c}{\omega} \boldsymbol{x} \cdot \boldsymbol{E}\, k^\mu \tag{4.30}$$

can be obtained via the gauge function

$$\chi = -\boldsymbol{A} \cdot \boldsymbol{x} \,. \tag{4.31}$$

In our physical configuration we investigate tunnel-ionization of the ground state of a H-like ion. The ground state is given by

$$\phi_0^s(\boldsymbol{x}, t) = \frac{(2\kappa)^{\gamma+1/2}}{\sqrt{4\pi}} \sqrt{\frac{1+\gamma}{2\Gamma(1+2\gamma)}} \exp(-\kappa r - i\varepsilon_0 t)\, r^{\gamma-1} u_s \tag{4.32}$$

with the ground state spinor

$$u_\pm = \begin{pmatrix} \varsigma_\pm \\ \dfrac{ic(1-\gamma)}{\kappa} \hat{\boldsymbol{r}} \cdot \boldsymbol{\sigma}\, \varsigma_\pm \end{pmatrix} . \tag{4.33}$$

Here $\varepsilon_0 = c^2 - I_p$ is the ground state energy with the ionization potential $I_p = c^2(1-\gamma)$, $\gamma = \sqrt{1 - \kappa^2/c^2}$, and the charge of the ion κ [57].

After plugging the wave functions (4.27) and (4.32) into the transition matrix (4.16), we obtain

$$M_{s\to s'} = N\int_{-\infty}^{\infty} dt \int d^3x\, \exp\left(-iS - i\sigma\frac{\boldsymbol{A}\cdot\boldsymbol{x}}{c} + iI_p t - \kappa r\right) r^{\gamma-2} P_{s\to s'}\,, \tag{4.34}$$

where the constant N is given by

$$N = i\kappa\sqrt{\frac{c^2}{\varepsilon}}\frac{(2\kappa)^{\gamma+1/2}}{\sqrt{4\pi}}\sqrt{\frac{1+\gamma}{2\Gamma(1+2\gamma)}} \tag{4.35}$$

and the relevant spin transition matrix is

$$P_{s\to s'} = v^{\dagger}_{s'}\left(1 - \frac{1}{2c\,k\cdot p}\not{k}\not{A}\right)^{\dagger} u_s\,. \tag{4.36}$$

Furthermore, we have introduced the parameter σ in Eq. (4.34) in order to select the gauge at any step such that $\sigma = 0$ denotes the velocity gauge, while $\sigma = 1$ is for the length gauge.

If we employ the coordinate transformation $(t, \boldsymbol{x}) \to (\eta, \boldsymbol{x})$ and if we further define

$$\Phi(\eta) = \frac{\varepsilon_0 - \varepsilon}{\omega}\eta + \frac{1}{c\,k\cdot p}\int^{\eta} d\eta' \left(p\cdot A + \frac{1}{2c}A^2\right), \tag{4.37}$$

$$\boldsymbol{q}(\eta) = \boldsymbol{p} + \sigma\frac{\boldsymbol{A}(\eta)}{c} + \hat{\boldsymbol{k}}\frac{\varepsilon_0 - \varepsilon}{c}\,, \tag{4.38}$$

the transition matrix (4.34) yields

$$M_{s\to s'} = \frac{N}{\omega}\int_{-\infty}^{\infty} d\eta\, \exp\left(-i\Phi(\eta)\right)\int d^3x\, \exp\left(-i\boldsymbol{q}(\eta)\cdot\boldsymbol{x} - \kappa r\right) r^{\gamma-2} P_{s\to s'}\,. \tag{4.39}$$

The spin transition matrix $P_{s\to s'}$ can be written as

$$P_{s\to s'} = v^{\dagger}_{s'}\left(1 + \frac{\omega}{2c^2\,k\cdot p}\boldsymbol{\alpha}\cdot\boldsymbol{A}\left(1 + \boldsymbol{\alpha}\cdot\hat{\boldsymbol{k}}\right)\right) u_s\,. \tag{4.40}$$

When the space integral in Eq. (4.39) acts on the spin transition matrix $P_{s\to s'}$, the relevant position dependency comes from the ground state spinor u_s. As a consequence, let us define the following space integrals

$$I_0(\eta) = \int d^3x\, \exp\left(-i\boldsymbol{q}(\eta)\cdot\boldsymbol{x} - \kappa r\right) r^{\gamma-2}\,, \tag{4.41}$$

$$\boldsymbol{\sigma}\cdot\boldsymbol{I}_1(\eta) = \int d^3x\, \exp\left(-i\boldsymbol{q}(\eta)\cdot\boldsymbol{x} - \kappa r\right) r^{\gamma-2}\hat{\boldsymbol{r}}\cdot\boldsymbol{\sigma}\,. \tag{4.42}$$

These integrals can be calculated via the plane wave expansion [112]

$$e^{-i\boldsymbol{q}\cdot\boldsymbol{x}} = 4\pi\sum_{l=0}^{\infty}\sum_{m=-l}^{l}(-i)^l j_l(qr)Y_{lm}(\Omega_q)Y^*_{lm}(\Omega_r) \tag{4.43}$$

where Y_{lm} and j_l are the Spherical Harmonics and the Spherical Bessel functions, respectively. The results yield

$$I_0(\eta) = 4\pi\, \Upsilon_0(\eta)\,, \tag{4.44}$$

$$\boldsymbol{\sigma}\cdot\boldsymbol{I}_1(\eta) = -i4\pi\, \boldsymbol{\sigma}\cdot\hat{\boldsymbol{q}}\Upsilon_1(\eta) \tag{4.45}$$

with

$$\Upsilon_n(\eta) = \int_0^\infty dr\, r^\gamma \exp\left(-\kappa r\right) j_n(qr)\,. \tag{4.46}$$

Therefore, with the defined integrals, the strong field transition matrix reads

$$M_{s\to s'} = \frac{4\pi N}{\omega}\int_{-\infty}^{\infty} d\eta\, \exp\left(-i\Phi(\eta)\right)\Upsilon_0(\eta)\, v_{s'}^\dagger\left(1+\frac{\omega}{2c^2\, k\cdot p}\boldsymbol{\alpha}\cdot\boldsymbol{A}\left(1+\boldsymbol{\alpha}\cdot\hat{\boldsymbol{k}}\right)\right)\tilde{u}_s(\eta)\,. \tag{4.47}$$

with

$$\tilde{u}_s(\eta) = \begin{pmatrix} \varsigma_\pm \\ \dfrac{c(1-\gamma)}{\kappa}\dfrac{\Upsilon_1(\eta)}{\Upsilon_0(\eta)}\boldsymbol{\sigma}\cdot\hat{\boldsymbol{q}}\,\varsigma_\pm \end{pmatrix}. \tag{4.48}$$

The η integral in the above expression can be evaluated via the saddle point approximation. Then, the transition matrix (4.47) becomes

$$M_{s\to s'} = \frac{4\pi N}{\omega}\sqrt{\frac{2\pi}{i\ddot{\Phi}(\eta_s)}}\exp\left(-i\Phi(\eta_s)\right)\Upsilon_0(\eta_s) v_{s'}^\dagger\left(1+\frac{\omega}{2c^2\, k\cdot p}\boldsymbol{\alpha}\cdot\boldsymbol{A}\left(1+\boldsymbol{\alpha}\cdot\hat{\boldsymbol{k}}\right)\right)\tilde{u}_s(\eta_s) \tag{4.49}$$

where the saddle phase η_s is given by

$$\left.\frac{d\Phi(\eta)}{d\eta}\right|_{\eta=\eta_s} = 0\,. \tag{4.50}$$

At this stage we should discuss the saddle point conditions. The saddle point implies that $q(\sigma = 1) = i\kappa$ in an arbitrary gauge for the tunneling regime. This further indicates that in the length gauge the integration (4.46) has a singular point at the saddle. Therefore, in order to use the saddle point approximation in the length gauge one has to use a modified saddle point method for integrals with a singularity [113] (see also the discussion in [114]). However, since our aim is to evaluate the corresponding ratios, i.e., spin-flip SF, spin-flip asymmetry A and the ensemble averaged asymmetry parameter $\langle A\rangle$, the ordinary saddle point method is sufficient to deduce the result. In fact the ration for the length gauge in the limit of $\eta\to\eta_s$ yields

$$\lim_{\eta\to\eta_s}\frac{\Upsilon_1(\eta)}{\Upsilon_0(\eta)} = i\,. \tag{4.51}$$

Finally, the relevant terms in the transition matrix (4.49) reduce to

$$M_{s\to s'} = v_{s'}^\dagger\left(1+\frac{\omega}{2c^2\, k\cdot p}\boldsymbol{\alpha}\cdot\boldsymbol{A}(\eta_s)\left(1+\boldsymbol{\alpha}\cdot\hat{\boldsymbol{k}}\right)\right)\tilde{u}_s(\eta_s) \tag{4.52}$$

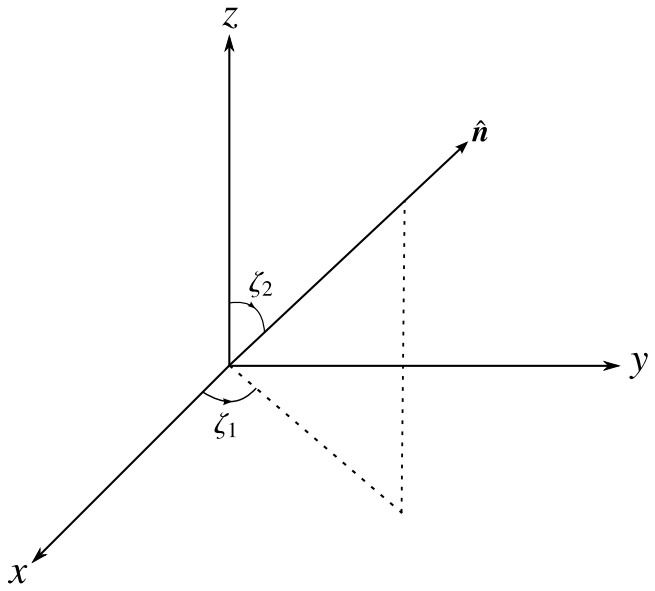

Figure 4.1. – Any quantization axis can be aligned with two angles.

where we have omitted the common factors for the ratios.

In the present work, we investigate the spin dynamics in the tunneling regime for a right circularly polarized electromagnetic plane wave, though the result can be generalized to an arbitrary polarization. The most general vector potential for an arbitrary polarized plane propagating along z direction can be written as

$$\boldsymbol{A} = \sqrt{2}\,A_0\left(\cos(\frac{\xi}{2})\cos(\eta)\hat{x} - \sin(\frac{\xi}{2})\sin(\eta)\hat{y}\right) \tag{4.53}$$

with the polarization parameter ξ such that $\xi = 0$ corresponds to the linear polarization while $\xi = \pm\pi/2$ correspond to the right and left circular polarization, respectively. The right circularly polarized plane wave

$$\boldsymbol{A} = A_0\left(\cos(\eta)\hat{x} - \sin(\eta)\hat{y}\right)\,, \tag{4.54}$$

then, yields the following fields

$$\boldsymbol{E} = E_0\left(\sin(\eta)\hat{x} + \cos(\eta)\hat{y}\right)\,, \tag{4.55}$$

$$\boldsymbol{B} = B_0\left(-\cos(\eta)\hat{x} + \sin(\eta)\hat{y}\right) \tag{4.56}$$

with $E_0 = B_0 = \omega A_0/c$.

The spin quantization axis, on the other hand, can be aligned with any preferred direction, which enables us to investigate different configurations for the spin dynamics. The corresponding spinors of both the Volkov state and the ground state can be written down for an arbitrary quantization axis using a rotation matrix [115]. Let z-axis be the initial quantization axis (propagating direction of the laser). For a given state $|j\,,m\rangle$ where j and m label corresponding angular momentum of the state and its component along the quantization axis, respectively, the rotated state is defined as

$$D(R)\,|j\,,m\rangle = \sum_{m'} D^{(j)}_{m\,,m'}(R)\,|j\,,m'\rangle \tag{4.57}$$

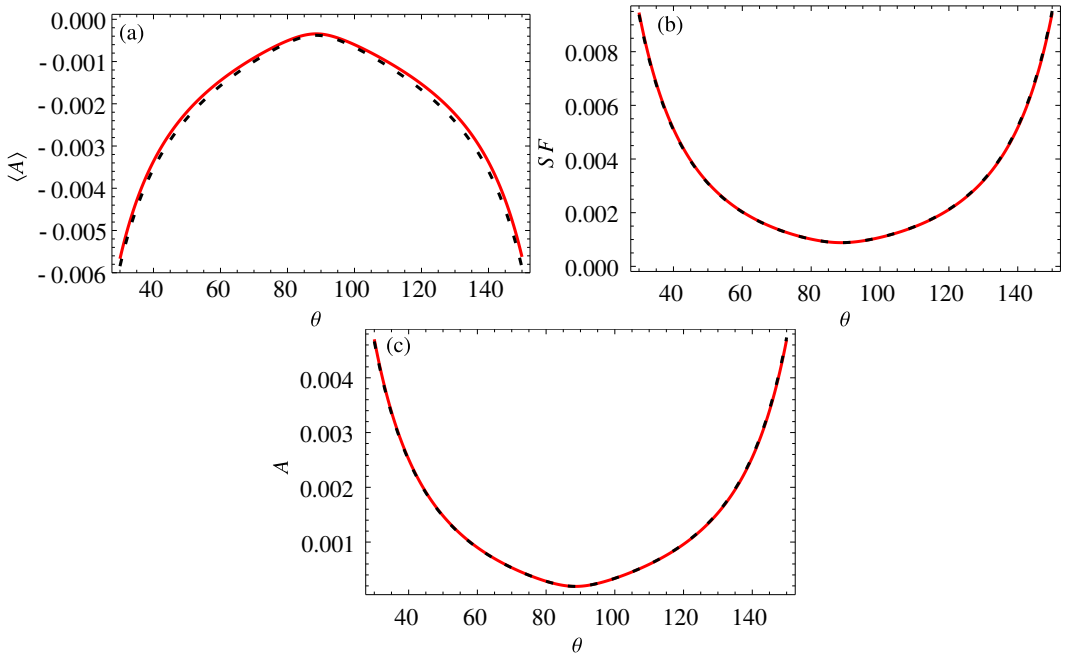

Figure 4.2. – Comparison of the nonrelativistic results of the standard SFA performed in the velocity gauge (solid red lines) and in the length gauge (black dashed lines) for (a) the ensemble averaged asymmetry parameter $\langle A \rangle$, (b) the spin-flip SF, and (c) the spin-flip asymmetry A as a function of the ionization angle θ. The applied parameters are $\kappa = 1$, $\omega = 0.05$ and $E_0/E_a = 1/(2\sqrt{2})$.

with the spin-j representation of the rotation matrix $D^{(j)}_{m,m'}(R)$ [115]. Both the Volkov state and the ground state of a H-like ion can be rotated via the $j = 1/2$ representation as

$$v_s^R = \sum_{s'} D^{(j=1/2)}_{s,s'}(R) v_{s'} \,, \tag{4.58}$$

$$u_s^R = \sum_{s'} D^{(j=1/2)}_{s,s'}(R) u_{s'} \,. \tag{4.59}$$

Then, the spinor along an arbitrary quantization axis $\hat{\boldsymbol{n}}$, see Fig. 4.1, can be evaluated with the following $j = 1/2$ representation of the rotation matrix

$$D^{(j=1/2)}_{s,s'}(R) = \begin{pmatrix} e^{-i\zeta_1/2}\cos(\zeta_2/2) & e^{i\zeta_1/2}\sin(\zeta_2/2) \\ -e^{-i\zeta_1/2}\sin(\zeta_2/2) & e^{i\zeta_1/2}\cos(\zeta_2/2) \end{pmatrix} . \tag{4.60}$$

Putting all together, the standard SFA transition matrix for a generic quantization axis reads

$$M^R_{s\to s'} = v^{R\,\dagger}_{s'} \left(1 + \frac{\omega}{2c^2\, k\cdot p} \boldsymbol{\alpha}\cdot\boldsymbol{A}\left(1 + \boldsymbol{\alpha}\cdot\hat{\boldsymbol{k}}\right)\right) \tilde{u}^R_s(\eta_s) \tag{4.61}$$

or in terms of the transition matrix for the initial alignment $M_{j\to k}$, Eq. (4.61) yields

$$M^R_{i\to f} = D^*_{k,f} M_{j\to k} D_{i,j} \,. \tag{4.62}$$

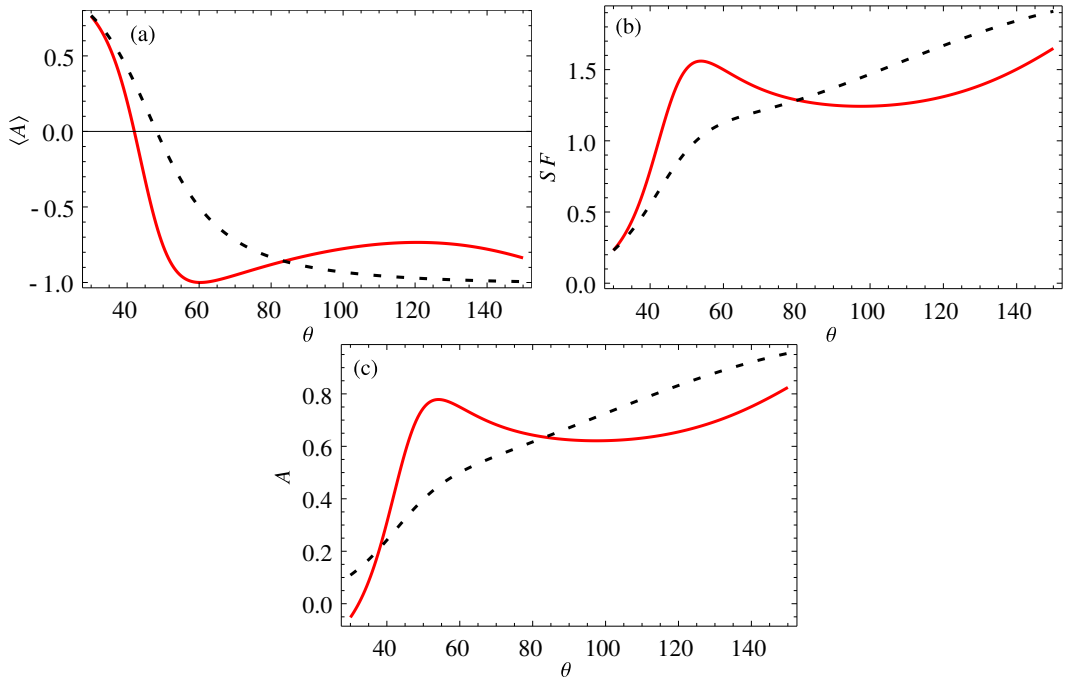

Figure 4.3. – Comparison of the relativistic results of the standard SFA performed in the velocity gauge (solid red lines) and in the length gauge (black dashed lines) for (a) the ensemble averaged asymmetry parameter $\langle A \rangle$, (b) the spin-flip SF, and (c) the spin-flip asymmetry A as a function of the ionization angle θ. The applied parameters are $\kappa = 90$, $\omega = 0.05$ and $E_0/E_a = 1/(2\sqrt{2})$.

We consider the most interesting case where the quantization axis is perpendicular to the plane of the magnetic field, it is aligned with the laser's propagation direction. The corresponding angles can, then, be defined

$$\zeta_1 = 0\,, \quad \zeta_2 = 0\,. \tag{4.63}$$

We first start with the nonrelativistic regime where we set $\kappa = 1$. The ensemble averaged asymmetry parameter $\langle A \rangle$, the spin-flip SF, and the spin-flip asymmetry A as a function of the ionization angle

$$\theta = -\arctan\left(\frac{p_x}{p_z}\right) \tag{4.64}$$

with $p_y = 0$, are shown in Fig. 4.2. In the figures, the solid red lines correspond to the result performed in the velocity gauge, while the dashed black lines are for the length gauge. It is clearly seen that both gauges agree with each other for nonrelativistic parameters. However, with the increasing atomic number which characterizes signature of the relativistic regime, the two results start to deviate. The difference between two gauges becomes larger as κ increases. The Fig. 4.3 demonstrates the extreme case where we have set $\kappa = 90$.

4.4. Dressed SFA

In the previous section we have calculated the spin asymmetries using the standard SFA. Nevertheless, the standard SFA does not take into account the electromagnetic field on the bound state. In this section we will also consider the influence of the laser field on the bound state dynamics via employing a different partition of the Hamiltonian. Consider the full Hamiltonian (4.18) in the length gauge

$$H = c\boldsymbol{\alpha}\cdot\boldsymbol{p} + c^2\beta - \frac{\kappa}{r} - \boldsymbol{E}\cdot\boldsymbol{r}\,\boldsymbol{\alpha}\cdot\hat{\boldsymbol{k}} + \boldsymbol{E}\cdot\boldsymbol{r}\,, \tag{4.65}$$

we can partition it as

$$H_i = c\boldsymbol{\alpha}\cdot\boldsymbol{p} + c^2\beta - \frac{\kappa}{r} - \boldsymbol{E}\cdot\boldsymbol{r}\,\boldsymbol{\alpha}\cdot\hat{\boldsymbol{k}}, \quad V_i = \boldsymbol{E}\cdot\boldsymbol{r}, \tag{4.66}$$

$$H_f = c\boldsymbol{\alpha}\cdot\boldsymbol{p} + c^2\beta - \boldsymbol{E}\cdot\boldsymbol{r}\,\boldsymbol{\alpha}\cdot\hat{\boldsymbol{k}} + \boldsymbol{E}\cdot\boldsymbol{r}, \quad V_f = -\frac{\kappa}{r} \tag{4.67}$$

where the last term in H_i gives rise to the Zeeman splitting and the spin precession in the bound state [111].

The transition matrix, then, reads

$$M_{s\to s'} = -i\int_{-\infty}^{\infty} dt \int d^3x\, \Psi_V^{s'\dagger}(\boldsymbol{x},t)\boldsymbol{E}\cdot\boldsymbol{r}\varphi_0^s(\boldsymbol{x},t) \tag{4.68}$$

or via Eq. (4.16) it can be written as

$$M_{s\to s'} = i\kappa\int_{-\infty}^{\infty} dt \int d^3x\, \Psi_V^{s'\dagger}(\boldsymbol{x},t)\frac{1}{r}\varphi_0^s(\boldsymbol{x},t)\,. \tag{4.69}$$

Here $\Psi_V^s(\boldsymbol{x},t)$ is the Volkov wave function in the length gauge, while $\varphi_0^s(\boldsymbol{x},t)$ is the ground state solution of the Coulomb potential including the Zeeman term $-\boldsymbol{E}\cdot\boldsymbol{r}\,\boldsymbol{\alpha}\cdot\hat{\boldsymbol{k}}$.

The dressed bound state $\varphi_0^s(\boldsymbol{x},t)$ can be solved exactly within the long wave approximation. Since the typical length scale for the bound dynamics is much smaller than the wavelength of the plane wave [91], which is called the long wave approximation, one can neglect the spatial dependency of the field and approximate $\eta \sim \omega t$ for the bound state dynamics. Based on the following ansatz

$$|\varphi_0^s(t)\rangle \equiv C^{s\,s'}(t)\,|\phi_0^{s'}(t)\rangle \tag{4.70}$$

with the ground state solution of H-like ion $|\phi_0^{s'}(t)\rangle$ defined in Eq. (4.32) and the superposing coefficients $C^{s\,s'}(t)$, we can split up the Hamiltonian H_i in Eq. (4.66) as

$$H_0 = c\boldsymbol{\alpha}\cdot\boldsymbol{p} + c^2\beta - \frac{\kappa}{r}\,, \tag{4.71}$$

$$H_I = -\boldsymbol{E}\cdot\boldsymbol{r}\,\boldsymbol{\alpha}\cdot\hat{\boldsymbol{k}}\,. \tag{4.72}$$

The Schrödinger equation

$$i\partial_t\,|\varphi_0^s(t)\rangle = (H_0 + H_I)\,|\varphi_0^s(t)\rangle\,, \tag{4.73}$$

then, reduces to

$$i\,\dot{C}^{s\,s''}(t) = C^{s\,s'}(t)\,\langle\phi_0^{s''}|H_I|\phi_0^{s'}\rangle\ . \tag{4.74}$$

First observe that the matrix element vanishes for the same spin states, i.e., $\langle\phi_0^s|H_I|\phi_0^s\rangle = 0$. Next, calculating the relevant matrix elements, we end up with the following solutions

$$C^{++}(t) = \sqrt{\frac{\Gamma+1}{2\Gamma}}\exp\left(\frac{i\omega t}{2}(1-\Gamma)\right), \tag{4.75a}$$

$$C^{+-}(t) = -\sqrt{\frac{\Gamma-1}{2\Gamma}}\exp\left(\frac{i\omega t}{2}(-1-\Gamma)\right), \tag{4.75b}$$

$$C^{-+}(t) = \sqrt{\frac{\Gamma-1}{2\Gamma}}\exp\left(\frac{i\omega t}{2}(1+\Gamma)\right), \tag{4.75c}$$

$$C^{--}(t) = \sqrt{\frac{\Gamma+1}{2\Gamma}}\exp\left(\frac{i\omega t}{2}(-1+\Gamma)\right), \tag{4.75d}$$

where

$$\Gamma = \frac{\sqrt{4E_0^2(1+2\gamma)^2/(6c)^2+\omega^2}}{\omega}\,. \tag{4.76}$$

Finally, the approximated ground state is given by the following replacement

$$C^{s\,s'}(t) \to C^{s\,s'}(\eta/\omega)\,. \tag{4.77}$$

Similar to the calculation performed in the previous Sec. 4.3, employing the coordinate transformation $(t,\boldsymbol{x}) \to (\eta,\boldsymbol{x})$, the transition matrix in the dressed SFA reads

$$M^D_{s\to s'} = \frac{N}{\omega}\int_{-\infty}^{\infty} d\eta\,\exp\left(-i\Phi(\eta)\right)\int d^3x\,\exp\left(-i\boldsymbol{q}(\eta)\cdot\boldsymbol{x}-\kappa r\right)r^{\gamma-2}P^D_{s\to s'} \tag{4.78}$$

where the spin transition matrix $P^D_{s\to s'}$ is defined as

$$P^D_{s\to s'} = v^\dagger_{s'}\left(1+\frac{\omega}{2c^2\,k\cdot p}\boldsymbol{\alpha}\cdot\boldsymbol{A}\left(1+\boldsymbol{\alpha}\cdot\hat{\boldsymbol{k}}\right)\right)C^{s\,s''}u_{s''}\,. \tag{4.79}$$

Evaluation of the space integral can be performed identical to the calculation in the standard SFA in the length gauge. The saddle point integration, on the other hand, needs a further consideration due to presence of phase dependent exponential terms given in Eq. (4.75). However in the tunneling regime, since

$$\frac{\Gamma\,\omega}{\varepsilon_0-\varepsilon} \ll 1\,, \tag{4.80}$$

the saddle point is still determined by $\dot{\Phi}(\eta_s) = 0$.

After the space integral and the saddle point integration and further omitting common factors we end up with

$$M^D_{s\to s'} = v^\dagger_{s'}\left(1+\frac{\omega}{2c^2\,k\cdot p}\boldsymbol{\alpha}\cdot\boldsymbol{A}(\eta_s)\left(1+\boldsymbol{\alpha}\cdot\hat{\boldsymbol{k}}\right)\right)\tilde{\tilde{u}}_s(\eta_s)\,. \tag{4.81}$$

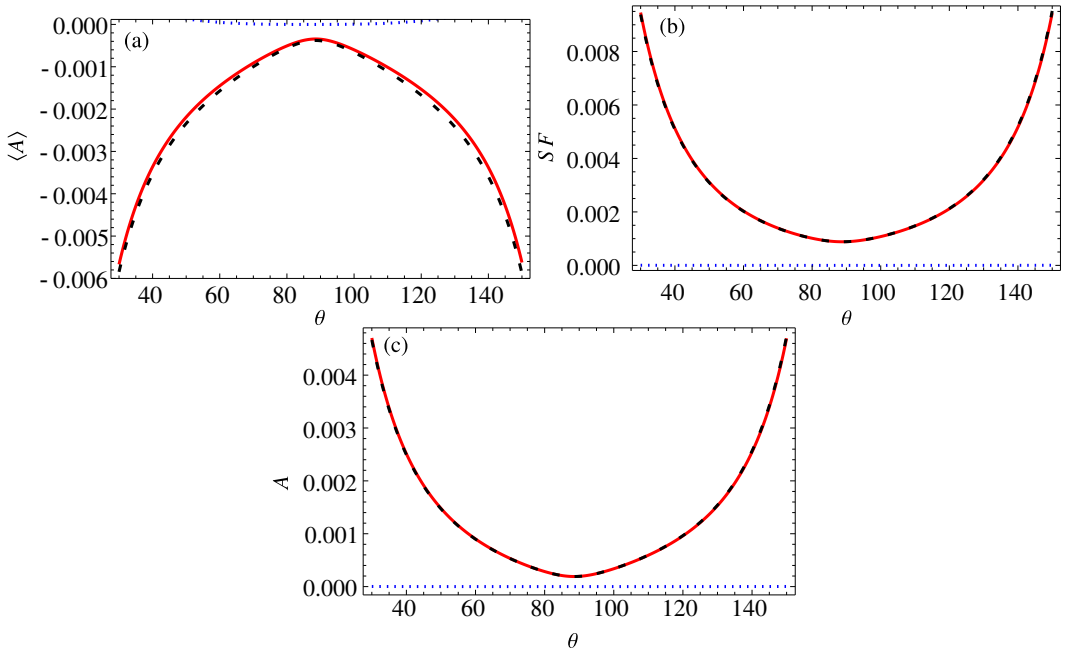

Figure 4.4. – Comparison between nonrelativistic results of the standard SFA and the dressed SFA (blue dotted lines) for (a) the ensemble averaged asymmetry parameter $\langle A \rangle$, (b) the spin-flip SF, and (c) the spin-flip asymmetry A as a function of the ionization angle θ. The applied parameters are $\kappa = 1$, $\omega = 0.05$ and $E_0/E_a = 1/(2\sqrt{2})$.

Here the Fourier transform of the ground state spinors read

$$\tilde{\tilde{u}}_+(\eta_s) = 4\pi\sqrt{\frac{\Gamma+1}{2\Gamma}}\exp\left(i\eta_s(1-\Gamma)/2\right)\begin{pmatrix} \varsigma_+ \\ \dfrac{ic(1-\gamma)}{\kappa}\,\hat{\boldsymbol{q}}\cdot\boldsymbol{\sigma}\,\varsigma_+ \end{pmatrix}$$
$$- 4\pi\sqrt{\frac{\Gamma-1}{2\Gamma}}\exp\left(i\eta_s(-1-\Gamma)/2\right)\begin{pmatrix} \varsigma_- \\ \dfrac{ic(1-\gamma)}{\kappa}\,\hat{\boldsymbol{q}}\cdot\boldsymbol{\sigma}\,\varsigma_- \end{pmatrix}, \tag{4.82}$$

$$\tilde{\tilde{u}}_-(\eta_s) = 4\pi\sqrt{\frac{\Gamma-1}{2\Gamma}}\exp\left(i\eta_s(1+\Gamma)/2\right)\begin{pmatrix} \varsigma_+ \\ \dfrac{ic(1-\gamma)}{\kappa}\,\hat{\boldsymbol{q}}\cdot\boldsymbol{\sigma}\,\varsigma_+ \end{pmatrix}$$
$$+ 4\pi\sqrt{\frac{\Gamma+1}{2\Gamma}}\exp\left(i\eta_s(-1+\Gamma)/2\right)\begin{pmatrix} \varsigma_- \\ \dfrac{ic(1-\gamma)}{\kappa}\,\hat{\boldsymbol{q}}\cdot\boldsymbol{\sigma}\,\varsigma_- \end{pmatrix}, \tag{4.83}$$

where we have used the limit (4.51). Finally, one can extend the result for an arbitrary quantization axis via the rotation matrix and ends up with Eq. (4.62).

Now we can compare the results obtained in the dressed SFA with figures 4.2 and 4.3 for case of that the quantization axis is parallel to the propagation direction of the right circular polarized laser. For nonrelativistic parameters the comparison is shown

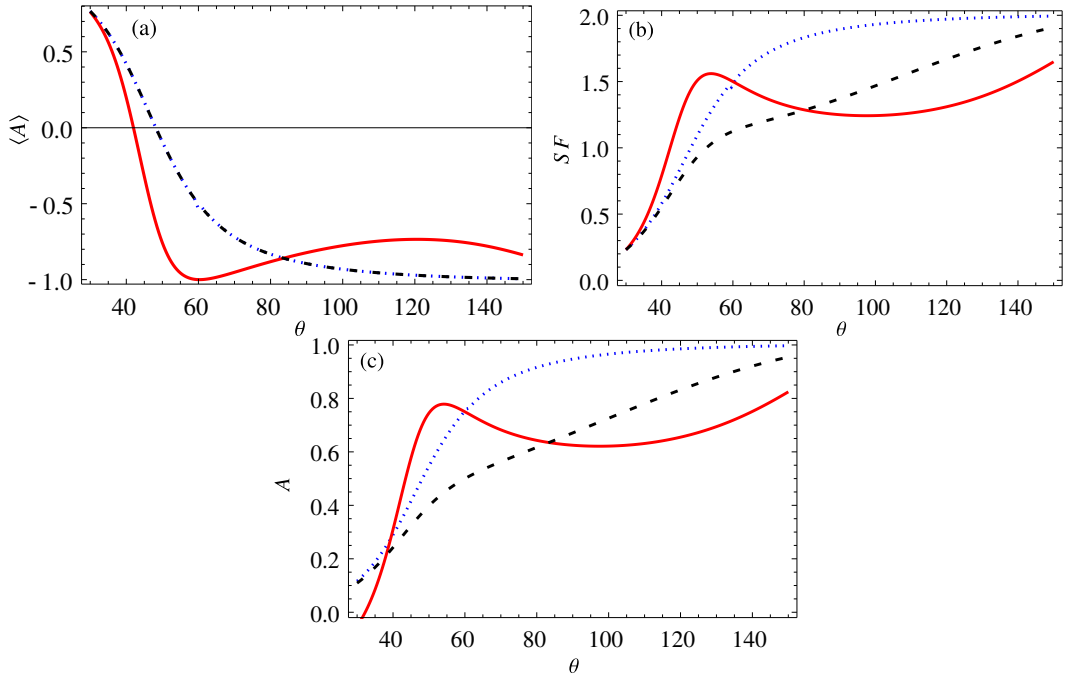

Figure 4.5. – Comparison between relativistic results of the standard SFA and the dressed SFA (blue dotted lines) for (a) the ensemble averaged asymmetry parameter $\langle A \rangle$, (b) the spin-flip SF, and (c) the spin-flip asymmetry A as a function of the ionization angle θ. The applied parameters are $\kappa = 90$, $\omega = 0.05$ and $E_0/E_a = 1/(2\sqrt{2})$.

in Fig. 4.4. It can be seen that the asymmetries are suppressed in the dressed SFA for nonrelativistic parameters. However, when we approach the relativistic regime, the previously suppressed results of the dressed SFA reach the same order of the results obtained in the standard SFA. For instance, the highly relativistic regime is plotted in Fig. (4.5). Another observation based on the graphs is that the qualitative behavior of the asymmetries obtained in the standard SFA in the length gauge and the dressed SFA is similar.

4.5. Conclusion

As a conclusion we have investigated the spin dynamics in relativistic tunnel-ionization using the spin asymmetries. After developing the SFA on the base of different partitions of the Hamiltonian, we calculated the differential ionization rate for the spin resolved ionization for H-like ions in the standard SFA. A comparison of velocity and length gauge is illustrated for a circular polarized electromagnetic plane wave, where we set the quantization axis along the laser's propagation direction. Later, the result was extended to the dressed SFA. In the nonrelativistic regime, asymmetries are suppressed by the dressed SFA in comparison to the results obtained in the standard SFA. However, it is shown that the qualitative and quantitative behavior of the results of the standard SFA in the length gauge and the dressed SFA is similar for the relativistic parameters.

5. The relativistic propagator via the path-dependent vector potential

5.1. Introduction

For those potentials which vary much more slowly than the corresponding wave function, the wave function can be calculated using Wentzel-Kramers-Brilluin (WKB) approximation [70]. In a sense, we are in the quasiclassical regime where the de Broglie wavelength of the particle varies only slightly over the distance that characterizes the problem [86]. In fact, if the Lagrangian of a point particle is a quadratic function of the coordinate and the velocity, then the corresponding exact propagator coincides with the quasiclassical propagator, i.e., the classical path dominates the Feynman path integral [116–119]. It is interesting that the exact Volkov propagator, the propagator of a charged particle interacting with a plane electromagnetic wave, also coincides with the quasiclassical limit [88, 120–123], though the Lagrangian is not quadratic. Furthermore, there are many cases where the quasiclassical propagator is a good approximation. In this chapter, we show that the calculation of the quasiclassical propagator can be significantly simplified by employing the path dependent formulation of the vector potential within the proper time formalism.

The propagator of a particle in an electromagnetic field can be calculated via the Feynman path integral [116, 117], where the propagator is expressed in terms of the action (2.64). When additionally the path-dependent formulation of the gauge representation is used, the interaction part of the action of the Feynman path integral can be expressed in terms of the electromagnetic flux through the area between the arbitrary Feynman path and the gauge path which generates the associated path-dependent vector potential [69]. The significant simplification of the quasiclassical propagator expression verifies when one specifies the gauge path to coincide with the classical trajectory. In fact, as we will show here, the electromagnetic flux vanishes in this case and, consequently, the interaction part of the action vanishes in the Feynman path integral.

The straightforward calculation of the relativistic propagator via the Feynman path integral is cumbersome due to the presence of the particle's infinitesimal proper time [116–119]. However, one can overcome this difficulty via introducing a fifth parameter to the theory which is known as the proper time formalism [16,124–129]. In

this method one defines an effective Lagrangian associated to the super-Hamiltonian $\mathcal{H}(P, X)$. The latter is defined by quantum mechanical equation. Any quantum mechanical equation can be written in the form of

$$\mathcal{H}(P, X)\,|\psi\rangle = 0 \tag{5.1}$$

with the four-momentum operator P and four-position operator X. Then, the relativistic propagator derived by the standard rules of the nonrelativistic Feynman path integral for an effective system governed by effective Lagrangian.

In this chapter, we unite two powerful methods for the calculation of the propagator of a relativistic charged particle interacting with an external electromagnetic field. In particular, the path-dependent formulation of gauge theory is incorporated in the proper time formalism for propagators. This allows us to obtain simple expressions of the quasiclassical propagators for a constant and uniform electromagnetic field, for an arbitrary plane wave and for an arbitrary plane wave combined with an arbitrary constant and uniform electromagnetic field. In all these cases, the quasiclassical propagator coincides with the exact result.

The structure of the chapter is the following: In Sec. 5.2, the proper time formalism for calculation of propagators is introduced, which incorporates the path-dependent gauge formalism. The explicit expressions for the propagators of a spinless charged particle interacting with a constant and uniform electromagnetic field, with a plane wave and with a plane wave combined with a constant and uniform electromagnetic field, respectively, are derived in Sec. 5.3. The conclusion is given in Sec. 5.4.

The CGS units are used throughout the chapter and the operators and the corresponding eigenvalues label with the uppercase letters and lowercase, respectively. Further, the chapter is based on [69, 130].

5.2. The Proper Time Formalism

The calculation of the relativistic propagator is, in general, tedious due to the presence of the particle's infinitesimal proper time. Nevertheless, this can be overcome via the proper time (eigentime, fifth parameter or einbein) formalism [16, 124–129].

The proper time formalism is based on the fact that any quantum mechanical equation can be written in the form

$$\mathcal{H}(P, X)\,|\psi\rangle = 0 \tag{5.2}$$

with a certain operator $\mathcal{H}(P, X)$, so called super-Hamiltonian. For instance, in the case of Klein-Gordon equation the super-Hamiltonian is

$$\mathcal{H} = \left(P - \frac{e}{c}\mathcal{A}(\mathcal{P}_G, X)\right)^2 - m^2c^2\,. \tag{5.3}$$

The four-momentum operator P^μ and the four-position operator X^μ in Eq. (5.2) satisfy the eigenvalue equations

$$P^\mu |p\rangle = p^\mu |p\rangle , \tag{5.4}$$

$$X^\mu |x\rangle = x^\mu |x\rangle , \tag{5.5}$$

respectively, with $p^\mu = (E/c, \boldsymbol{p})$ and $x^\mu = (c\,t, \boldsymbol{x})$. Further, the assumption of the canonical commutation relation $[X^\mu, P^\nu] = i\hbar\, g^{\mu\nu}$ implies the relations $\langle x| P_\mu |\psi\rangle = i\hbar\partial_\mu\psi(x)$, $\langle x| X_\mu |\psi\rangle = x_\mu\psi(x)$,

$$\langle x|p\rangle = \frac{1}{(2\pi\hbar)^2} \exp\left[-\frac{ix\cdot p}{\hbar}\right] , \tag{5.6}$$

$$\langle x|x'\rangle = \delta^4(x-x') = \int \frac{d^4p}{(2\pi\hbar)^4} \exp\left[-\frac{ip\cdot(x-x')}{\hbar}\right] . \tag{5.7}$$

In position space, the fundamental equation (5.2) yields

$$\langle x|\, \mathcal{H}\,(P,X)\, |\psi\rangle = \mathcal{H}\,(i\hbar\,\partial, x)\ \psi(x) = 0\,. \tag{5.8}$$

Then, the corresponding Green's function satisfies

$$\mathcal{H}\,(i\hbar\,\partial, x)\ G(x,x') = \delta^4(x-x')\,. \tag{5.9}$$

Hence, the Green's function can be identified as

$$G(x,x') = \mathcal{H}^{-1}\,(i\hbar\,\partial, x)\,\delta^4(x-x') \tag{5.10}$$

which can be written as

$$G(x,x') = \langle x|\,\mathcal{H}^{-1}\,(P,X)\,|x'\rangle = \langle x|\,\frac{1}{\mathcal{H}\,(P,X)+i\epsilon}\,|x'\rangle \tag{5.11}$$

with the Feynman $i\epsilon$ prescription. Furthermore, Eq. (5.11) may also be defined as

$$G(x,x') = -\frac{i}{\hbar}\alpha \int_0^\infty d\tau\ \langle x| \exp\left[\frac{i}{\hbar}\mathcal{H}\,(P,X)\,\alpha\,\tau\right] |x'\rangle\, e^{-\epsilon\tau} \tag{5.12}$$

with an auxiliary field α (einbein field). Here the parameter α is introduced in order to fix the right classical equations of motion of the corresponding super-Hamiltonian $\mathcal{H}(P,X)$ [128, 129].

Let us define the integrand in Eq. (5.12) as a Feynman kernel

$$K_F(x,x';\tau) = \langle x| \exp\left[\frac{i}{\hbar}\mathcal{H}\,(P,X)\,\alpha\,\tau\right] |x'\rangle\,, \tag{5.13}$$

with the effective Hamiltonian $\alpha\mathcal{H}$ and "time" parameter τ, which determines the propagator

$$G(x,x') = -\frac{i}{\hbar}\alpha \int_0^\infty d\tau\, K_F(x,x';\tau) e^{-\epsilon\tau}\,. \tag{5.14}$$

The Feynman kernel can be expressed using a path integral

$$K_F(x,x';\tau) = \int D(\mathcal{P}_F)\, \exp\left(-\frac{i}{\hbar}S(\mathcal{P}_F)\right) , \tag{5.15}$$

with a action $S(\mathcal{P}_F)$, which is derived by introducing an effective Lagrangian via a Legendre transformation

$$\mathcal{L} = p \cdot \dot{x} - \alpha \mathcal{H} \tag{5.16}$$

with $p^\mu = \partial \mathcal{L} / \partial \dot{x}_\mu$. Then,

$$K_F(x, x'; \tau) = \int D[y] \exp\left(-\frac{i}{\hbar} \int_0^\tau d\sigma \mathcal{L}(y, \dot{y}) \right), \tag{5.17}$$

where the parametrized path $y(\sigma)$ satisfies the boundary conditions $y^\mu(0) = x'^\mu$, $y(\tau) = x^\mu$.

In the present work, we restrict ourselves to spinless charged particles, although the results can be easily generalized to Fermionic particles. Then using Eq. (5.16) for Eq. (5.3), the corresponding effective Lagrangian is given by

$$\mathcal{L} = \frac{1}{4\alpha} \dot{y}^2 + \frac{e}{c} \dot{y} \mathcal{A}(\mathcal{P}_G, y) + \alpha\, m^2 c^2 \,. \tag{5.18}$$

The Euler-Lagrange equation for the effective Lagrangian provides the effective equation of motion

$$\frac{1}{2\alpha} \ddot{y}(\sigma)_c{}^\mu = \frac{e}{c} F^\mu{}_\nu(y_c) \dot{y}(\sigma)_c{}^\nu \tag{5.19}$$

which coincides with the classical equation of motion in the given external electromagnetic field for $\alpha = 1/(2m)$ as long as the path is parametrized with the particle's proper time τ [1].

In chapter 2 we have proposed a convenient gauge choice, the classical path gauge. This gauge fixing removes the interaction term from the action, see Sec. 2.3. As a consequence, in the quasiclassical approximation using this gauge, see Eq. (2.67), the Feynman kernel becomes

$$K_F(x, x') = \sqrt{\left(\frac{1}{2\pi i \hbar} \right)^4 \det\left(\frac{\partial^2 S_c}{\partial x_\mu \partial x'_\nu} \right)} \exp\left(-\frac{i}{\hbar} m^2 c^2 \alpha \tau - \frac{i}{\hbar} \int_0^\tau d\sigma \, \frac{\dot{y}_c^2}{4\alpha} \right). \tag{5.20}$$

Finally, the Green function is obtained via Eq. (5.14).

Eq. (5.20) is the main result of this chapter, which shows how to derive the fundamental Feynman kernel for the quasiclassical Green's function in a simple way, when the classical equation of motion Eq. (5.19) is integrable for the given field.

5.3. Examples

In this section we will apply the developed formalism to some important cases where the quasiclassical propagator coincides with the exact propagator.

5.3.1. Constant and uniform electromagnetic (EM) field

Let us first consider a spinless charged particle interacting with a constant and uniform electromagnetic field $F_{\mu\nu}$. Since the Lagrangian for a constant and uniform electromagnetic field (5.18) is a quadratic function of y and $\dot{y}$, the quasiclassical formula gives the exact result.

The Euler-Lagrange equation derived from the effective Lagrangian (5.18) gives the effective Lorentz force law

$$\ddot{y}(\sigma)_c{}^{\mu} = \lambda F^{\mu}{}_{\nu}\, \dot{y}(\sigma)_c{}^{\nu} \tag{5.21}$$

with $\lambda = 2\alpha e/c$ and the field strength tensor

$$F^{\mu}{}_{\nu} = \begin{pmatrix} 0 & E_x & E_y & E_z \\ E_x & 0 & B_z & -B_y \\ E_y & -B_z & 0 & B_x \\ E_z & B_y & -B_x & 0 \end{pmatrix}. \tag{5.22}$$

Then, the classical path with boundary conditions $y(0)_c{}^{\mu} = x'^{\mu}$, $y(\tau)_c{}^{\mu} = x^{\mu}$ yields

$$y(\sigma)_c{}^{\mu} = \left(\frac{e^{\lambda F\sigma} - 1}{e^{\lambda F\tau} - 1}\right)^{\mu}_{\nu} (x - x')^{\nu} + x'^{\mu}\,. \tag{5.23}$$

Here it should be understood that

$$\left(\frac{e^{\lambda F\sigma} - 1}{e^{\lambda F\tau} - 1}\right)^{\mu}_{\nu} = \frac{\sigma}{\tau} g^{\mu}{}_{\nu} + \frac{\lambda\left(\sigma^2 - \sigma\tau\right)}{2\tau} F^{\mu}{}_{\nu} + \frac{\lambda^2\left(2\sigma^3 - 3\sigma^2\tau + \sigma\tau^2\right)}{12\tau} F^{\mu}{}_{\alpha} F^{\alpha}{}_{\nu} + \cdots \tag{5.24}$$

As a result, in the classical path gauge, the Feynman kernel (5.20) reads

$$K_F(x, x'; \tau) = \sqrt{\frac{\det\left[-\frac{\lambda^2 F^2 \tau}{8\alpha} \sinh^{-2}(\frac{\lambda F\tau}{2})\right]}{(2\pi i\hbar)^4}} \times \exp\left(-\frac{i}{4\alpha\hbar}(x - x')\left(\frac{\lambda^2 F^2 \tau}{4} \sinh^{-2}(\frac{\lambda F\tau}{2})\right)(x - x') - \frac{im^2c^2\alpha\tau}{\hbar}\right). \tag{5.25}$$

The kernel in an arbitrary gauge, then, is given by the transformation

$$K_F(x, x'; \tau) \to \exp\left(-\frac{ie}{\hbar c}\Phi_{EM}(x)\right) K_F(x, x'; \tau) \exp\left(\frac{ie}{\hbar c}\Phi_{EM}(x')\right) \tag{5.26}$$

where the electromagnetic flux Φ_{EM} is calculated for the area bounded by the loop $\partial\Sigma = \mathcal{P}_c - \mathcal{P}_G$ with desired gauge $\mathcal{P}_G$. Equivalently, the kernel in an arbitrary gauge can also be found as follows. The vector potential for the classical path can be expressed as

$$\mathcal{A}_{\mu}(\mathcal{P}_c, x) = -\frac{1}{\lambda}\int_0^{\tau} d\sigma\, \frac{\partial^2 y_c{}^{\nu}}{\partial\sigma^2} \frac{\partial y_{c\nu}}{\partial x^{\mu}} \tag{5.27}$$

where we have used Eq. (5.19) in Eq. (2.35). Then, the desired gauge is obtained via the corresponding gauge function χ.

The constant and uniform crossed field with equal amplitude

$$\boldsymbol{E} = E_0\,\hat{\boldsymbol{x}}\,, \quad \boldsymbol{B} = E_0\,\hat{\boldsymbol{y}}\,, \tag{5.28}$$

is an important spacial case of a constant field, corresponding to the limit $\omega \to 0$ in the domain of interest with the frequency of the electromagnetic field. Since the third power of the field strength matrix (5.22) vanishes for the above fields, the Feynman kernel in the classical path gauge yields

$$K_F(x,x';\tau)_{FS} = \frac{1}{(4\pi\hbar\alpha\tau)^2}\exp\left(-\frac{i}{\hbar}\frac{(x-x')^2}{4\alpha\tau} + \frac{i\lambda^2\tau}{48\,\hbar\alpha}(x-x')F^2(x-x') - \frac{im^2c^2\alpha\tau}{\hbar}\right) \tag{5.29}$$

which corresponds to the vector potential in the classical path gauge

$$\mathcal{A}_\mu(\mathcal{P}_c,x) = -\frac{1}{2}\left(F + \frac{\lambda\tau}{3}F^2\right)_{\mu\nu}(x-x')^\nu\,. \tag{5.30}$$

For comparison, in the Fock-Schwinger gauge, the vector potential

$$\mathcal{A}_\mu(\mathcal{P}_{FS},x) = -\frac{1}{2}F_{\mu\nu}(x-x')^\nu \tag{5.31}$$

is obtained via the gauge function

$$\chi = \frac{\lambda\tau}{12}(x-x')^\mu F^2{}_{\mu\nu}(x-x')^\nu\,. \tag{5.32}$$

In terms of the gauge paths, the above gauge function corresponds to the flux through the area bounded by the classical path (5.23) and the Fock-Schwinger path which is a straight line

$$\mathcal{P}_{FS}\,:\; y^\mu(\sigma) = \sigma x^\mu + (1-\sigma)x'^\mu \tag{5.33}$$

with the boundary conditions $y^\mu(1) = x^\mu$, $y^\mu(0) = x'^\mu$.

5.3.2. Plane wave: Volkov propagator

Another case where the quasiclassical approximation yields the exact result is the interaction of a charged particle with a plane electromagnetic wave [88, 120–123]. The corresponding propagator for this case is called Volkov propagator. The field strength tensor $F_{\mu\nu}$ of a linearly polarized plane wave can be written as

$$F_{\mu\nu}(\phi) = \epsilon_{\mu\nu}f'(\phi) \tag{5.34}$$

where the phase of the wave is defined as $\phi = nx$ and the antisymmetric tensor $\epsilon_{\mu\nu} = n_\mu\epsilon_\nu - n_\nu\epsilon_\mu$ with the propagation and polarization directions n_μ and ϵ_μ, respectively.

The classical trajectory $\mathcal{P}_c$ via Eq. (5.19) for a plane wave reads:

$$ny_c(\sigma) = \frac{\sigma}{\tau} n(x - x') + nx' \,, \tag{5.35}$$

$$\epsilon y_c(\sigma) = \frac{\sigma}{\tau} \epsilon(x - x') + \epsilon x' + \frac{\lambda}{\tau} \left(\tau g_1(\sigma) - \sigma g_1(\tau)\right) \,, \tag{5.36}$$

$$\overline{\epsilon} y_c(\sigma) = \frac{\sigma}{\tau} \overline{\epsilon}(x - x') + \overline{\epsilon} x' \,, \tag{5.37}$$

$$\begin{aligned} \overline{n} y_c(\sigma) = {} & \frac{\lambda \left(\tau g_1(\sigma) - \sigma g_1(\tau)\right)}{n(x - x')\tau} \left(\epsilon(x - x') - \lambda\, g_1(\tau)\right) \\ & + \frac{\lambda^2}{2\, n(x - x')} \left(\tau g_2(\sigma) - \sigma g_2(\tau)\right) + \frac{\sigma}{\tau} \overline{n}(x - x') + \overline{n} x' \,, \end{aligned} \tag{5.38}$$

where

$$g_m(\sigma) = \int_0^\sigma f(n y_c)^m d\sigma' \tag{5.39}$$

and the basis n^μ, ϵ^μ, $\overline{\epsilon}^\mu$, $\overline{n}^\mu$ is introduced such that it satisfies $n^2 = \overline{n}^2 = \epsilon n = \overline{\epsilon} n = \epsilon \overline{n} = \overline{\epsilon n} = \epsilon \overline{\epsilon} = 0$, $\epsilon^2 = \overline{\epsilon}^2 = -1$, and $n\overline{n} = 1$.

Furthermore, the classical action in the classical path gauge can be written in terms of the new basis as

$$S_c = m^2 c^2 \alpha \tau + \int_0^\tau d\sigma \, \frac{1}{4\alpha} \left(2 n\dot{y}_c \, \overline{n}\dot{y}_c - \epsilon \dot{y}_c^2 - \overline{\epsilon} \dot{y}_c^2\right) \tag{5.40}$$

where we have used the fact that any four-vector can be expanded in terms of the new basis as

$$A^\mu = \overline{n} A \, n^\mu + nA \, \overline{n}^\mu - \epsilon A \, \epsilon^\mu - \overline{\epsilon} A \, \overline{\epsilon}^\mu \,. \tag{5.41}$$

Consequently, the Feynman kernel in the classical path gauge yields

$$\begin{aligned} K_F(x, x'; \tau) = {} & \frac{1}{(4\pi\hbar\alpha\tau)^2} \\ & \times \exp\left(-\frac{i}{\hbar} \frac{(x - x')^2}{4\alpha\tau} - \frac{i m^2 c^2 \alpha \tau}{\hbar} - \frac{i\lambda^2}{4\hbar\alpha\tau} \left(\int_0^\tau d\sigma \, f(n y_c)\right)^2 + \frac{i\lambda^2}{4\hbar\alpha} \int_0^\tau d\sigma \, f(n y_c)^2\right) . \end{aligned} \tag{5.42}$$

The result is more compact due to the absence of the interaction term (see for instance Eq. (31) of [122]). For a constant and uniform plane wave one naturally recovers Eq. (5.29) and in the absence of the field one obtains the relativistic propagator for a free particle (see Eq. (19.28) of [119]). Furthermore, the Volkov propagator can be written in an arbitrary gauge via the transformation (5.26).

5.3.3. Plane wave combined with a constant and uniform EM field

In the last example we will obtain the relativistic propagator for a charged particle interacting with an arbitrary plane wave combined with a constant and uniform electromagnetic field.

The associated field strength tensor can be written as

$$F^{\mu\nu}(\phi) = {F_0}^{\mu\nu} + f^{\mu\nu}(\phi) \tag{5.43}$$

where ${F_0}^{\mu\nu}$ and $f^{\mu\nu}(\phi)$ are the field strength tensors of the constant and uniform electromagnetic field (5.22) and the plane wave (5.34), respectively.

Before calculating the classical action, we note that, since the action is a Lorentz scalar, one can calculate it in an arbitrary frame of reference. In fact, in an arbitrary reference frame, there are two fundamental Lorentz invariants which can be constructed using field strength tensor

$$F_{\mu\nu}F^{\mu\nu} = 2\,(\boldsymbol{B}^2 - \boldsymbol{E}^2)\,, \tag{5.44}$$

$$G_{\mu\nu}F^{\mu\nu} = -4\,\boldsymbol{E}\cdot\boldsymbol{B} \tag{5.45}$$

with the dual of the field strength tensor $G_{\mu\nu} = \epsilon^{\mu\nu\alpha\beta}F_{\alpha\beta}/2$. Hence, for a constant and uniform electromagnetic field a reference frame exists, where the magnetic field and the electric field can be parallel to each other [1]. Furthermore, the direction of the parallel magnetic and electric fields can be chosen along the propagation direction of the plane wave [131]. As a consequence, the field strength tensor for a constant and uniform electromagnetic field ${F_0}^{\mu\nu}$ can be written as

$${F_0}^{\mu\nu} = E_0\,(n^\mu\overline{n}^\nu - n^\nu\overline{n}^\mu) - iB_0\,(\epsilon_+^\mu\epsilon_-^\nu - \epsilon_+^\nu\epsilon_-^\mu)\,, \tag{5.46}$$

where E_0 and B_0 are the electric field and magnetic field in the aforementioned frame, respectively, and the new basis ${\epsilon_\pm}^\mu = \frac{1}{\sqrt{2}}(\epsilon \pm i\overline{\epsilon})^\mu$ satisfy $\epsilon_+\epsilon_- = -1$, $\epsilon_\pm^2 = 0$. Moreover, one can recover the field strength tensor as

$$E_0 = \frac{1}{2}\sqrt{\sqrt{I_1^2 + I_2^2} - I_1}\,, \tag{5.47}$$

$$B_0 = -\frac{1}{2}\sqrt{\sqrt{I_1^2 + I_2^2} + I_1} \tag{5.48}$$

with $I_1 = F_{0\mu\nu}{F_0}^{\mu\nu}$ and $I_2 = G_{0\mu\nu}{F_0}^{\mu\nu}$.

Then in the frame of reference where the electric field and the magnetic field of $F_0^{\mu\nu}$ and the propagation direction of $f^{\mu\nu}(\phi)$ are all parallel to each other, the equations of motion are governed by

$$n\ddot{y}_c(\sigma) = -\lambda E_0\, n\dot{y}_c(\sigma)\,, \tag{5.49}$$

$$\overline{n}\ddot{y}_c(\sigma) = \lambda E_0\,\overline{n}\dot{y}_c(\sigma) + \frac{\lambda\epsilon\dot{y}_c\,\dot{f}}{n\dot{y}_c}\,, \tag{5.50}$$

$$\epsilon_+\ddot{y}_c(\sigma) = -i\lambda B_0\,\epsilon_+\dot{y}_c(\sigma) + \frac{\lambda\dot{f}}{\sqrt{2}}\,, \tag{5.51}$$

$$\epsilon_-\ddot{y}_c(\sigma) = i\lambda B_0\,\epsilon_-\dot{y}_c(\sigma) + \frac{\lambda\dot{f}}{\sqrt{2}}\,. \tag{5.52}$$

[1] It should be noted here that this particular frame cannot exist for a crossed field. Consequently, the constant and uniform field strength tensor $F_0^{\mu\nu}$ cannot include a constant and uniform crossed field for this analysis.

As a consequence, the Feynman kernel becomes

$$K_F(x,x') = \sqrt{\left(\frac{1}{2\pi i\hbar}\right)^4 \det\left(\frac{\partial^2 S_c}{\partial x_\mu \partial x'_\nu}\right)} \exp\left(-\frac{i}{\hbar} S_c\right), \tag{5.53a}$$

where the classical action reads

$$S_c = m^2c^2\alpha\tau + \int_0^\tau d\sigma \, \frac{1}{2\alpha}\,(n\dot{y}_c\,\overline{n}\dot{y}_c - \epsilon_+\dot{y}_c\,\epsilon_-\dot{y}_c) \tag{5.53b}$$

with the following solutions of the equations of motion

$$ny_c(\sigma) = nx' + \frac{e^{-\lambda E_0\sigma}-1}{e^{-\lambda E_0\tau}-1} n(x-x'), \tag{5.53c}$$

$$\epsilon_+ y_c(\sigma) = \epsilon_+ x' + \frac{e^{-i\lambda B_0\sigma}-1}{e^{-i\lambda B_0\tau}-1}\left[\epsilon_+(x-x')\right. \tag{5.53d}$$
$$\left. - \frac{i}{\sqrt{2}B_0}\left(\frac{e^{i\lambda B_0(\sigma-\tau)}-1}{1-e^{i\lambda B_0\sigma}}\int_0^\sigma (1-e^{i\lambda B_0\rho})\dot{f}d\rho + \int_\tau^\sigma (1-e^{i\lambda B_0(\rho-\tau)})\dot{f}d\rho\right)\right],$$

$$\epsilon_- y_c(\sigma) = \epsilon_- x' + \frac{e^{i\lambda B_0\sigma}-1}{e^{i\lambda B_0\tau}-1}\left[\epsilon_-(x-x')\right. \tag{5.53e}$$
$$\left. + \frac{i}{\sqrt{2}B_0}\left(\frac{e^{-i\lambda B_0(\sigma-\tau)}-1}{1-e^{-i\lambda B_0\sigma}}\int_0^\sigma (1-e^{-i\lambda B_0\rho})\dot{f}d\rho + \int_\tau^\sigma (1-e^{-i\lambda B_0(\rho-\tau)})\dot{f}d\rho\right)\right],$$

$$\overline{n}y_c(\sigma) = \overline{n}x' + \frac{e^{\lambda E_0\sigma}-1}{e^{\lambda E_0\tau}-1}\left[\overline{n}(x-x')\right. \tag{5.53f}$$
$$\left. - \frac{1}{E_0}\left(\frac{e^{\lambda E_0\tau}-e^{\lambda E_0\sigma}}{e^{\lambda E_0\sigma}-1}\int_0^\sigma (1-e^{-\lambda E_0\rho})\frac{\epsilon\dot{y}_c\,\dot{f}}{n\dot{y}_c}d\rho + \int_\tau^\sigma (1-e^{-\lambda E_0(\rho-\tau)})\frac{\epsilon\dot{y}_c\,\dot{f}}{n\dot{y}_c}d\rho\right)\right].$$

Although the closed expression for the Feynman kernel is very cumbersome and is not shown here, it could be derived by straightforward calculation when the plane wave function $f'(\phi)$ and the components of the field strength tensor of the constant and uniform electromagnetic field ${F_0}^{\mu\nu}$ are known. Moreover, the form of the Feynman kernel given by Eq. (5.53) provides considerable convenience for numerical calculations. Simpler expressions for the propagator can be obtained in the limit $E_0 \to 0$ ($B_0 \to 0$), corresponding to a plane wave combined with a constant and uniform magnetic (electric) field along the propagation direction of the plane wave.

5.4. Conclusion

We have applied the path-dependent formulation of gauge theory within the Feynman path integral formalism of quantum mechanics for a Klein-Gordon particle in an external electromagnetic field. The applied formalism points to a specific gauge when a significant simplification of the expression for quasiclassical propagators is obtained. The simplification is due to the fact that the interaction part of the classical action vanishes in this gauge. In the path-dependent formulation the optimal gauge corresponds to the choice of the classical path in the definition of the vector potential.

Specifically, we have calculated the quasiclassical propagators of a scalar charged particle interacting with an arbitrary constant and uniform electromagnetic field, an arbitrary plane wave and, finally, an arbitrary plane wave combined with an arbitrary constant and uniform electromagnetic field. It is shown that in the classical path gauge the expressions for the quasiclassical propagators, which yield the exact result for above configurations, are more compact.

6. Tunneling time delay

6.1. Introduction

A particular controversial aspect of tunneling and hence tunnel-ionization is the issue of whether the motion of a particle under a barrier is instantaneous or not. The question of whether the tunneling phenomenon contradicts special theory of relativity has been raised [132]. The main difficulty in the definition of the tunneling time delay is due to the lack of a well-defined time operator in quantum mechanics.

In quantum mechanics time, as it stands, is a parameter and not an observable. Furthermore, as it is discussed by Pauli [34, 35], it cannot be upgraded to an operator which is conjugate to the Hamiltonian. In essence, this is due to the fact that the time can take any value, but the spectrum of allowed energy levels of a given Hamiltonian cannot span the entire real line. Namely, either the Hamiltonian is bounded from below or it may take discrete values due to bound states. Nevertheless, a time delay problem can be formulated in quantum mechanics. It is possible to answer in a reasonable way within quantum mechanics the question on how much time an electron spends in a specified space region during its motion and, in particular, to determine the time delay for the tunneling through a potential barrier [33, 36–40, 43, 133–135].

For the generic problem of the tunneling time delay [33] different definitions have been proposed and the discussion of their relevance still continues [36–43, 136]. Recent interest to this problem has been renewed by a unique opportunity offered by attosecond angular streaking techniques for measuring the tunneling time delay during laser-induced tunnel-ionization [137–141]. Here we investigate the tunneling time problem for ionization in nonrelativistic as well as in relativistic settings [45].

Within the quasiclassical description, using either the Wentzel-Kramers-Brillouin (WKB) approximation or a path integration in Euclidean space-time along the imaginary time axis [142–146], the under-the-barrier motion is instantaneous. Thus, we address the time delay problem by going beyond the quasiclassical description [45].

In the present work, we adopt the Eisenbud-Wigner-Smith definition of the time delay (here refered to as the Wigner time delay.) [36–38] which, pictorially, allows to follow the peak of the tunneled wave packet. In this chapter, we find conditions when a non-vanishing Wigner time delay under the barrier for tunnel-ionization is expected to be measurable by attosecond angular streaking techniques [45].

The structure of this chapter is the following. In Sec. 6.2 the tunneling time delay and its corresponding quasiclassical counterpart are investigated and in Sec. 6.3 it is

applied to tunnel-ionization. Later, in Sec. 6.4, we obtain the Wigner trajectory from the phase of the fixed energy propagator . Our conclusions and further remarks are given in Sec. 6.5.

In the reminder of this chapter, we consider tunnel-ionization by a monochromatic plane wave in the infrared ($\omega = 0.05$ a.u.) and we use two extreme but feasible sets of parameters, which ensure that we are in the tunneling regime, viz. $\kappa = 90$ and $E_0/E_a = 1/30$ for the deep-tunneling regime and $E_0/E_a = 1/17$ for the near-threshold-tunneling regime. Formal definitions of these two regimes will be given in Sec. 6.4.3.

Atomic units (a. u.) are used throughout this chapter. The results and the discussion can be partly found in [31, 45] and most of the figures are taken from [45].

6.2. General aspects of the Wigner time delay

The definition of the Wigner time delay is based on the trajectory of the peak of the electron wave packet, as long as the wave packet has a unique peak. Let us illustrate it considering the motion of the following wave packet in position space

$$\langle x|\psi(t)\rangle = \frac{1}{\sqrt{2\pi}} \int_{-\infty}^{\infty} dp \, \exp(ipx) \langle p|\psi(t)\rangle \,, \tag{6.1}$$

assuming that the wave packet in momentum space $\langle p|\psi(t)\rangle$ is centered around p_0 and is expressed in the form

$$\langle p|\psi(t)\rangle = g(p) \exp(-i\phi(p,t)) \tag{6.2}$$

with real functions g and ϕ. The peak of the wave packet in position space at a moment t

$$\langle x|\psi(t)\rangle = \frac{1}{\sqrt{2\pi}} \int_{-\infty}^{\infty} dp \, \exp(i(px - \phi(p,t))) \, g(p) \tag{6.3}$$

can be found in the limit $\Delta p_g \gg \phi'(p_0)$, where Δp_g is the width of the density g, by the stationary phase approximation, and is given by the stationary phase condition

$$\frac{\partial}{\partial p}(px - \phi(p,t))\bigg|_{p_0} = 0 \quad \Rightarrow \quad x = \frac{\partial \phi(p,t)}{\partial p}\bigg|_{p_0} . \tag{6.4}$$

In the limit $\Delta p_g \ll \phi'(p_0)$, the phase ϕ can be linearized, viz., $\phi(p) = \phi(p_0) + \phi'(p_0)(p - p_0)$ and the maximum of the wave-packet is shifted from 0 to $\phi'(p_0)$ due to the coordinate translation operator $\exp[ip\phi'(p_0)]$. Therefore, in both cases the phase derivative at p_0 yields the coordinate of the maximum of the wave-packet. In fact, this result is consistent with the expectation value of the position operator

$$\langle x\rangle = \langle\psi(t)|\, x \,|\psi(t)\rangle = \int_{-\infty}^{\infty} dp \, \left(ig(p)g(p)' + g(p)^2 \phi(p,t)' \right) . \tag{6.5}$$

In the latter expression, the first term vanishes because the wave packet is initially formed symmetrically around p_0, while from the second term one obtains $\langle x\rangle \approx$

$\phi(p_0,t)'$, if the phase $\phi(p,t)'$ is expanded around p_0 and the third and higher-order derivatives are neglected.

Similarly, the wave packet in position space can be expanded in energy eigenfunctions with energy eigenvalues ε [147]

$$\langle x|\psi(t)\rangle = \int_0^\infty d\varepsilon\ \langle x|\varepsilon\rangle\langle\varepsilon|\psi(t)\rangle = \int_0^\infty d\varepsilon\, f(x,\varepsilon)\exp\left(i\varphi(x,\varepsilon) - i\varepsilon(t-t_0)\right)\ , \quad (6.6)$$

where $f(x,\varepsilon) \equiv \langle\varepsilon|\psi(t_0)\rangle\,|\langle x|\varepsilon\rangle|$ and $\langle\varepsilon|\psi(t_0)\rangle$ is the energy distribution of the initial wave packet at $t = t_0$, which is symmetrically centered around ε_0, and $\varphi(x,\varepsilon)$ is the phase of $\langle x|\varepsilon\rangle$, which is the steady-state solution. Analogously to the discussion of the coordinate maximum, the condition

$$\tau \equiv t - t_0 = \left.\frac{\partial\varphi(x,\varepsilon)}{\partial\varepsilon}\right|_{\varepsilon_0} \quad (6.7)$$

determines the moment when the wave packet is maximal at a given point with coordinate x, i. e. , the Wigner trajectory. Eq. (6.7) indicates that the phase of the steady state solution to the Schrödinger equation is sufficient to deduce the Wigner trajectory. The difference between the Wigner trajectory and the classical trajectory, no time interval is spent under the barrier and the trajectory obeys Newton's law outside the barrier[1], at points far behind the barrier we call Wigner time delay [37]. In the following we will apply the Wigner time delay formalism to some exactly solvable basic systems under the dynamics of the Schrödinger equation with some potential $V(x)$. These examples will give us some hints for the analysis of the tunnel-ionization process.

6.2.1. Square potential

As a first example we consider the Wigner time delay during the penetration of a wave packet through a box potential

$$V(x) = V_0\left(\theta(x) - \theta(x-a)\right) \quad (6.8)$$

with $\theta(x)$ denoting the Heaviside step function. The wave packet propagating to the barrier and tunneling through it is constructed via superposing the steady-state solutions with energy eigenvalues $\varepsilon < V_0$,

$$\langle x|\psi(t)\rangle = \int_0^{V_0} d\varepsilon\, \exp\left(-i\varepsilon(t-t_0) + i\phi(x,\varepsilon)\right) g(x,\varepsilon) \quad (6.9)$$

with $g(x,\varepsilon) = \langle\varepsilon|\psi(t_0)\rangle\,|u(x,\varepsilon)|$. Here $\langle\varepsilon|\psi(t_0)\rangle$ is the initial wave packet centered around $\varepsilon_0 < V_0$, $|u(x,\varepsilon)|$ and $\phi(x,\varepsilon)$ are the amplitude and the phase of the steady-state solution $u(x,\varepsilon)$, respectively. We only consider the steady-state solution $u(x,\varepsilon)$

[1] In essence, it is the quasiclassical trajectory since it has a portion under the barrier.

for $\varepsilon < V_0$ due to the assumption that the initial wave packet $\langle\varepsilon|\psi(t_0)\rangle$ has a sharp enough profile such that the integral

$$\langle x|\psi(t)\rangle = \int_{V_0}^{\infty} d\varepsilon \, \exp\left(-i\varepsilon(t-t_0)\right) u(x,\varepsilon) \, \langle\varepsilon|\psi(t_0)\rangle \tag{6.10}$$

vanishes.

Generally, the wave packet in Eq. (6.9) includes both transmitted and reflected waves. To define the Wigner trajectory for the transmitted wave packet, we omit the reflected wave packet from the barrier and utilize the steady-state solutions with positive current

$$u_+(x,\varepsilon) = \begin{cases} e^{ik_1 x} & x < 0 \\ C_1\left(e^{-k_2 x} + ie^{k_2 x}\right) + C_2\left(e^{-k_2 x} - ie^{k_2 x}\right) & 0 \le x \le a \\ Te^{ik_1 x} & x > a \end{cases} \tag{6.11}$$

with $k_1 = \sqrt{2\varepsilon}$, $k_2 = \sqrt{2V_0 - 2\varepsilon}$, and the matching coefficients C_1, C_2 and T[2]. The Wigner trajectory for the transmitted wave can then be defined implicitly via

$$\tau(x) = \left.\frac{\partial\varphi_+(x,\varepsilon)}{\partial\varepsilon}\right|_{\varepsilon=\varepsilon_0} \tag{6.12}$$

where $\varphi_+(x,\varepsilon)$ is the phase of $u_+(x,\varepsilon)$.

The Wigner trajectory for the outgoing wave packet defined in Eq. (6.12), is shown in Fig. 6.1(a) and is compared with the classical trajectory. From the latter one can see that the Wigner trajectory, which initially coincides with the classical one, deviates during tunneling from the classical trajectory. In the quasiclassical limit $\kappa a \gg 1$, the Wigner time delay is $\tau = 1/2\sqrt{(V_0 - \varepsilon_0)\varepsilon_0}$, which is formed when the wave packet enters and exits the barrier.

This simple example provides us the opportunity to compare Wigner's approach with the exact trajectory of the wave packet's maximum which can be calculated via Eq. (6.9). Let us choose the initial normalized wave packet in momentum space as the following Gaussian

$$\langle p|\psi(t_0=0)\rangle = \frac{e^{-ix_0(p-p_0)}}{(2\pi\delta p^2)^{1/4}} \exp\left[-\left(\frac{p-p_0}{2\delta p}\right)^2\right], \tag{6.13}$$

with initial position x_0 and initial momentum $p_0 = \sqrt{2\varepsilon_0}$. The position x_0 is assumed to be far away from the barrier and the energy spread $\delta\varepsilon$ of the wave packed so small that $\varepsilon_0 + \delta\varepsilon < V_0$ with $\delta\varepsilon = p_0\delta p$. To be consistent with the tunnel-ionization case, where the wave packet has a sharp energy, we assume that $\delta p/p \ll 1$. Then, the time evolution of the wave packet becomes

$$\langle x|\psi(t)\rangle = \int_0^{\infty} d\varepsilon \, \frac{\langle x|\varepsilon\rangle}{(2\pi\delta p^2)^{1/4}} e^{-i\varepsilon t - ix_0(\sqrt{2\varepsilon} - \sqrt{2\varepsilon_0}) - \left(\frac{\sqrt{2\varepsilon} - \sqrt{2\varepsilon_0}}{2\delta p}\right)^2}. \tag{6.14}$$

[2]Note that the coefficients are matched by requiring continuity of the wave function $u(x,\varepsilon)$, which includes the reflected portion of the wave function rather than $u_+(x,\varepsilon)$. Furthermore, one can also omit the reflected portion of the wave packet valid for the under-the-barrier motion by setting C_2 to zero in Eq. (6.11). However it does not affect the Wigner time delay.

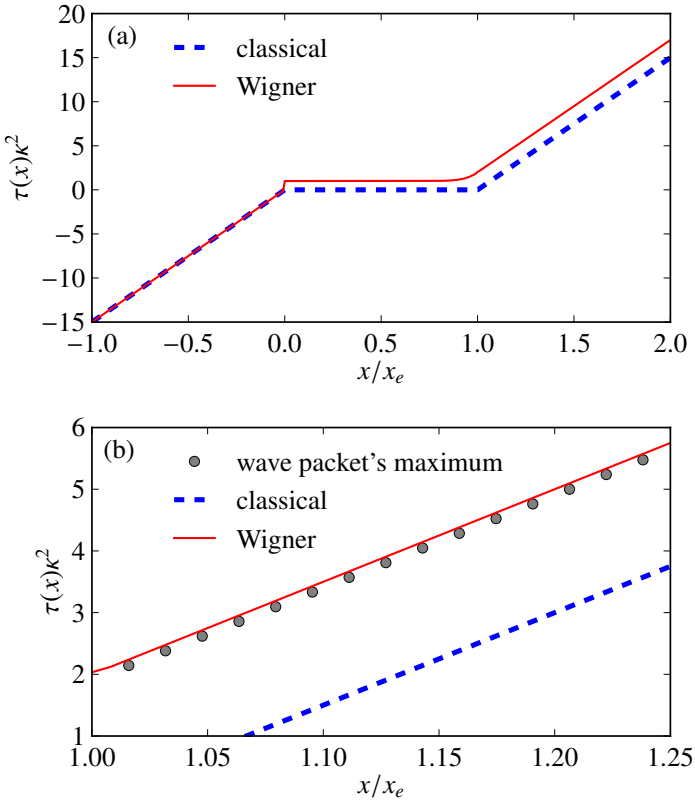

Figure 6.1. – (a) Comparison of the Wigner trajectory (6.12) (solid red line) and the classical (dashed blue line) trajectory for tunneling through a square potential barrier (6.8). The applied parameters are $V_0 = 2\varepsilon_0$, $\varepsilon_0 = I_p$, $I_p = c^2 - \sqrt{c^4 - c^2\kappa^2}$ with $\kappa = 90$ and $a = 14/\kappa$. (b) Close-up of (a) with additionally showing the position of the wave packet's maximum.

If we trace the maximum of the wave packet outside the barrier, we see that it overlaps with Wigner trajectory defined in Eq. (6.12). The result can be seen in Fig. 6.1(b).

To investigate the role of the magnetic field in relativistic tunnel-ionization, we modify the previous configuration by applying an additional static magnetic field within the square potential. The vector potential which generates the magnetic field $\boldsymbol{B} = -E_0\,(\theta(x) - \theta(x-a))\,\hat{y}$ may be written as

$$\boldsymbol{A} = E_0\,(x\,(\theta(x) - \theta(x-a)) + a\theta(x-a))\,\hat{z}\,. \tag{6.15}$$

Then, the Hamiltonian for this field configuration is given by

$$H = \frac{p_x^2}{2} + \frac{[p_z + A_z(x)/c]^2}{2} + V(x)\,. \tag{6.16}$$

Since the canonical momentum p_z is conserved, $[p_z, H] = 0$, the energy eigenfunctions have the form

$$\langle x, z|\varepsilon, p_z\rangle = \frac{u(x, p_z, \varepsilon)}{\sqrt{2\pi}} e^{ip_z z}, \tag{6.17}$$

and the motion along the x coordinate is separable

$$\left[-\frac{1}{2}\frac{d^2}{dx^2} + \frac{(p_z + A_z(x)/c)^2}{2} + V(x)\right] u(x, p_z, \varepsilon) = \varepsilon\, u(x, p_z, \varepsilon)\,. \tag{6.18}$$

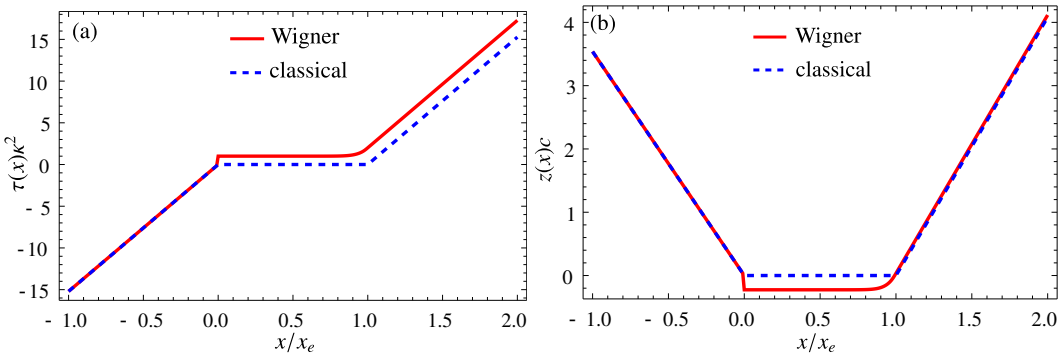

Figure 6.2. – Tunneling through a square potential with an additional magnetic field with $E_0 = \kappa^3/30$ and other parameters as in Fig. 6.1. Sub-figures (a) and (b) compare the Wigner (red solid lines) and the classical (blue dashed lines) trajectories along the x direction and in the x-z-plane, respectively.

The solution of Eq. (6.18) outside the barrier is given by

$$u(x, p_z, \varepsilon) = \begin{cases} u_1(x, p_z, \varepsilon) = e^{ik_1 x} + Re^{-ik_1 x} & x < 0 \\ u_3(x, p_z, \varepsilon) = Te^{ik_3 x} & x > a \end{cases} \tag{6.19}$$

with $k_1 = \sqrt{2\varepsilon - p_z^2}$, $k_3 = \sqrt{2\varepsilon - (p_z + aE_0/c)^2}$, and the reflection and transmission coefficients are R and T, respectively. For the dynamics under the barrier ($0 \le x \le a$, $\varepsilon < V_0$) the Schrödinger equation

$$\left[-\frac{1}{2}\frac{d^2}{dx^2} + \frac{(p_z - xE_0/c)^2}{2} + V_0\right] u_2(x, p_z, \varepsilon) = \varepsilon\, u_2(x, p_z, \varepsilon) \tag{6.20}$$

has two linearly independent solutions, which can be expressed using the parabolic cylinder function D [148] as

$$\begin{aligned} u_2(x, p_z, \varepsilon) = {} & C_1\, D\left(-\frac{E_0 + 2cV_0 - 2c\varepsilon}{2E_0}, \frac{\sqrt{2}(cp_z + E_0 x)}{\sqrt{cE_0}}\right) \\ & + C_2\, D\left(-\frac{E_0 - 2cV_0 + 2c\varepsilon}{2E_0}, \frac{i\sqrt{2}(cp_z + E_0 x)}{\sqrt{cE_0}}\right). \end{aligned} \tag{6.21}$$

Here, the matching coefficients C_1 and C_2 can be found by using the continuity of the wave function at the borders of the potential ($x = 0$ and $x = a$). The wave packet which has tunneled out of the potential barrier is

$$\begin{aligned} \langle x, z|\psi(t)\rangle &= \int_{-\infty}^{\infty} dp_z \int_0^{V_0} d\varepsilon\, \langle x, z|\varepsilon, p_z\rangle \langle \varepsilon, p_z|\psi(t)\rangle\,, \\ &= \frac{1}{\sqrt{2\pi}} \int_{-\infty}^{\infty} dp_z \int_0^{V_0} d\varepsilon\, e^{izp_z - i\varepsilon(t-t_0) + i\phi_+(x,p_z,\varepsilon)} g(x, p_z, \varepsilon)\,, \end{aligned} \tag{6.22}$$

where $g(x, p_z, \varepsilon) = \langle \varepsilon, p_z|\psi(t_0)\rangle\, |u(x, p_z, \varepsilon)|$, $\langle \varepsilon, p_z|\psi(t_0)\rangle$ is the initial wave packet centered around p_{z0} and ε_0, and $\phi_+(x, p_z, \varepsilon)$ is the phase of the outgoing part of $u(x, p_z, \varepsilon)$.

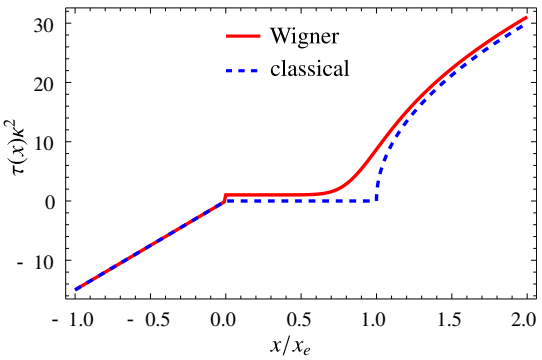

Figure 6.3. – Comparison of the Wigner trajectory (red solid line) and the classical trajectory (blue dashed line) for tunneling through a linear potential barrier (6.25) for $V_0 = 2\varepsilon_0$, $\varepsilon_0 = I_p$, with the numerical parameters $\kappa = 90$, and $E_0/E_a = 1/30$.

Calculating the transition probability $|T|^2$ as a function of p_z, we find that the maximum is reached at $p_{z0} = -I_p/(2c)$ which equals the kinetic momentum at the tunneling entry $x = 0$, $q_z(0) = -I_p/(2c)$. At the tunneling exit $x = a$ the kinetic momentum with maximal tunneling probability is $q_z(a) = p_{z0} + A_z(a)/c = I_p/(2c)$.

As the phase now depends also on p_z, Eq. (6.12) generalizes to

$$\tau(x) = \left.\frac{\partial \varphi_+(x, p_z, \varepsilon)}{\partial \varepsilon}\right|_{\varepsilon=\varepsilon_0} . \tag{6.23}$$

Thus, for each choice of p_z, Eq. (6.23) defines a different trajectory and setting $p_z = p_{z0}$ in Eq. (6.23) gives the most probable trajectory, which is shown in Fig. 6.2(b) together with the classical one. Comparing Figs. 6.1(a) and 6.2(a) shows that the presence of the magnetic field does not change the Wigner time delay.

In analogy to Eq. (6.4), one can also define the coordinate z as a function of x

$$z = -\left.\frac{\partial \phi_+(x, p_z, \varepsilon_0)}{\partial p_z}\right|_{p_z=p_{z0}} , \tag{6.24}$$

which gives the most probable trajectory (path) in the x-z-plane as shown in Fig. 6.2(b) together with the corresponding classical trajectory. Outside the barrier both the Wigner and the classical trajectory nearly coincide; under the barrier, however, the Wigner trajectory shows a clear spatial drift into the z-direction, that is perpendicular to the tunneling direction. Nevertheless, this spatial drift is (in contrast to the Wigner time delay) not observable on the detector at remote distances. This is intuitively plausible, because the drift at the entry point to the barrier $\Delta z_d(0) = q_z(0)\tau = -(I_p/2c)\tau$ is exactly compensated by the drift at the exit point $\Delta z_d(a) = q_z(a)\tau = (I_p/2c)\tau$.

6.2.2. Linear potential

As a second example, we consider tunneling through a linear potential barrier

$$V(x) = \theta(x)\,(E_0 x + V_0) \ . \tag{6.25}$$

The solution of the corresponding Schrödinger equation is given for the domain

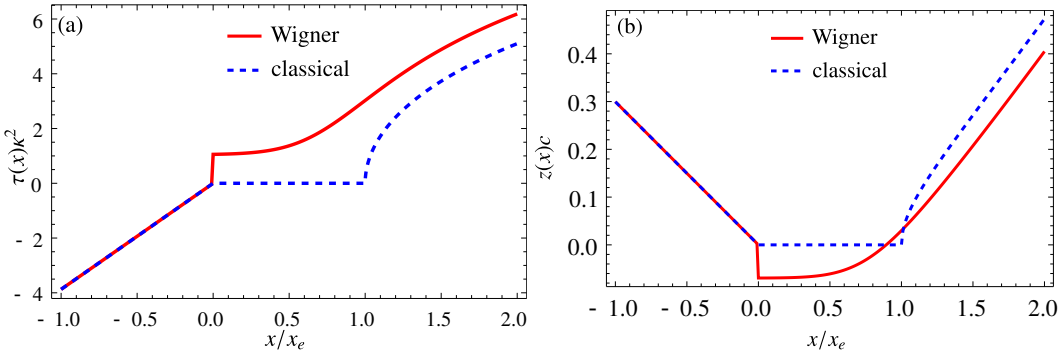

Figure 6.4. – (a) Comparison of the Wigner trajectory (red solid line) and the classical trajectory (blue dashed line) for tunneling through the parabolic potential barrier (6.27) for $V_0 = 2\varepsilon_0$, $\varepsilon_0 = I_p$ with the numerical parameters $\kappa = 90$, and $\beta = 1/30$. (b) The coordinate z as a function of x for tunneling through a parabolic potential barrier in the presence of a magnetic field.

$x < 0$ by

$$u_1(x,\varepsilon) = e^{ik_1 x} + Re^{-ik_1 x} \tag{6.26a}$$

with $k_1 = \sqrt{2\varepsilon}$ and the reflection coefficient R. In the region $x \geq 0$, the solution can be written as

$$\begin{aligned} u_2(x,\varepsilon) &= T\left(\mathrm{Ai}\left(\frac{2E_0x + 2(V_0-\varepsilon)}{(2E_0)^{2/3}}\right) + i\,\mathrm{Bi}\left(\frac{2E_0x + 2(V_0-\varepsilon)}{(2E_0)^{2/3}}\right)\right) \\ &= T\,\mathrm{Ai}\left(e^{-2\pi i/3}\frac{2E_0x + 2(V_0-\varepsilon)}{(2E_0)^{2/3}}\right), \end{aligned} \tag{6.26b}$$

where Ai and Bi are the Airy function of first and second kind, respectively. Under the barrier, that is $0 \leq x \leq x_e$ with the tunneling exit point $x_e = -\varepsilon_0/E_0$, the wave function (6.26b) is a superposition of reflected and transmitted portions. The transmission coefficient T in (6.26b) is deduced from matching the wave functions at the border $x = 0$. The phase of the total wave function (6.26) is used to calculate the Wigner trajectory (6.7), which is compared in Fig. 6.3 with the classical one. This comparison shows that shortly before the tunneling exit x_e, a substantial time delay builds up, which is reduced after tunneling. Finally, a non-vanishing Wigner time delay remains which is detectable at a remote detector. This time delay is induced during entering the barrier and equals in magnitude $\tau = 1/(2\sqrt{(V_0-\varepsilon_0)\varepsilon_0})$.

6.2.3. Parabolic potential

As a last example we examine the Wigner time delay for tunneling through a parabolic potential barrier

$$V(x) = \theta(x)\left(-\beta\kappa^4 x^2 + V_0\right), \tag{6.27}$$

with a dimensionless parameter β. In this case, the exact solution for the region $x \geq 0$ is given by

$$u_2(x,\varepsilon) = T\,D\left(-\frac{1}{2} - \frac{i(V_0-\varepsilon)}{\sqrt{2}\sqrt{\beta}\kappa^2}, -(-2)^{3/4}x\beta^{1/4}\kappa\right), \tag{6.28}$$

with the transmission coefficient T and D denoting parabolic cylinder functions [148]. The Wigner and the classical trajectories for tunneling through the parabolic potential are compared in Fig. 6.4(a). Qualitatively, the Wigner time delay behaves similar as for the case of a linear potential. In the barrier close to the exit a time delay is built up, which is reduced after tunneling and eventually a small non-vanishing Wigner time delay remains.

In analogy to Sec. 6.2.1 we add now to the parabolic potential (6.27) a static magnetic field in the region $x > 0$ and investigate the spatial drift in the Wigner time delay which is induced by the magnetic field. Introducing the vector potential $A_z(x) = \theta(x)E_0x$, this scenario can be described by the Hamiltonian

$$H = \frac{p_x^2}{2} + \frac{[p_z + A_z(x)/c]^2}{2} + V(x)\,. \tag{6.29}$$

The canonical momentum that maximizes the tunneling probability equals $p_z = -0.15I_p/c$. The coordinate z as a function of x is shown in Fig. 6.4(b) for this canonical momentum. As in the case of a square potential with magnetic field, the spatial shift between the classical and the Wigner trajectories is small.

6.3. Time delay in tunnel-ionization

The previous sections' techniques can also be employed to analyze tunnel-ionization in Hydrogenic ions as considered in Sec. 3.4. The fundamental difference between the above one-dimensional model systems and tunnel-ionization in Hydrogenic ions is that in the former cases there is a source that produces a positive current incident on the tunneling barrier. In the latter case, however, a bound state tunnels through a barrier and consequently the continuum wave function has to be matched with the bound state wave function, instead of the incident and the reflected plane waves as in the model systems. In the model systems of Sec. 6.2 the Wigner trajectory and the classical trajectory coincide before they enter the tunneling barrier.

This, however, is no longer true for tunnel-ionization from bound states, which can be explained by observing that some portion of the bound state resides always in the barrier. In order to define a meaningful Wigner time delay, one has to match the classical trajectory with the Wigner one at the entry point x_0. As a consequence, the Wigner trajectory for tunnel-ionization $\tau_{\mathrm{TI}}(x)$ may be defined via the relation

$$\tau_{\mathrm{TI}}(x) = \tau(x) - \tau(x_0)\,. \tag{6.30}$$

Hence the corresponding Wigner time delay for tunnel-ionization is identified as

$$\tau_{\mathrm{W}} = \tau_c(\infty) - \tau_{\mathrm{TI}}(\infty) \tag{6.31}$$

with the classical trajectory $\tau_c(x)$. Since the coefficients that match the bound wave function and the continuum wave function are position independent, the Wigner trajectory $\tau_{\mathrm{TI}}(x)$ for tunnel-ionization is solely determined by the phase of the wave

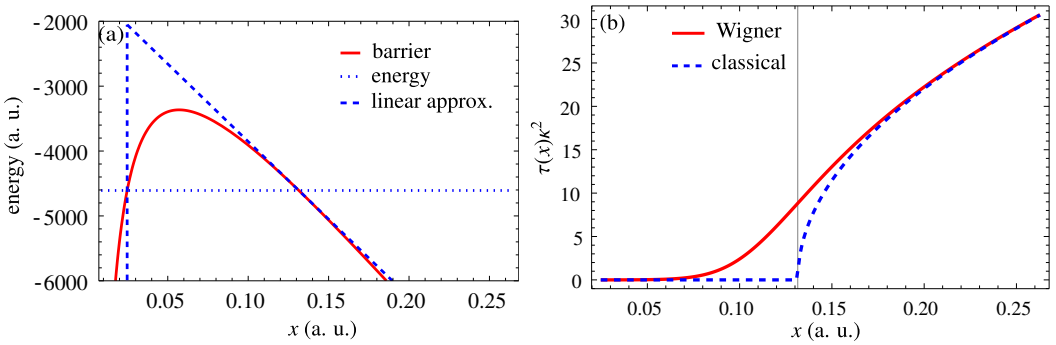

Figure 6.5. – (a) The potential barrier (6.32) (red solid line) and its linear approximation (6.34) (blue dashed line) in the deep-tunneling regime. The blue dotted line indicates the energy level of the bound state with $\varepsilon = -I_p$. (b) The Wigner trajectory (red solid line) and the classical trajectory (blue dashed line) in the deep-tunneling regime for nonrelativistic tunnel-ionization with $\kappa = 90$ and $E_0/E_a = 1/30$. The vertical black line indicates the exit coordinate.

function which is the solution of the corresponding Schrödinger equation for the potential

$$V(x) = \theta(x - x_0)(xE_0 - \kappa/x) \tag{6.32}$$

and represents asymptotically a plane wave. Although there is no analytical solution for this potential, approximate solutions can be found in limiting cases which we will discuss in this section.

6.3.1. Nonrelativistic case

In the one-dimensional tunneling picture, the relevant Schrödinger equation is, within the electric dipole approximation, is given by

$$\left(-\frac{1}{2}\frac{d^2}{dx^2} + xE_0 - \frac{\kappa}{|x|}\right)\psi(x) = \varepsilon\,\psi(x)\,. \tag{6.33}$$

When the tunneling potential is of sufficient height (deep-tunneling regime), the potential barrier (6.32) can be approximated near the tunneling exit point x_e by a linear potential

$$V(x) = V(x_e) + V'(x_e)(x - x_e)\,, \tag{6.34}$$

see Fig. 6.5(a). With this approximation the problem of tunnel-ionization in Hydrogenic ions resembles the case of a linear potential as discussed in Sec. 6.2.2. Therefore, in the deep-tunneling regime, the solution of the Schrödinger equation is given by the Airy function

$$\psi(x) = \mathrm{Ai}\left(e^{-2\pi i/3}\frac{-2xV'(x_e) - 2\left(\varepsilon + V(x_e) - x_eV'(x_e)\right)}{2^{2/3}\left(-V'(x_e)\right)^{2/3}}\right). \tag{6.35}$$

Note, that the potentials considered in Sec. 6.2.2 and here differ in their positions, heights, and slopes. The comparison between the Wigner trajectory and the classical

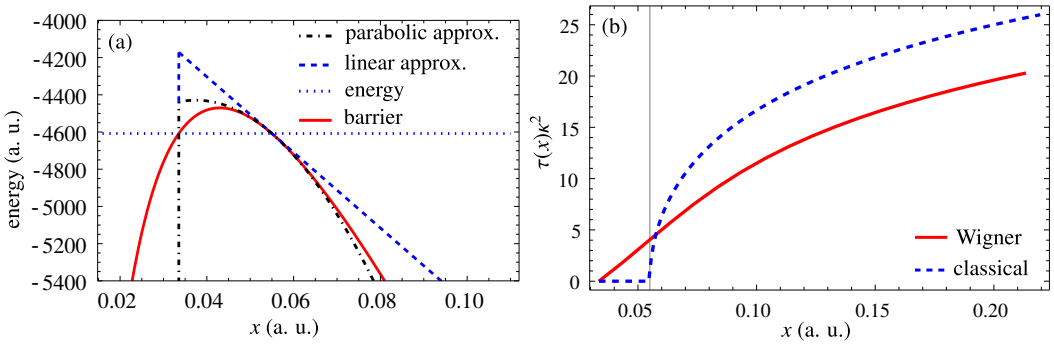

Figure 6.6. – (a) The tunneling barrier (6.32) (red solid line), its linear approximation (6.34) (blue dashed line), and the quadratic approximation (6.36) (black dash-dotted line) in the near-threshold-tunneling regime. The blue dotted line indicates the energy level of the bound state with $\varepsilon = -I_p$. (b) The Wigner (red solid line) and the classical trajectories (blue dashed line) in the near-threshold-tunneling regime for nonrelativistic tunnel-ionization with $\kappa = 90$ and $E_0/E_a = 1/17$. The vertical black line indicates the exit coordinate.

trajectory are plotted in Fig. 6.5(b). In contrast to the linear potential case of Sec. 6.2.2 the Wigner trajectory catches up the classical one at far distance and consequently the Wigner time delay vanishes.

When the electric field strength is increased, but the dynamics still remains in the tunneling regime, the linear approximation (6.34) becomes invalid. We may call this regime near-threshold-tunneling regime of ionization. In this regime the potential may be approximated by including the next quadratic term

$$V(x) = V(x_e) + V'(x_e)(x - x_e) + V''(x_e)\frac{(x - x_e)^2}{2}, \tag{6.36}$$

see Fig. 6.6(a). As a consequence, the solution of the Schrödinger equation in the near-threshold-tunneling regime can be expressed using the parabolic cylinder function as

$$\psi(x) = D(a, b) \tag{6.37a}$$

with

$$a = -\frac{i\left(V'(x_e)^2 - \left(2\varepsilon + 2V(x_e) + i\sqrt{V''(x_e)}\right)V''(x_e)\right)}{2V''(x_e)^{3/2}}, \tag{6.37b}$$

$$b = \frac{(1-i)\left(V'(x_e) + (x - x_e)V''(x_e)\right)}{V''(x_e)^{3/4}}. \tag{6.37c}$$

A comparison of the Wigner and the classical trajectories in the near-threshold-tunneling regime is shown in Fig. 6.6(b). A non-vanishing Wigner time delay exists in this case due to the parabolic character of the potential barrier near the tunneling exit x_e.

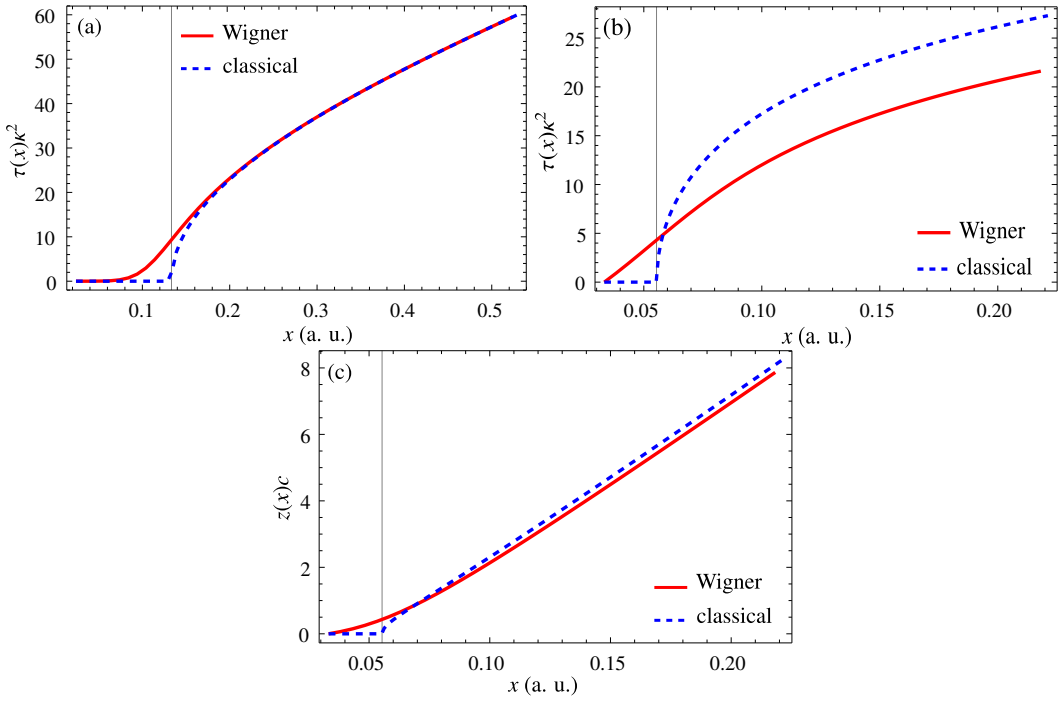

Figure 6.7. – Comparison of the Wigner (red solid line) and the classical trajectories (blue dashed line) for tunnel-ionization taking into account leading effects in $1/c$ (magnetic dipole effects): (a) for the deep-tunneling regime with the most probable momentum at the exit $q_z(x_e) = 0.28I_p/c$, $\kappa = 90$ and $E_0/E_a = 1/30$; (b) for the near-threshold-tunneling regime with $q_z(x_e) = 0.12I_p/c$, $\kappa = 90$ and $E_0/E_a = 1/17$. Corresponding classical and Wigner trajectories z as a function of x are presented in (c) for parameters of (b). The vertical black lines indicate the exit coordinate.

6.3.2. Magnetic dipole effects

When the laser's magnetic field is taken into account, tunnel-ionization in Hydrogenic systems can be described by a one-dimensional model if one introduces a position dependent energy level inside the barrier as discussed in Sec. 3.4. In this one-dimensional model the role of the curvature of the potential barrier and, therefore, its approximations are the same as in the nonrelativistic case within the electric dipole approximation. As for the square and the parabolic potentials with magnetic field we calculate the Wigner time delay when the tunneling probability is maximal. This happens at a certain non-vanishing momentum along the laser's propagation direction.

The leading term in $1/c$ is the magnetic dipole correction. Including the latter into the Schrödinger equation in the electric dipole approximation yields

$$\left[-\frac{1}{2}\frac{d^2}{dx^2} + \frac{(p_z - xE_0/c)^2}{2} + xE_0 - \frac{\kappa}{|x|}\right]\psi(\boldsymbol{x}) = \varepsilon\psi(\boldsymbol{x})\,. \tag{6.38}$$

As a consequence of the presence of the vector potential term, for both deep-tunneling and near-threshold-tunneling regimes, the relevant solutions are given by parabolic

cylinder functions. Since the quadratic approximation covers also the deep-tunneling regime, in the former case the solution yields

$$\psi(x) = D\,(a, b) \tag{6.39a}$$

with

$$\begin{aligned} a = & \frac{c\left(-cV''(x_e)\sqrt{c^2V''(x_e)+E_0^2} - E_0^2\sqrt{E_0^2/c^2+V''(x_e)}\right)}{2\left(c^2V''(x_e)+E_0^2\right)^{3/2}} \\ & + \frac{c^3\left(V''(x_e)\left(p_z^2+2V(x_e)-2\varepsilon\right)-V'(x_e)^2\right)}{2\left(c^2V''(x_e)+E_0^2\right)^{3/2}} \\ & + \frac{c\left(-2cE_0p_z\left(V'(x_e)-x_eV''(x_e)\right)\right)}{2\left(c^2V''(x_e)+E_0^2\right)^{3/2}} + \frac{c\left(E_0^2\left(x_e^2V''(x_e)-2\left(x_eV'(x_e)+\varepsilon\right)+2V(x_e)\right)\right)}{2\left(c^2V''(x_e)+E_0^2\right)^{3/2}}, \end{aligned} \tag{6.39b}$$

$$b = -\frac{i\sqrt{2}\left(c^2(x-x_e)V''(x_e)+c^2V'(x_e)+E_0(cp_z+E_0x)\right)}{c^2\left(E_0^2/c^2+V''(x_e)\right)^{3/4}}. \tag{6.39c}$$

In the deep-tunneling regime, where the potential barrier is approximately linear, the Wigner time delay vanishes as plotted in Fig. 6.7(a). However, when tunneling happens in the near-threshold-tunneling regime, there exists a non-zero Wigner time delay, see Fig. 6.7(b). Its order of magnitude equals the result of the nonrelativistic near-threshold-tunneling regime ionization, compare Figs. 6.6(b) and 6.7(b). Moreover, due to the non-vanishing Wigner time delay, a spatial shift between the classical trajectory and the Wigner trajectory along the laser's propagation direction is expected because of the Lorentz force. Both trajectories are shown in Fig. 6.7(c).

6.3.3. Relativistic effects

In order to investigate relativistic effects in the relevant weakly relativistic regime, the leading relativistic corrections to the kinetic energy are expected to be dominant with regard to the Wigner time delay. For simplicity, the exact Klein-Gordon equation is solved in a regime where, the higher order relativistic effects play no significant role. Other leading relativistic effects of order $1/c^2$ like those depending on the spin and on the magnetic field are conjectured to be smaller than the leading relativistic correction to the kinetic energy. In our one-dimensional intuitive picture of Sec. 3.4, the corresponding Klein-Gordon equation yields

$$\left(-c^2\frac{d^2}{dx^2}+c^4\right)\psi(x) = \left(\varepsilon - V(x)\right)^2\psi(x) \tag{6.40}$$

with the potential barrier (6.32).

In the deep-tunneling regime, we can linearize the potential barrier, i. e., $V(x) = V(x_e) + V'(x_e)(x - x_e)$. The corresponding solution which, asymptotically, has the

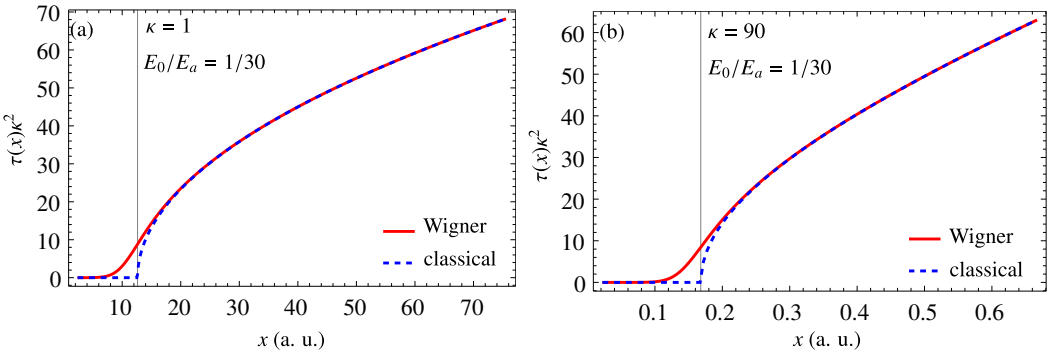

Figure 6.8. – Comparison of the Wigner trajectory (red solid line) and the classical trajectory (blue dashed line) for tunnel-ionization taking into account kinematic relativistic effects for the deep-tunneling regime employing nonrelativistic (part (a)) and relativistic (part (b)) parameters. In both parameter regimes no non-zero time delay is detectable at remote distance. The vertical black line indicates the exit coordinate.

form of a plane wave, reads

$$\psi(x) = D\,(a, b) \tag{6.41a}$$

with

$$a = -\frac{1}{2} + \frac{ic^3}{2V'(x_e)}\,, \quad b = -\frac{(1+i)\,((x-x_e)V'(x_e) + V(x_e) - \varepsilon)}{\sqrt{c}\,\sqrt{V'(x_e)}}\,. \tag{6.41b}$$

For the deep-tunneling regime, where the Wigner time delay is zero in the nonrelativistic case, the relativistic corrections to the kinetic energy are also not able to induce a non-zero Wigner time delay as illustrated in Fig. 6.8.

As pointed out in Sec. 6.3.1, an analysis of tunneling from a Coulomb potential in the near-threshold-tunneling regime employs best a quadratic fitting of the tunneling barrier in the vicinity of the tunneling exit. However, there is still no analytic solution to this problem. Therefore, we replace now the Coulomb potential again with a zero-range potential rendering the linear approximation applicable again apart for the singular position of the core. Note that the high nonlinearity of the effective potential barrier near the core is still maintained. Then, the solution indicates that the leading relativistic correction to the kinetic energy has a negligible effect on the Wigner time delay as illustrated in Fig. 6.9. In this figure, the scaled Wigner time delay $\tau_W I_p$ for the nonrelativistic (dashed lines) as well as relativistic case (solid lines) is shown for different values of I_p and of E_0/E_a.

6.4. The phase of the fixed energy propagator

In the previous sections we have related the Wigner time delay to the phase of the corresponding steady-state wave function. This way of identifying the time delay is convenient, especially for tunnel-ionization, due to the fact that the relevant phase is independent of the matching coefficients, see Sec. 6.3. Alternatively, one can

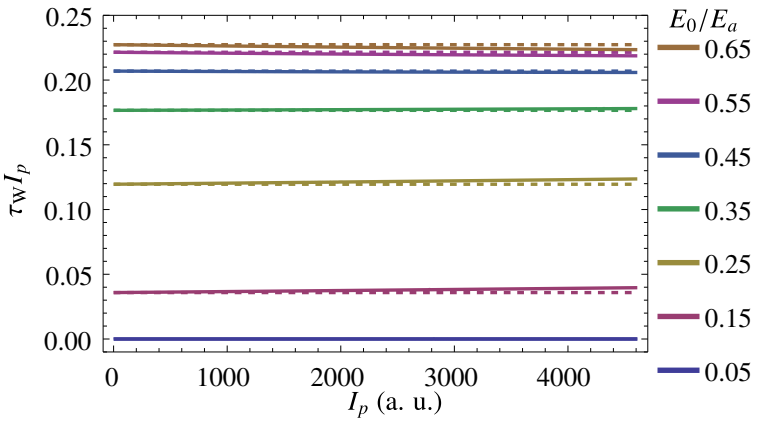

Figure 6.9. – The scaled Wigner time delay $\tau_W I_p$ as a function of I_p for different values of E_0/E_a for tunnel-ionization taking into account relativistic kinematic effects (solid lines) and for nonrelativistic tunnel-ionization (dashed lines) for the zero-range potential. Note the increasing small deviations of the scaled Wigner time delay with increasing I_p(relativistic effects).

identify the Wigner trajectory in terms of the phase of the corresponding fixed energy propagator. This identification is not only of intellectual interest, but also provides an easier way to calculate the Wigner trajectory in particular cases, for instance, in the highly relativistic case, where the associated phase is harder to handle.

The basic idea is to reveal the phase of the steady-state wave function via the fixed energy propagator. The steady-state wave function is the solution of the corresponding Schödinger equation for constant electromagnetic field. In fact, the steady-state solution is only valid in certain set of gauges, where the Hamiltonian coincides with the total energy operator. As a consequence, in order to reveal the phase, we need to calculate the fixed energy propagator in these gauges. In general, this can be accomplished by the Göppert-Mayer gauge which, in the absence of the magnetic field, reduces to the length gauge, see Sec. 2.2.1.

Here, we stick to the one-dimensional intuitive picture of tunneling, Sec. 3.4, and hence we will either calculate the propagators for one spatial dimension (electric field direction) or reduce the full propagator along the electric field direction via the Fourier transforms on the other coordinates.

Our fundamental definition of the Wigner trajectory follows from the relation between the spacetime propagator $G(x, x'; t)$ and the fixed energy propagator $\tilde{G}(x, x'; \varepsilon)$

$$G(x, x'; t) = \frac{1}{2\pi} \int_{-\infty}^{\infty} d\varepsilon \, \exp(-i\varepsilon t) \, \tilde{G}(x, x'; \varepsilon) \, . \tag{6.42}$$

Similarly to the case discussed in Sec. 6.2, the fixed energy propagator can be split into its phase ϕ and its amplitude A. Then the spacetime propagator reads

$$G(x, x'; t) = \frac{1}{2\pi} \int_{-\infty}^{\infty} d\varepsilon \, A(x, x', \varepsilon) \exp\left(-i\varepsilon t + i\phi(x, x', \varepsilon)\right) \, . \tag{6.43}$$

Finally, applying the stationary phase condition, the Wigner trajectory can be expressed as

$$\tau(x, x') = \left.\frac{\partial\phi(x, x', \varepsilon)}{\partial\varepsilon}\right|_{\varepsilon=\varepsilon_0} \tag{6.44}$$

with the energy of the incoming wave packet ε_0. Here we should stress that the identification of the Wigner trajectory by means of the phase of the electron's propagator is similar to the procedure given in Sec. 6.2. Nevertheless, Eq. (6.44) is based on a more fundamental approach that prevents us to discuss the appropriate conditions in order to identify a well-defined Wigner trajectory by means of wave packets.

In the tunnel-ionization case we have argued that the classical trajectory and the Wigner trajectory have to coincide at the entry point of the tunneling barrier x_i. Therefore, we impose the same condition here and we obtain the Wigner trajectory for the tunnel-ionization in terms of the phase of the fixed energy propagator as

$$\tau_{\mathrm{TI}}(x) \equiv \left.\frac{\partial\phi(x, x_i, \varepsilon)}{\partial\varepsilon}\right|_{\varepsilon=\varepsilon_0} - \left.\frac{\partial\phi(x_i, x_i, \varepsilon)}{\partial\varepsilon}\right|_{\varepsilon=\varepsilon_0} \tag{6.45}$$

with $\varepsilon_0 = c^2 - I_p$, where $I_p = c^2 - \sqrt{c^4 - c^2\kappa^2}$ is the ionization energy of the ground state of H-like ion.

The remaining task is to calculate the fixed energy propagator and its phase. Here we will focus on the relativistic tunnel-ionization from a zero-range potential under the effect of the constant and uniform electric field and the constant and uniform crossed fields (6.57). The relativistic fixed energy propagator can be identified via the inverse Fourier transform as

$$\tilde{G}(x, x'; \varepsilon) = \int_0^\infty dt\, \exp(i\varepsilon t)\, G(x, x'; t)\,, \tag{6.46}$$

where the corresponding spacetime propagators $G(x, x'; t)$ were already calculated in chapter 5.

6.4.1. Constant and uniform electric field

Let us apply the developed formalism first to tunnel-ionization from a zero-range potential under the effect of a constant and uniform electric field

$$\boldsymbol{E} = E_0\, \hat{\boldsymbol{x}}\,. \tag{6.47}$$

Following the calculation performed in Sec. 5.3.1, the spacetime propagator along the electric field direction x in the length gauge $A^\mu = (-xE_0, 0)$ can be written as

$$\begin{aligned} G(x, 0; t) = &-\frac{iE_0 \exp(-iE_0 t x/2)}{8\pi c} \int_0^\infty d\tau\, \mathrm{csch}\left(\frac{E_0\tau}{2c}\right) \\ &\times \exp\left(-\frac{i\left(2c^3\tau - E_0 x^2 \coth\left(\frac{E_0\tau}{2c}\right)\right)}{4c} - \frac{i}{4}E_0 c t^2 \coth\left(\frac{E_0\tau}{2c}\right) - \epsilon\tau\right). \end{aligned} \tag{6.48}$$

with the Feynman $i\epsilon$ prescription. Here the tunneling entry point for the tunnel-ionization form a zero-range potential can be set as $x_i = 0$.

Then using the inverse Fourier transform (6.46), the corresponding fixed energy propagator in the length gauge reads

$$\tilde{G}(x,0;\varepsilon) = -i\sqrt{\frac{E_0}{2\pi i\, c^3}}\int_0^\infty d\tau\, \frac{1}{\sqrt{\sinh(E_0\tau/c)}} \tag{6.49}$$
$$\times \exp\left(-i\frac{\tau c^2}{2} + i\frac{E_0 x^2}{4c}\coth\left(\frac{E_0\tau}{2c}\right) + i\frac{(E_0 x - 2\varepsilon)^2}{4E_0 c}\tanh\left(\frac{E_0\tau}{2c}\right) - \epsilon\tau\right),$$

where we have omitted the complementary error function for the sake of simplicity due to the fact that it does not affect the phase.

Before calculating the Wigner trajectory via the phase of Eq. (6.49), we will present the classical trajectory via the proper time parametrization.

The classical equations of motion are governed by Eq. (5.19)

$$\ddot{y}(\sigma)_c{}^\mu = -\frac{1}{c}F^\mu{}_\nu(y_c)\dot{y}(\sigma)_c{}^\nu\,. \tag{6.50}$$

The solutions for a constant and uniform electric field (6.47) read

$$y^0(\tau) = \frac{cu_0{}^0\sinh\left(\frac{E_0\tau}{c}\right) - cu_0{}^1\cosh\left(\frac{E_0\tau}{c}\right) + cu_0{}^1 + E_0 x_0{}^0}{E_0}\,, \tag{6.51}$$

$$y^1(\tau) = \frac{-cu_0{}^0\cosh\left(\frac{E_0\tau}{c}\right) + cu_0{}^1\sinh\left(\frac{E_0\tau}{c}\right) + cu_0{}^0 + E_0 x_0{}^1}{E_0} \tag{6.52}$$

with the initial conditions $y^\mu(0) = x_0{}^\mu$ and $\dot{y}^\mu(0) = u_0{}^\mu$, where $x_0{}^\mu$ and $u_0{}^\mu$ are the initial spacetime point and the initial four-velocity, respectively. After setting $x_0{}^0 = 0$, i.e., $y^0(0) = 0$, without loss of generality and further using the Lorentz invariant relation of the four-velocity $\dot{y}^\mu\dot{y}_\mu = c^2$, initial conditions yield

$$x_0{}^\mu = (0, x_e)\,, \tag{6.53}$$

$$u_0{}^\mu = (c, 0) \tag{6.54}$$

with the tunnel exit point $x_e = I_p/E_0$, where the classical trajectory starts. Hence, the equations of motion read

$$\frac{1}{c}y^0(\tau) = \frac{c^2\sinh\left(\frac{E_0\tau}{c}\right)}{E_0}\,, \tag{6.55}$$

$$y^1(\tau) = \frac{c^2\left(-\cosh\left(\frac{E_0\tau}{c}\right)\right) + c^2 + E_0 x_e}{E_0}\,. \tag{6.56}$$

In principle, one can eliminate the proper time τ and write down the equation of motion in terms of the parameter time t as $x(t)$ via identifying $\frac{1}{c}y^0(\tau) = t$ and $y^1(\tau) = x$. However, we will keep this form in order to be consistent with the case of constant

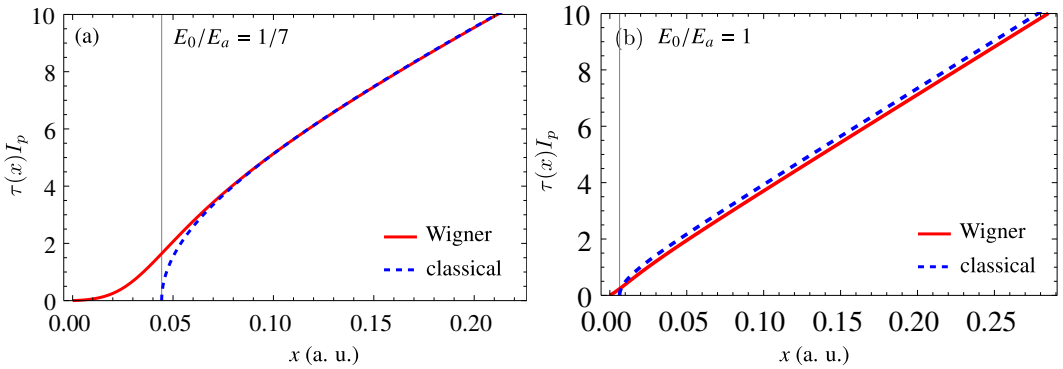

Figure 6.10. – Comparison of the Wigner trajectory (red solid line) and the classical trajectory (blue dashed line) for tunnel-ionization from a zero-range potential under the effect of a constant and uniform electric field; the deep-tunneling regime (a) with $E_0/E_a = 1/7$ and the near-threshold-tunneling regime (b) with $E_0/E_a = 1$. The vertical black line indicates the exit coordinate and the applied parameter is $\kappa = 90$.

and uniform crossed fields, where writing down the equation of motion in terms of the time is quite difficult.

Now, we can compare the classical trajectory (6.55), (6.56) with the Wigner trajectory (6.45) for tunnel-ionization from a zero-range potential. We did comparisons for two sets of parameters: First for $E_0/E_a = 1/7$, $\kappa = 90$, corresponding to the deep-tunneling regime, and for $E_0/E_a = 1$, $\kappa = 90$, which represents the near-threshold-tunneling regime of tunnel-ionization, see Fig. 6.10. The results exactly match with the previous analysis based on the phase of the steady-state wave function. For the deep-tunneling regime the Wigner time delay vanishes, while for the near-threshold-tunneling regime it persists and is detectable at remote distance.

6.4.2. Constant and uniform crossed fields

The next consideration is based on the more realistic scenario of tunnel-ionization from a zero-range potential under the influence of a constant and uniform crossed fields

$$\boldsymbol{E} = E_0\,\hat{\boldsymbol{x}}\,, \tag{6.57}$$

$$\boldsymbol{B} = E_0\,\hat{\boldsymbol{y}}\,. \tag{6.58}$$

In chapter 5.3.1, we have already calculated the propagator for a constant and uniform crossed field (5.29). The corresponding (3+1) dimensional spacetime propagator in the Göppert-Mayer gauge $A^\mu = -xE_0\,n^\mu$, then, reads

$$G(x^\mu, 0) = -\frac{i}{2}\exp\left(\frac{iE_0}{2c}P\cdot x\, n\cdot x\right)\int_0^\infty d\tau\,\frac{1}{(2\pi\tau)^2}$$
$$\times\exp\left(-i\frac{x\cdot x}{2\tau} - \frac{i\tau}{24c^2}x\cdot F\cdot F\cdot x - \frac{ic^2\tau}{2} - \epsilon\tau\right) \tag{6.59}$$

with the wave vector $n^\mu = (1, 0, 0, 1)$ and the polarization vector $P^\mu = (0, 1, 0, 0)$, where we set the initial spatial position $x'^\mu = 0$.

The fixed energy and the fixed transversal momenta propagator along the laser's polarization direction can be calculated via the Fourier transform

$$\tilde{G}(x, 0; \varepsilon, p_z, p_y) = \int d\varepsilon \, dp_z \, dp_y \, G(x^\mu, 0) \exp\left(i\varepsilon t - ip_z z - p_y y\right) , \tag{6.60}$$

which reads

$$\tilde{G}(x; \varepsilon, p_z, p_y) = -\frac{(-1)^{3/4}}{2c} \int_0^\infty d\tau \, \frac{1}{\sqrt{2\pi\,\tau}} \tag{6.61}$$
$$\exp\left(\frac{ix^2}{2\tau} - \frac{i\tau\left(c^2 + p_y^2 + p_z^2\right)}{2} + \frac{i\tau(cE_0 p_z x + \varepsilon(\varepsilon - E_0 x))}{2c^2} - \frac{i\tau^3 E_0^2 (\varepsilon - cp_z)^2}{24c^4} - \epsilon\tau \right) .$$

Here we set the initial spatial position $x' = 0$.

The tunneling probability for a given energy ε_0 can be obtained via

$$|T|^2 = \frac{\left|\tilde{G}(x_e; \varepsilon_0, p_z)\right|^2}{\left|\tilde{G}(0; \varepsilon_0, p_z)\right|^2} , \tag{6.62}$$

where we further set $p_y = 0$ without loss of generality and the tunnel exit point x_e can be calculated via the condition

$$\left(c^2 - I_p - x_e E_0\right)^2 = c^2 \left(p_z - x_e \frac{E_0}{c}\right)^2 + c^4 , \tag{6.63}$$

which yields

$$x_e = \frac{I_p^2 - c^2(2I_p + p_z^2)}{2E_0(c^2 - I_p - cp_z)} . \tag{6.64}$$

The transition probability (6.62) reveals the most probable tunneling probability for a certain transversal momentum p_z, see Fig. 6.11. This indicates that during the tunneling there is a momentum transfer along the propagation direction of the crossed fields. The kinetic momentum $q_z(x) = p_z - xE_0/c$ with maximal tunneling probability at the tunneling entry is $q_z(0) = p_z \sim -2I_p/(3c)$, whereas at the exit it is $q_z(x_e) \sim I_p/(3c)$. As a consequence, the momentum transfer along the laser's propagation direction is I_p/c. Furthermore, contrary to tunnel-ionization from a Coulomb potential case, the momenta at the entry and the exit, and hence the momentum transfer are independent from the barrier suppression parameter E_0/E_a for a zero-range potential, which is consistent with Fig. 3.6.

In order to compare the Wigner trajectory with the classical trajectory, we need to evaluate the classical equations of motion. For a constant and uniform crossed

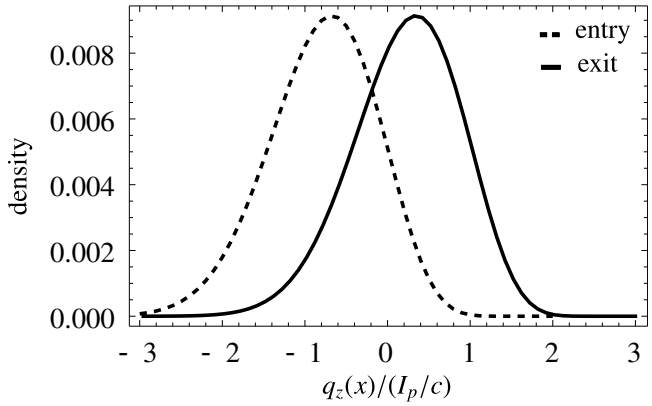

Figure 6.11. – Tunneling probability vs. the kinetic momentum along the propagation direction of the crossed fields at the tunnel entry (dashed line) and tunnel exit (solid line). In the case of tunnel-ionization from a zero-range potential, the values are independent from the barrier suppression parameter E_0/E_a and the transversal momentum transfer is I_p/c. The applied parameters for the figure are $E_0/E_a = 1/7$ and $\kappa = 90$.

fields (6.57), the solutions are given by

$$\frac{1}{c}y^0(\tau) = \frac{\tau}{6c^3}\sqrt{c^2+v_{z0}^2}\left(6c^2+E_0^2\tau^2\right) - \frac{E_0^2\tau^3 v_{z0}}{6c^3}\,, \tag{6.65}$$

$$y^1(\tau) = \frac{E_0\tau^2}{2c}\left(v_{z0} - \sqrt{c^2+v_{z0}^2}\right) + x_e\,, \tag{6.66}$$

$$y^3(\tau) = \frac{E_0^2\tau^3}{6c^2}\left(\sqrt{c^2+v_{z0}^2} - v_{z0}\right) + \tau v_{z0} \tag{6.67}$$

with the initial conditions $y^\mu(0) = (0, x_e, 0)$ and $\dot{y}^\mu = \left(\sqrt{c^2+v_{z0}^2}, 0, v_{z0}\right)$, where $v_{z0} = q_z(x_e) = p_z - x_e E_0/c$ is the initial velocity along the propagation direction of the crossed fields. Moreover, the tunnel exit is given by

$$x_e = -\frac{I_p}{E_0}\left(\frac{18c^2-5I_p}{18c^2-6I_p}\right), \tag{6.68}$$

where we have used $p_z = -2I_p/(3c)$ in Eq. (6.64).

Similarly to the previous case, we can compare the Wigner trajectory with the classical trajectory in two distinct regimes. In the deep tunneling regime, $E_0/E_a = 1/7$, the Wigner time delay vanishes. For the near-threshold-tunneling regime, $E_0/E_a = 1$ the Wigner time delay is detectable.

Furthermore, one can compare the Wigner and the classical trajectories in terms of the transversal coordinate z. The stationary phase condition identifies the transversal coordinate as

$$z_{\mathrm{TI}}(x) \equiv -\left.\frac{\partial\phi(x,\varepsilon_0,p_z)}{\partial p_z}\right|_{p_z=p_{z0}} + \left.\frac{\partial\phi(0,\varepsilon_0,p_z)}{\partial p_z}\right|_{p_z=p_{z0}} \tag{6.69}$$

with the most probable momentum $p_{z0} = -2I_p/(3c)$. Due to the existence of a non-zero Wigner time delay, there exists also a spatial drift along the propagation direction at the tunnel exit, which, however, vanishes at remote distance, see Fig. 6.12(c).

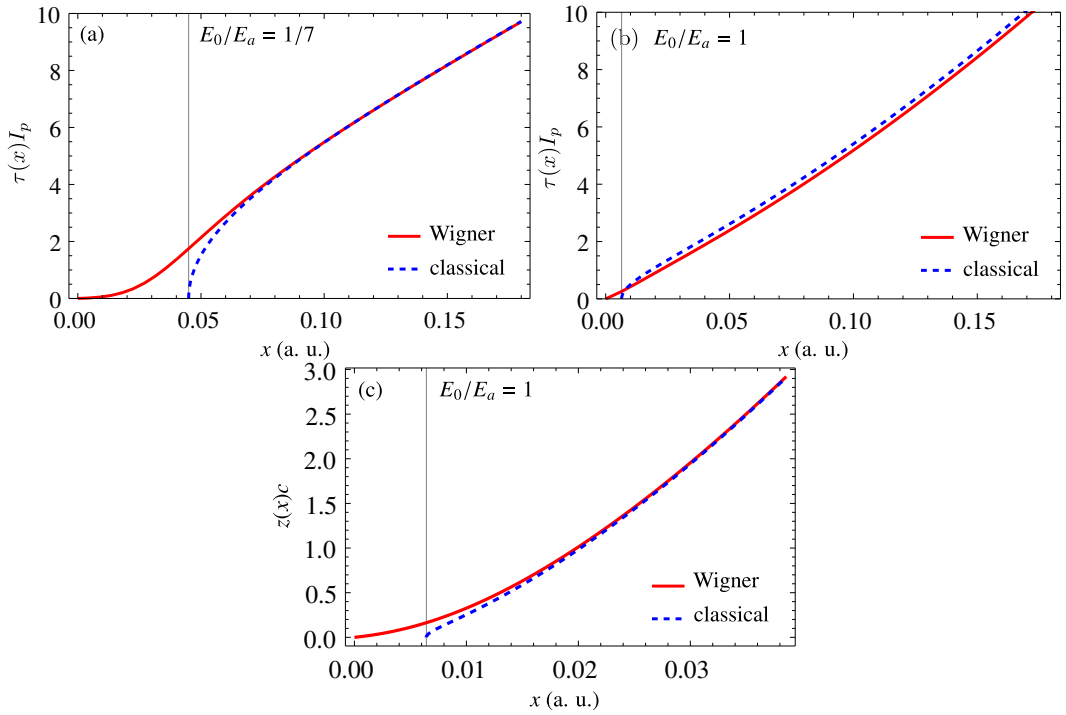

Figure 6.12. – Comparison of the Wigner trajectory (red solid line) and the classical trajectory (blue dashed line) for tunnel-ionization from a zero-range potential under the effect of constant and uniform crossed fields; the deep-tunneling regime (a) with $E_0/E_a = 1/7$ and the near-threshold-tunneling regime (b) with $E_0/E_a = 1$. Comparison of the Wigner and the classical trajectories in terms of the transversal coordinate z (path) for the parameters $E_0/E_a = 1$ (c). The vertical black line indicates the exit coordinate and the applied parameter is $\kappa = 90$.

6.4.3. Intuitive explanation of the Wigner time delay

Finally, we address the formal definition of deep-tunneling and near-threshold-tunneling and clarify the reason for the differing behavior of the Wigner time delay in these regimes. A general rule for the validity of the linear approximation, which allows us to neglect the quadratic and the higher-order terms in the expansion of the potential barrier, can be given via the condition

$$\left|\frac{V''(x_e)}{V'(x_e)}\,\delta x\right| \ll 1 \tag{6.70}$$

for the characteristic distance δx that will be quantified later. Indeed, this condition defines the deep-tunneling regime. The regime, which meets the condition

$$\left|\frac{V''(x_e)}{V'(x_e)}\,\delta x\right| \sim 1 \tag{6.71}$$

is identified as the near-threshold-tunneling regime. In the latter case the potential has to be approximated by including also at least the quadratic term, which is sufficient unless it is too close to the threshold

$$V(x) = V(x_e) + V'(x_e)(x - x_e) + V''(x_e)\frac{(x - x_e)^2}{2}\,. \tag{6.72}$$

In Sec. (6.3) we characterized the Wigner time delay as the asymptotic deviation of the maximum of the wavepacket position from its corresponding classical path. Therefore, the typical distance δx can be identified with the deviation of the maximum of the wavepacket position with respect to the classical one, viz. $x = x_e + \delta x$, and similarly for the momentum $p = p_e + \delta p$, with x_e and p_e denoting the classical position and momentum at the tunnel exit. The typical distance δx may be estimated by considering the Hamiltonian for a nonrelativistic particle which tunnels trough a potential barrier $V(x)$. The corresponding Schrödinger Hamiltonian

$$H = \frac{p^2}{2} + V(x) \tag{6.73}$$

can be written in terms of δx and δp as

$$\frac{\delta p^2}{2} + \delta x\, V'(x_e) = 0\,, \tag{6.74}$$

with $V(x_e) = -I_p$ and $p_e = 0$. Employing the uncertainty relation $\delta x\, \delta p \sim 1$, the deviation from the classical trajectory is obtained as

$$|\delta x| \sim \left| V'(x_e)^{-1/3} \right| . \tag{6.75}$$

Inserting Eq. (6.75) into Eq. (6.70), the condition for the validity of the linear approximation reads

$$\left| \frac{V''(x_e)}{V'(x_e)^{4/3}} \right| \ll 1. \tag{6.76}$$

The latter condition which also quantifies the transition regime between the deep-tunneling and the near-threshold-tunneling regime can be also expressed via the parameter E_0/E_a in the case of the one-dimensional potential (111) as

$$\left(\frac{16 E_0}{E_a} \right)^{5/3} \ll 1\,. \tag{6.77}$$

For instance, $(16E_0/E_a)^{5/3} \approx 0.3$ for the deep tunneling regime with $E_0/E_a = 1/30$, whereas $(16E_0/E_a)^{5/3} \approx 0.9$ for the near-threshold-tunneling regime with $E_0/E_a = 1/17$. In the case of a short-range atomic potential, where $V''(x_e) = 0$, the condition of the near-threshold-tunneling regime, Eq. (6.76), should be modified. The tunneling potential is not linear in this case due to the edge of the triangular shaped effective barrier, which becomes essential for the tunneling time at $\delta x \sim x_e$. Therefore, in the case of a short-range atomic potential Eq. (6.77) is replaced by $\delta x / x_e \sim (E_0/E_a)^{2/3} \ll 1$.

It should be noted here that the nonrelativistic Schrödinger equation

$$\left(-\frac{1}{2}\nabla^2 + xE_0 - \frac{\kappa}{r} \right) \psi(\boldsymbol{x}) = \varepsilon\, \psi(\boldsymbol{x}) \tag{6.78}$$

can be separated in cylindrical parabolic coordinates such that the three-dimensional problem reduces effectively to a one-dimensional one with the one-dimensional potential for the ground state [86, 139]

$$V(\zeta) = -\frac{1}{4\zeta} - \frac{1}{8\zeta^2} - \frac{1}{8} E_0 \zeta\,. \tag{6.79}$$

A calculation of the tunneling time delay utilizing the potential (6.79) instead of (6.32) would give qualitatively the same results in both tunneling regimes because both potentials have the same behavior in the continuum range of the potential barrier. The quantitative difference comes only from a numerical value in the transition regime between the deep-tunneling and the near-threshold-tunneling regime. Namely, the condition (6.77) can be written for the potential (6.79) as

$$\left(\frac{9E_0}{E_a}\right)^{5/3} \ll 1 \tag{6.80}$$

where $E_0/E_a = 1/9$ is in the border between tunnel-ionization and over-the-barrier ionization.

Further, this classification of the tunneling regimes allows to formulate a condition for a non-zero Wigner time delay. When the potential barrier is linear on the typical distance δx around the exit, i.e., in the deep tunneling regime, the time delay vanishes at far distances. If this is not the case, in the near-threshold-tunneling regime, a non-zero tunneling time is expected. This is consistent with our results in Fig. 2

To sum up, a possible experimental verification of the tunneling time delay is expected to be feasible in the near-threshold-tunneling regime. This delay is approximately proportional to $1/I_p$ as shown in Fig. 6.9.

6.5. Conclusions

In this chapter, the problem of tunneling time delay has been considered. Although there is no well-defined time operator in quantum mechanics, it is possible to infer information about the tunneling time delay via tracing the peak of the wave packet, which brings in the so-called Wigner time concept. The Wigner time formalism was applied to the nonrelativistic as well as to the relativistic tunnel-ionization process. It was shown that the Wigner time formalism can be simplified further for the tunnel-ionization process, due to the fact that the quasiclassical trajectory starts at the entry point of the barrier. In the nonrelativistic case, it was illustrated that the Wigner time delay vanishes for the deep-tunneling regime when the potential barrier at the tunneling exit can be approximated by solely its tangent line. At larger laser field strength, in the near-threshold-tunneling regime of tunnel-ionization, the potential barrier is not linear in coordinate at the tunnel exit. Consequently, the Wigner time delay is preserved at far distances. Finally, our results were extended to the relativistic regime via the phase of the fixed energy propagator. It was shown that the Wigner time delay is characterized mainly by the nonrelativistic dynamics.

7. On the quantization of the electromagnetic flux

This additional chapter including the figures is based on [69] and it can be read independently of the rest of the thesis.

7.1. Introduction

Historically, the introduction of gauge potentials may seem to appear just as a mathematical convention in order to calculate the electromagnetic fields. However, as elegantly described by Aharanov and Bohm, the gauge potential has a significant role in quantum mechanics [60]. Namely, the gauge potential does not only provide a compact mathematical formulation of the associated field strength tensor, but also it leads to predictions such as Aharanov-Bohm effect [60–62], flux quantization [63–66] and Dirac's charge quantization condition when the existence of a magnetic monopole is assumed [67, 68]. Furthermore, in their celebrated paper [71], Wu and Yang gave a complete description of electromagnetism based on the concept of the nonintegrable (path-dependent) phase factor. Wu and Yang pointed out that the field strength tensor underdescribes the complete electromagnetic phenomena. In other words, the different physical realization of electromagnetic phenomena may have the same field strength tensor $F_{\mu\nu}$ in a local theory. In fact, in terms of the paradigm of modern physics, gauge potentials (gauge fields) emerge from requiring the theory invariant under a group of local internal continuous symmetry transformations [6–8]. Non-abelian gauge theories are the consequence of such an inclusive approach [10]. This approach stems from the fact that conservation of electric charge follows from the invariance of the theory under a global symmetry transformation, viz. global gauge invariance of the theory. This connection was made first by Herman Weyl when he attempted to unify electromagnetism and general relativity [5]. Demanding a further local gauge invariance introduces gauge potentials. In this connection, the gauge invariance is equivalent to the phase invariance of a wave function. For instance, the Dirac equation for a relativistic spin-$1/2$ particle

$$\left[i\hbar\gamma^{\mu}\left(\partial_{\mu}-\frac{iq}{\hbar c}A_{\mu}(x)\right)-mc\right]\psi(x)=0 \tag{7.1}$$

is invariant under the transformations

$$\psi(x)\rightarrow\exp\left(\frac{iq\chi(x)}{\hbar c}\right)\psi(x)\,, \tag{7.2}$$

where the gauge potentials obey the transformation law

$$A^\mu \to A^\mu + \partial^\mu \chi \,. \tag{7.3}$$

After the introduction of gauge potentials, the local phase invariance (or the group of local continuous symmetry transformations) can also be accomplished by

$$\exp\left(-\frac{iq}{\hbar c}\int_{\mathcal{P}}^{x} A_\nu dy^\nu\right), \tag{7.4}$$

where the integration path $\mathcal{P}$ starts at a point where the field is zero and runs up to the point of interest x [8]. This phase factor (7.4) is known as the Wilson line [72]. Historically, such kind of line integrals of the potentials have previously been suggested in [46,47,71,73,74], and it was shown by DeWitt [46] and Mandelstam [47] that the phase factor Eq. (7.4) can replace the gauge freedom of the theory with the path freedom. The resulting formalism can be called the path-dependent formulation of gauge theory.

Although the path-dependent formalism was discussed in various places and in different contexts in the literature [8, 46–49, 72, 75], in this additional chapter, we are confident that we present a complete framework for the path-dependent formulation of gauge theory. We discuss and explore the quantum mechanical topological effects in the light of the path-dependent formalism. Although the results are well-known in the literature, we will present a clear geometric picture for the electromagnetic flux quantization. We further discuss the electric charge quantization via the developed formalism.

The CGS units are used throughout this chapter.

7.2. The path-dependent formalism

The complete description of a gauge theory can be constructed demanding the invariance of the theory under a local phase transformation via the Wilson line as (after the introduction of gauge potentials)

$$\psi(x) \to \Psi(x) = \exp\left(-\frac{iq}{\hbar c}\int_{\mathcal{P}}^{x} A_\nu dy^\nu\right)\psi(x)\,. \tag{7.5}$$

In fact, Eq. (7.5) corresponds to defining the gauge function χ via the path integral $\chi = -\int_{\mathcal{P}}^{x} A_\nu dy^\nu$. However, it should be noted that this particular choice of gauge function is not a gauge fixing in the conventional sense because the path freedom of the Wilson line covers all possible gauge functions.

Then, in order to require the invariance of the theory under a local symmetry transformation, gauge potentials satisfy the transformation law

$$A_\mu(x) \to \mathcal{A}_\mu(x) \equiv A_\mu(x) - \frac{\partial}{\partial x^\mu}\int_{\mathcal{P}}^{x} A_\nu dy^\nu\,. \tag{7.6}$$

The latter defines "gauge invariant" but path dependent gauge potentials $\mathcal{A}_\mu(x)$. The gauge potential $\mathcal{A}_\mu(x)$ is invariant under the transformation (7.3) and its gauge freedom is recovered by the path freedom. Since, instead of gauge functions, we have a path freedom in this equivalent formulation of gauge theory, we will label both the gauge potential $\mathcal{A}_\mu$ and the wave function Ψ with the path index $\mathcal{P}$. This leads to a completely path-dependent but gauge-function-free theory. For instance, the Dirac equation reads

$$\left[i\hbar\gamma^\mu\left(\partial_\mu - \frac{iq}{\hbar c}\mathcal{A}_\mu(\mathcal{P},x)\right) - mc\right]\Psi(\mathcal{P},x) = 0\,, \tag{7.7}$$

and furthermore it is invariant under the path transformation

$$\Psi[\mathcal{P}',x] = \exp\left(\frac{iq}{\hbar c}\oint_{\partial\Sigma}^{x} A_\mu dy^\mu\right)\Psi[\mathcal{P},x]\,, \tag{7.8}$$

as long as the gauge potentials obey the following path transformation

$$\mathcal{A}_\mu(\mathcal{P}',x) = \mathcal{A}_\mu(\mathcal{P},x) + \partial_\mu\oint_{\partial\Sigma}^{x} A_\nu dy^\nu \tag{7.9}$$

with the closed loop $\partial\Sigma = \mathcal{P} - \mathcal{P}'$. Here the gauge invariant generator of the path transformation is called the Wilson loop [72].

The Wilson loop further provides a geometric picture of the gauge invariance. Using the four-dimensional Stokes' law, a loop integral can be converted to a surface integral, which yields the electromagnetic flux Φ_{EM} as

$$\oint_{\partial\Sigma}^{x} A^\mu dy_\mu = \frac{1}{2}\int_{\Sigma}^{x} F^{\mu\nu}d\sigma_{\mu\nu} = \Phi_{EM}(x)\,. \tag{7.10}$$

Consequently, if we compare conventional gauge theory (7.2) with the path-dependent formalism (7.8), we infer that a gauge function χ comes into existence as an electromagnetic flux Φ_{EM} through the surface bounded by two gauge paths whose end points are the same. It should be underlined that contrary to an electromagnetic flux appearing in the conventional gauge theory, which has a direct measurable physical implication, the flux of the path-dependent formalism is path dependent and hence it cannot have a physical implication. Nevertheless, when it becomes path independent, it has direct physical consequences as we will discuss later.

The gauge potential $\mathcal{A}_\mu(x)$ defined in Eq. (7.6) can be written in terms of gauge invariant physical expressions. Here, we first provide DeWitt's derivation and show that it is not complete. Then, we formulate the general expression for gauge potential applicable to all cases. We parametrize the path $\mathcal{P}$ as $y = y(\sigma,x)$ with boundary conditions

$$y(s,x) = x\,,\quad y(0,x) = x_0\,, \tag{7.11}$$

where the electromagnetic field vanishes at x_0, at which A_μ may, without loss of

generality, be set equal to zero. Then, Eq. (7.6) becomes

$$\begin{aligned}\mathcal{A}_\mu(\mathcal{P},x) &= A_\mu(x) - \frac{\partial}{\partial x^\mu}\int_0^s A_\nu(y)\frac{\partial y^\nu}{\partial\sigma}d\sigma\,,\\ &= A_\mu(x) - \int_0^s\left(\frac{A_\nu(y)}{\partial y^\lambda}\frac{\partial y^\lambda}{\partial x^\mu}\frac{\partial y^\nu}{\partial\sigma} + A_\nu(y)\frac{\partial}{\partial\sigma}\frac{\partial y^\nu}{\partial x^\mu}\right)d\sigma\,,\\ &= A_\mu(x) - \int_0^s\left(\frac{A_\lambda(y)}{\partial y^\nu}\frac{\partial y^\nu}{\partial\sigma}\frac{\partial y^\lambda}{\partial x^\mu} + A_\nu(y)\frac{\partial}{\partial\sigma}\frac{\partial y^\nu}{\partial x^\mu} - F_{\nu\lambda}(y)\frac{\partial y^\lambda}{\partial x^\mu}\frac{\partial y^\nu}{\partial\sigma}\right)d\sigma\,,\end{aligned} \tag{7.12}$$

where in last line we have used the definition of the field strength tensor as $A_{\nu,\lambda}(y) = A_{\lambda,\nu}(y) - F_{\nu\lambda}(y)$. The first two integrand terms in Eq. (7.12) can be written as $\frac{\partial}{\partial\sigma}\left(A_\lambda(y)\frac{\partial y^\lambda}{\partial x^\mu}\right)$ and using the boundary conditions (7.11),

$$\mathcal{A}_\mu(\mathcal{P},x) = \int_0^s F_{\nu\lambda}(y)\frac{\partial y^\nu}{\partial\sigma}\frac{\partial y^\lambda}{\partial x^\mu}d\sigma \tag{7.13}$$

is obtained. The expression (7.13) first is given in the DeWitt's paper [46]. Later, the correspondence between paths and gauge functions was discussed in a series of papers [48, 49].

However, the expression of the gauge potential $\mathcal{A}_\mu$ given in Eq. (7.13) is incomplete. In fact, it is only valid for nonconfined electromagnetic fields and it immediately violates the path transformation rule (7.9) for a confined field. Since Eq. (7.13) depends on the field strength tensor $F_{\mu\nu}$ as well as path choice, any path which does not pass through the field region of a confined field generates a vanishing gauge potential, though there may exist an electromagnetic flux through the area bounded by such kind of paths. However this obviously contradicts to the original definition of the path dependent gauge potential (7.6) as well as to the general path transformation rule (7.9). Furthermore, consider two paths $\mathcal{P}_1$ and $\mathcal{P}_2$, whose segments pass through the field region are common as shown in Fig. 7.1 and they generate the gauge potentials $\mathcal{A}_\mu(\mathcal{P}_1,x)$ and $\mathcal{A}_\mu(\mathcal{P}_2,x)$, respectively. Since only relevant segments which generate the gauge potential are those pass through the field region, both the paths yield the same gauge potential. However, according to the general path transformation (7.9), relation between the gauge potentials should be given by

$$\mathcal{A}_\mu(\mathcal{P}_2,x) = \mathcal{A}_\mu(\mathcal{P}_1,x) + \partial_\mu\Phi_{EM}(x) \tag{7.14}$$

with the electrodynamics flux $\Phi_{EM}(x)$ (the flux through pink region in Fig. 7.1).

The fundamental reason of the incompleteness of Eq. (7.13) is the fact that for a confined field the field strength tensor $F_{\mu\nu}$ vanishes outside the field region, however the corresponding gauge potential does not vanish and its loop integral has to be the electromagnetic flux. Nonetheless, we can provide a complete expression for the path-dependent gauge potential. Let us go back to the original definition of the path-dependent gauge potential given by Eq. (7.6). Any path $\mathcal{P}$ can be decomposed as

$$\mathcal{P} \equiv \mathcal{P}_F - \mathcal{P}_L\,, \tag{7.15}$$

where the path $\mathcal{P}_F$, which has the same end points as the path $\mathcal{P}$, passes through the field region, whereas $\mathcal{P}_L$ is a loop that connects with $\mathcal{P}_F$ to the path of interest $\mathcal{P}$. Then, Eq. (7.6) can be written as

$$\mathcal{A}_\mu(\mathcal{P}, x) = A_\mu(x) - \frac{\partial}{\partial x^\mu}\int_{\mathcal{P}_F}^{x} A_\nu dy^\nu + \frac{\partial}{\partial x^\mu}\int_{\mathcal{P}_L}^{x} A_\nu dy^\nu \,. \tag{7.16}$$

On the one hand, the first two terms in the above equation can be written in the form of Eq.(7.13), on the other hand, the last term is nothing else but the electromagnetic flux due to a confined field through the area bounded by the loop $\mathcal{P}_L$. As a result, we derive the complete expression for the path-dependent gauge potential as

$$\mathcal{A}_\mu(\mathcal{P}, x) = \int_0^s F_{\nu\lambda}(y)\frac{\partial y^\nu}{\partial\sigma}\frac{\partial y^\lambda}{\partial x^\mu}d\sigma + \frac{\partial \Phi_{EM}(\mathcal{P}_L, x)}{\partial x^\mu} \,. \tag{7.17}$$

Indeed, the expression (7.17) can also be directly obtained by means of the path transformation (7.14) as

$$\mathcal{A}_\mu(\mathcal{P}, x) = \mathcal{A}_\mu(\mathcal{P}_F, x) + \partial_\mu \Phi_{EM}(\mathcal{P}_L, x) \,. \tag{7.18}$$

In summary, existence of a confined field implies a not simply connected space where a path may not be continuously deformed into another path and a loop may not be contracted to a point due to a confined field. Consequently, the complete expression for the path dependent potential is given by Eq. (7.17). However, a nonconfined field corresponds to a simply connected topological space where every path can be continuously deformed into each other and every loop can shrink to a point. In this case, the loop path $\mathcal{P}_L$ can be omitted. This implies that $\mathcal{P} = \mathcal{P}_F$ and the expression (7.17) reduces to Eq. (7.13).

7.3. Quantization of the electromagnetic flux

In this section, we will apply the developed path-dependent formalism of gauge theory in order to analyze quantum mechanical topological effects.

In the case of a nonconfined field, the electromagnetic flux $\Phi_{EM}(x)$ depends on the gauge paths and it behaves like a gauge function. However, the electromagnetic flux of a confined field through the area bounded by the border of the field is path independent and, therefore, has physical implications. Due to the latter, the electromagnetic flux is either detectable in an Aharanov-Bohm type interference experiment or has to be quantized as we discuss below.

For this purpose, consider two arbitrary paths $\mathcal{P}_1$ and $\mathcal{P}_2$ in the case of a confined electromagnetic field as shown in Fig. 7.1, which have the same starting and terminating points. If the electromagnetic flux Φ_{EM} through the confined field is constant and uniform in the spacetime, then the path dependent gauge potentials $\mathcal{A}_\mu(\mathcal{P}_1, x)$ and $\mathcal{A}_\mu(\mathcal{P}_2, x)$ coincide. Since the gauge potential already overdescribes the physical

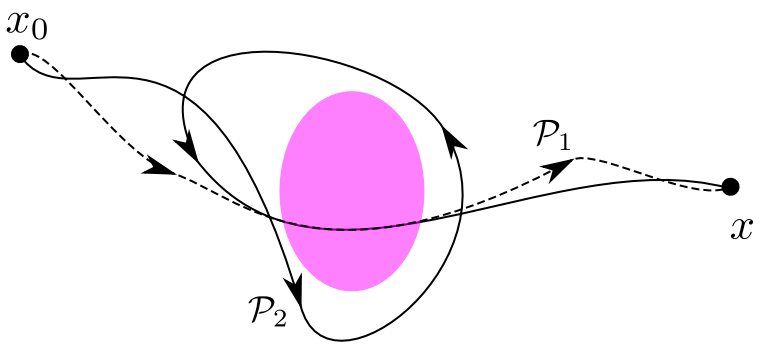

Figure 7.1. – Both gauge paths $\mathcal{P}_1$ and $\mathcal{P}_2$ generate the same gauge potential according to Eq. (7.13), which is inconsistent with the general path transformation (7.9). The complete expression for the path-dependent gauge potential can be given by Eq. (7.17). Furthermore, in terms of topological point of view, path $\mathcal{P}_2$ cannot be continuously deformed into $\mathcal{P}_1$ due to the presence of the confined field (pink region), which has direct physical consequences. If the electromagnetic flux Φ_{EM} through the area bounded by the loop $\partial\Sigma = \mathcal{P}_1 - \mathcal{P}_2$ is constant and uniform, then the flux is quantized.

reality [71], i.e., different gauge potentials can describe the same physics, the wave function for a given gauge potential has to be unique. As a result, the wave function defined via the path $\mathcal{P}_2$

$$\Psi[\mathcal{P}_2] = \exp\left(\frac{iq}{\hbar c}\Phi_{EM}\right)\Psi[\mathcal{P}_1] \tag{7.19}$$

should match with $\Psi[\mathcal{P}_1]$. Then it follows that the electromagnetic flux has to be quantized as

$$\frac{q\Phi_{EM}}{\hbar c} = 2\pi n, \quad n = \pm 1, \pm 2, \dots , \tag{7.20}$$

which can be interpreted as a condition of the flux quantization[1]. Here we want to stress that the constant and uniform phase appearing in Eq.(7.19) is a nontrivial phase based on the requirement of a local gauge invariance. On the contrary, the trivial phase of a global gauge invariance χ can be set equal to zero without loss of generality.

The validity of such a requirement can be further confirmed in the following way. If there exists a constant and uniform flux Φ_{EM} due to a confine field, then it is also possible to find another path $\mathcal{P}_3$ whose winding number N is greater than 1, i.e., a path which wraps the flux more than one time such that each turn can pass through different hypersurfaces. In this case the wave function defined for the path $\mathcal{P}_3$

$$\Psi[\mathcal{P}_3] = \exp\left(\frac{iq}{\hbar c}N\Phi_{EM}\right)\Psi[\mathcal{P}_1] \tag{7.21}$$

would depend on the winding number N, which is inconsistent with physical realization unless there exists an Aharanov-Bohm type experiment which can differentiate the winding number N.

[1] In general, further quantization conditions can be obtained by imposing other conditions like periodicity of the wave function.

Thus, the analysis of the gauge transformation of the wave function within the path-dependent formalism allows us to find a very simple geometric explanation for the topological quantum mechanical effects such as the Aharonov-Bohm effect and the flux quantization. From the topological point of view, one can give the following interpretation: If one gauge path cannot be continuously deformed into another gauge path relative to their endpoints due to the existence of a topological object on the deformation region, then this topological object - the electromagnetic flux - has to be quantized as long as these two gauge paths generate the same gauge potential. Meanwhile, when different gauge paths generates different gauge potentials, the path independent electromagnetic flux can be measurable via the wave function phase as an interference phenomena[2]. Specifically, consider a spatially confined magnetic field. Firstly, if the confined field is time dependent, than the field can be detectable in an Aharanov-Bohm experiment. Secondly, if the confined field is also time independent, then the associated flux is quantized, which can be referred to the flux quantization occurring in Type II superconductors [63–66].

Let us illustrate the flux quantization in two specific examples, where we choose two gauge paths which provide the same gauge potential and show that the electromagnetic flux bounded by these paths should be quantized.

As a first example, we consider a confined static magnetic field

$$\boldsymbol{B}(\boldsymbol{x}) = B_0 \left(1 - \theta(r - r_0)\right) \hat{z}\,, \tag{7.22}$$

with $r = \sqrt{x^2 + y^2}$, $r_0 = \sqrt{x_0^2 + y_0^2}$, and the Heaviside step function $\theta(x)$. The path $\mathcal{P}_1$, shown in Fig. 7.2, generates the following gauge potential

$$\mathcal{A}(\mathcal{P}_1, \boldsymbol{x}) = \begin{cases} B_0 \left(-y, x, 0\right)/2, & r \leq r_0\,, \\ \dfrac{B_0 r_0^2}{2r^2} \left(-y, x, 0\right), & r > r_0\,. \end{cases} \tag{7.23}$$

Similarly, the path $\mathcal{P}_2$ will also give the same gauge potential Eq. (7.23). Although these two paths give the same gauge potential, there is a non zero magnetic flux in the surface bounded by these paths, which appears as a local constant phase in the wave function defined on the path $\mathcal{P}_2$. In order to satisfy the uniqueness of the wave function, the flux of the confined static magnetic field has to be quantized as

$$\frac{qB_0 \pi r_0^2}{\hbar c} = 2\pi\, n\,. \tag{7.24}$$

In the second example, we investigate a constant and uniform electric field along x-direction, which is confined on a specific region of the spacetime as

$$\boldsymbol{E}(t, x) = E_0 \left(\theta(ct) - \theta(ct - c\Delta t)\right) \left(\theta(x) - \theta(x - \Delta x)\right) \hat{x}\,. \tag{7.25}$$

[2] In fact, the mathematical connection can be established in the framework of homotopy between the gauge paths, see the relevant references listed in [7].

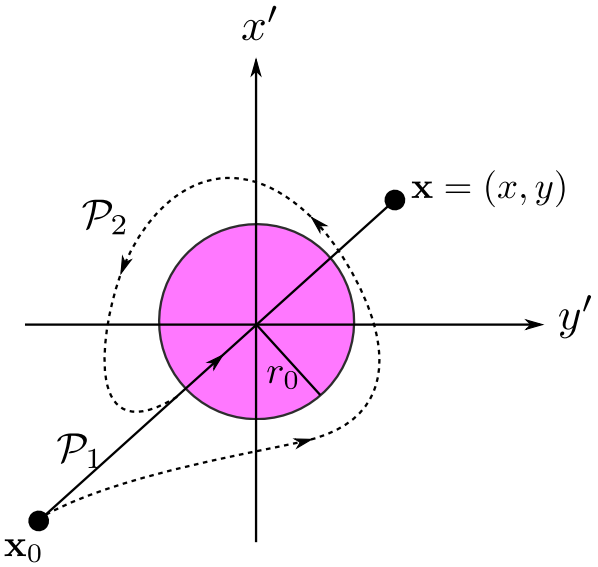

Figure 7.2. – Geometric configuration for the magnetic flux quantization. Both the path $\mathcal{P}_1$ (solid) and the path $\mathcal{P}_2$ (dashed) give the same gauge potential. As a consequence, the flux enclosed by the loop has to be quantized. The starting point is $x_0 = (-\infty, -\infty)$ at which the gauge potential is zero.

Following Fig. 7.3, both the path $\mathcal{P}_1$ and the path $\mathcal{P}_2$ give the same potential

$$\mathcal{A}^\mu = \begin{cases} -E_0\,(-x, ct, 0, 0)\,/2, & \Delta x \geq x \geq 0 \wedge \Delta t \geq t \geq 0\,, \\ -\dfrac{E_0 \Delta x^2}{2x^2}\,(x, ct, 0, 0)\,, & x > \Delta x > 0 \wedge \Delta t > t > 0\,, \\ -\dfrac{E_0 \Delta t^2}{2t^2}\,(x, ct, 0, 0)\,, & \Delta x > x > 0 \wedge t > \Delta t > 0\,. \end{cases} \tag{7.26}$$

Since there is a non-zero electromagnetic flux in the loop enclosed by the paths, the flux has to be quantized such that

$$\frac{q\,c\,E_0 \Delta x \Delta t}{\hbar\,c} = 2\pi\,n \tag{7.27}$$

holds.

7.4. On the electric charge quantization

Since the electric charge was measured by Millikan in 1913 [149], probably one of the most important long standing unresolved problems in theoretical physics is the quantization of electric charge [56]. In the early times of quantum mechanics the question was why electron and proton have the same but opposite electric charges. Later, with the discovery of quarks, the question was reformulated as why all particles have charges which are integer multiples of the charge $e/3$, the charge of down-type

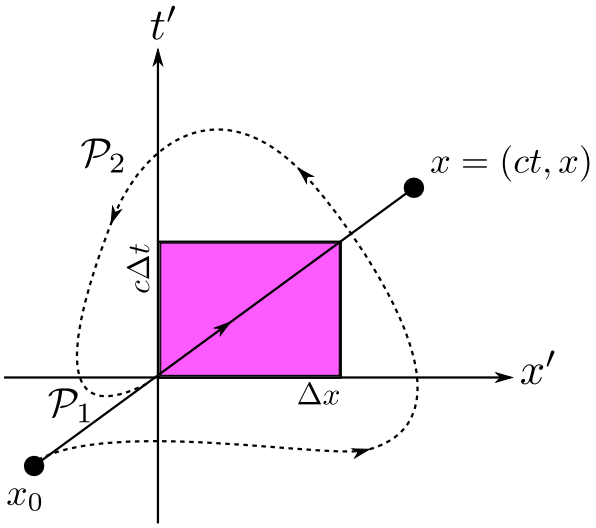

Figure 7.3. – Geometric configuration for the electric flux quantization. The starting point is $x_0 = (-\infty, -\infty)$ at which the gauge potential is zero.

quarks (down, strange, bottom) which can be identified as the fundamental unit of electric charge.

One particular interesting explanation of the problem is the possible existence of magnetic monopole[3] that is introduced by Dirac [67, 68]. Although quantum mechanics does not require the existence of magnetic monopoles, it does not also prohibit its presence even in the current formulation of electromagnetism. The fundamental relation, as it stands, $\boldsymbol{B} = \nabla \times \boldsymbol{A}$ with a non singular free gauge potential $\boldsymbol{A}$ allows to modify the associated Maxwell equation to $\nabla \cdot \boldsymbol{B} = 4\pi\rho_m$ with the magnetic monopole charge density ρ_m. Dirac's original derivation was based on the singular gauge potential whose singularity corresponds to the so-called Dirac string (see also Schwinger's discussion [153]). Later, the same result was obtained in [71] using a nonsingular gauge potential defined on a domain which is divided into two overlapping regions.

In the context of the path-dependent formalism such a derivation was done by Cabibbo and Ferrari in [75]. This elegant description can be illustrated as follows: Consider two gauge paths $\mathcal{P}_1$ and $\mathcal{P}_2$ which generate the associated gauge potential of a magnetic monopole with charge g. Then, using Eq. (7.8) and Eq. (7.10), the path transformation for the wave function of an electron interacting with a magnetic monopole reads

$$\Psi[\mathcal{P}_2] = \exp\left(\frac{ie}{2\hbar c}\int_{\Sigma_1} F^{\mu\nu} d\sigma_{\mu\nu}\right)\Psi[\mathcal{P}_1] = \exp\left(\frac{ie}{\hbar c}\int_{\Sigma_1} \boldsymbol{B}\cdot d\boldsymbol{\sigma}\right)\Psi[\mathcal{P}_1]\,, \qquad (7.28)$$

where e is electric charge of the electron and Σ_1 is a spacelike surface[4] bounded by the paths $\mathcal{P}_1$ and $\mathcal{P}_2$. However, a wave function can not depend on the particular

[3] see [150] for a comprehensive review and [151, 152] for the models of particles with both electric and magnetic charges.

[4] The derivation is not restricted to a spacelike surface, but it is general, see [75].

choice of the surface, and hence the wave function in the gauge path $\mathcal{P}_2$ can also be written as

$$\Psi[\mathcal{P}_2] = \exp\left(\frac{ie}{\hbar c}\int_{\Sigma_2} \boldsymbol{B}\cdot d\boldsymbol{\sigma}\right)\Psi[\mathcal{P}_1]\,. \tag{7.29}$$

Consequently, using the divergence theorem, we require

$$\exp\left(\frac{ie}{\hbar c}\int_V \nabla\cdot\boldsymbol{B}\,dv\right) = 1 \tag{7.30}$$

where V denotes the volume of the closed surface $\partial V = \Sigma_1 - \Sigma_2$. In the absence of a magnetic monopole, the requirement (7.30) is trivially satisfied. The nontrivial solution, which exists when the existence of a magnetic monopole is assumed, requires Dirac's charge quantization

$$\frac{2e\,g}{\hbar c} = n\,. \tag{7.31}$$

As a result, the existence of a magnetic monopole anywhere in the universe would explain electric charge quantization everywhere. However magnetic monopoles have not been observed so far [154].

Another elegantly described possible explanation is based on grand unified theories, where the $U(1)$ gauge group is embedded in a non-abelian gauge group [155]. The nontrivial Lie algebra of the non-abelian group implies the charge quantization [156] (see also magnetic monopoles in non-abelian gauge theories [6, 157, 158]). Lastly, we want to cite another notable idea which is based on constraints from the absence or cancellation of anomalies in the standard model [159–164]. In fact, there are many other further attempts that we cannot cite here, however, none of them provides a fully satisfactory resolution for the problem. Particularly appealing is the question considered by Dirac if it is possible to infer the fundamental unit of the charge from the theory. All the mentioned theories above and other existing theories fail to answer this question.

Here we discuss electric charge quantization within electromagnetism in the absence of a magnetic monopole on a toy model in a (1+1) dimensional causal spacetime.

In addition to the (1+1) dimensional causal spacetime, let us assume that there exists a quantum vacuum with a possibility of creation and annihilation of a pair of a charged particle and its antiparticle. Then, due to the particle-antiparticle pair creation-annihilation process in this universe, a confined electric field arises on the spacetime region bounded by the world lines of each one of the pair as shown in Fig. 7.4.

To find the field created by particles, we solve the Maxwell's equations in the (1+1) dimensional spacetime. The Maxwell's equations in an arbitrary (d+1) dimensional spacetime is given by [1]

$$\partial_\mu F^{\mu\nu} = \frac{2\pi^{d/2}}{\Gamma(d/2)}\frac{J^\nu}{c}\,, \tag{7.32}$$

$$\epsilon^{\alpha\beta\mu\nu}\partial_\mu F_{\alpha\beta} = 0\,, \tag{7.33}$$

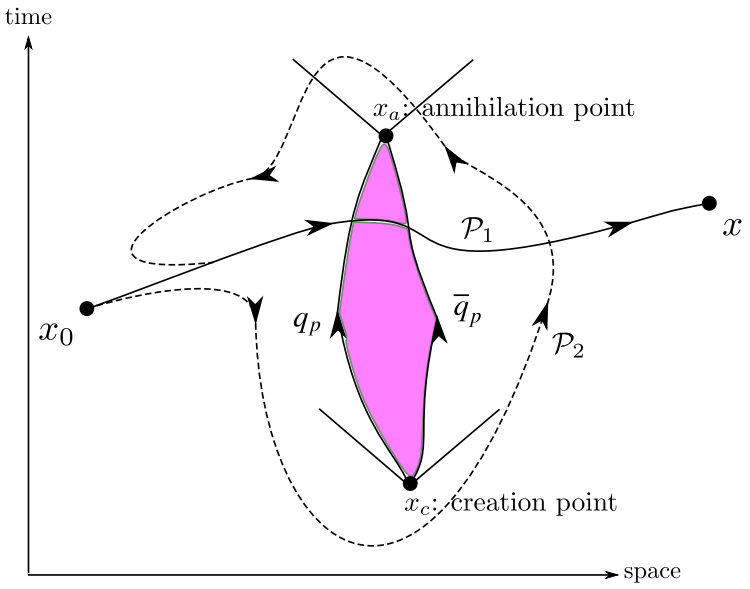

Figure 7.4. – The spacetime area bounded by the world lines of each one of the pair implies a constant uniform confined electric field in a (1+1) dimensional spacetime.

with the Gamma function $\Gamma(x)$, the vector current $J^\mu = (c\rho, \boldsymbol{J})$. The causal electric field of a point charge q moving on an arbitrary world line $r^\mu(\tau) = \left(r^0(\tau), r^i(\tau)\right)$ can be found via solving the Maxwell equation (7.32) with the retarded propagator [2]. In a (1+1) dimensional spacetime the causal electric field can be written as

$$E(t,x) = (k^{(1)})\, q\ \left(\theta\left(x - r(\tau_0)\right) - \theta\left(r(\tau_0) - x\right)\right)\ , \tag{7.34}$$

where the retarded time is given by $ct - r^0(\tau_0) = \left|x - r^1(\tau_0)\right|$, see appendix A, and the constant $k^{(1)}$, which appears in SI units, denotes the Coulomb constant for the (1+1) dimensional spacetime. Consequently, the flux defined on this spacetime area A reads

$$\Phi_{EM} = (k^{(1)})\, 2\, q_p\, A \tag{7.35}$$

with the charge of one of the pair q_p.

Then, the flux quantization condition (7.20) implies

$$(k^{(1)})\, q\, q_p \frac{A}{\hbar c} = \pi\, n\,. \tag{7.36}$$

We should underline that in Eq. (7.36) q is electric charge of a particle interacting with the potential generated by a charged particle q_p. In other words, q is electric charge of a receiver particle, while q_p is the charge of a source particle.

We can further consider a scenario where both the receiver and the source particle have the same electric charge q_p. If we assume that the area A has a fundamental value which is determined by the universe, then the fundamental unit of electric charge can be given by

$$q_p = \sqrt{\frac{\pi\,\hbar\, c}{A\,(k^{(1)})}}\,. \tag{7.37}$$

Finally, electric charge q of any particle can be written in terms of the fundamental unit of charge q_p as

$$q = q_p\, n\,, \tag{7.38}$$

which would explain why electric charge of any particle is an integer multiple of the elementary charge.

We may further estimate the area A for the confined field created by the electron-positron pair in (1+1) dimensional spacetime as follows. It is bounded as $A < c^2\tau^2/2$, with the lifetime of an electron τ which can be estimated from the Heisenberg uncertainty relation $\tau\, \Delta E \sim \hbar$, with $\Delta E \sim m_e c^2$, yielding $\tau \sim \lambda_C/c$ and

$$A \sim \lambda_C^2\,, \tag{7.39}$$

with the Compton wavelength $\lambda_C = \hbar/(m_e c)$, as long as the Planck constant $\hbar$, the speed of light c, the mass of the electron m_e, and the fundamental charge e remain the same in the (1+1) dimensional world. Then the fine structure constant for the (1+1) dimensional spacetime can be estimated from Eq. (7.37) as

$$\alpha^{(1)} \equiv \frac{(k^{(1)})q_p^2}{\hbar c} \approx \lambda_C^{-2}\,. \tag{7.40}$$

The derived scaling law for the fine structure constant of the one dimensional world, Eq. (7.40), can be tested in an effectively one-dimensional solid layers like quantum wires.

7.5. Conclusion

The Wilson line introduces a completely path-dependent but gauge-function-free theory. This equivalent formulation of gauge theory can provide a very simple description of the quantization of the electromagnetic flux on the basis of the topology of the gauge paths. In particular, we have shown that the path independent electromagnetic flux through the area bounded by two gauge paths has to be quantized if these paths generates the same gauge potential. The developed formalism was applied to a toy model where we discussed the electric charge quantization on a (1+1) dimensional spacetime.

8. Summary and outlook

In this concluding chapter we first highlight the main results of the thesis. Then we discuss and further point out aspects in connection with the thesis as an outlook.

Summary

The main scope of the present thesis is laid on relativistic features of laser-induced tunnel-ionization. In order to present a comprehensive study on the tunnel-ionization we approached the problem under different aspects with different tools. We have first discussed gauge theory in chapter 2. We introduced the gauge invariant energy operator for an arbitrary time independent electromagnetic field enabling us to define the tunneling barrier for tunnel-ionization without ambiguity. Consequently, it is clearly pointed out that the tunneling mechanism for the ionization is not an intuitive picture that is valid in the certain gauges, but it was identified as a gauge invariant physical mechanism [45].

Next in chapter 3, the relativistic character of tunnel-ionization was investigated. First, it was demonstrated that in the relativistic regime, where one cannot neglect the magnetic field component of the laser, the ionized electron experiences a momentum shift along the laser's propagation direction. This result was obtained in the WKB approximation by reducing the whole dynamics to the one dimensional picture. Then, this result was clearly corroborated using the strong field approximation. Further, an ab initio numerical calculation confirmed the aforementioned result [31, 45].

In chapter 4, spin dynamics was discussed as a further relativistic feature of tunnel-ionization [89, 91, 111]. This dynamics was investigated via spin asymmetries. It was shown that there is an asymmetry between the tunneling probabilities of different spin states. Even taking into account the effect of the laser on the bound state, it is shown that although the asymmetry is suppressed for nonrelativistic parameters, for relativistic parameters the spin asymmetry prevails.

One of the most controversial issues regarding tunneling, the tunneling time delay, was discussed in chapter 6. Although no well defined time operator conjugate to the Hamiltonian exists in quantum mechanics, the time delay problem can be investigated according to the rules of quantum mechanics. To this end, the Wigner's time delay definition was adopted. First, we investigated it for model problems given in Sec. 6.2 via comparing the Wigner trajectory with the quasiclassical one at remote distance. Then, the definition was extended to the tunnel-ionization process.

It was shown that for the deep tunneling regime, where the continuum side of the potential is approximated linearly, the time delay vanishes. However, at a large laser field strength, in the near-threshold-tunneling regime of the tunnel-ionization, it was demonstrated that the signature of the time delay can be measurable at the detector [31, 45].

The detailed investigation of gauge theory led us to a path-dependent formulation of gauge theory as we discussed in chapter 2. In this equivalent formulation, the vector potentials are expressed in terms of paths instead of the gauge function of conventional gauge theory. Furthermore, this formulation leads to a geometric interpretation of gauge theory. Specifically, it is of great convenience for the quasiclassical calculation of the propagator via canceling the interaction term of the action [130]. Therefore, in chapter 5 we have calculated the relativistic propagator for an arbitrary constant and uniform electromagnetic field, for an arbitrary plane wave, and for an arbitrary plane wave combined with an arbitrary constant and uniform electromagnetic field. In this calculation we have used the proper time formalism. These results were later used in order to redefine the Wigner trajectory in terms of the phase of the fixed energy propagator, which is a more fundamental approach.

Finally in chapter 7, one of the most significant long standing unresolved problem in theoretical physics, which is charge quantization, was discussed via the path-dependent formulation of gauge theory. It was shown that, in the absence of a magnetic monopole, the possible reasons for charge quantization can be the uniqueness of the wave function for different paths yielding the same vector potentials. The developed formalism was applied in a (1+1) dimensional spacetime where the confined electric field due to pair production not only explains the charge quantization but also predicts the fundamental unit of the charge [69].

Outlook

First of all, our intuitive picture for relativistic tunnel-ionization is based on a one dimensional approximation of the exact potential barrier. Although in the absence of a magnetic field the full problem can be reduced to a one dimensional problem via separation of variables in parabolic cylindrical coordinates, the reduction of the entire problem to one dimension is still missing in the presence of a magnetic field. Hence finding a coordinate system which can separate the full Schrödinger equation could be a significant achievement.

The strong field approximation (SFA) is a commonly used and powerful mathematical tool for the strong field ionization. However, the main deficiency of the SFA is its gauge dependence. Although the dressed SFA can produce gauge invariant results in certain partitions of the Hamiltonian, the partitioning of the Hamiltonian cannot be unique. Therefore, a new mathematical method that can yield gauge independent results would reveal further properties of strong field ionization.

The controversy on the tunneling time delay in the literature is due to the lack of a

well defined time operator in quantum mechanics. A successful attempt to raise the parameter time to an operator would be a milestone work in the understanding of the foundations of quantum mechanics. The main reason for the current status of time as a parameter is that while time can take any value, the spectrum of the eigenvalues of the Hamiltonian that is conjugate to time cannot span the entire real line. This main argument was given by Pauli in 1926 [34, 35]. One possible resolution of the problem might be to extend the Hamiltonian in such a way that the eigenvalues of the new Hamiltonian span the entire real line, but its eigenvalues on the physical state coincide with those of the ordinary Hamiltonian, as in the case of the covariant quantization of the electromagnetic field with the introduction of unphysical states.

In chapter 4, we investigated the spin asymmetries in the tunneling regime. Actually, the spin states of interest used in this chapter are eigenstates of the Hamiltonian as well as of the total angular momentum operator $\boldsymbol{J}$, but not of the spin operator $\boldsymbol{S}$. The standard spin operator found in all textbooks $\boldsymbol{S} = \hbar\boldsymbol{\Sigma}/2$ does not commute with the free Hamiltonian, nevertheless there is no physical background for it. Although there are many proposals for a relativistic spin operator, (see [165] for a comprehensive review for comparison of different spin operators), we have also proposed a relativistic spin operator which commutes with the free Dirac Hamiltonian as well as satisfies the corresponding rotation group algebra, $SU(2)$ algebra, in appendix B. As a consequence, an investigation of spin asymmetries in terms of the eigenstate of the "right" spin operator would be a very remarkable research.

We want to conclude with commenting on gauge theory. We are confident that the path dependent formulation of gauge theory may reveal further phenomena in electromagnetism as well as in other gauge theories. Moreover, it might take the initiative to connect gauge symmetry with spacetime symmetries due to the fact that the path-dependent formalism provides a geometric interpretation of gauge theory.

A. Liénard - Wiechert potential in a (1+1) dimensional spacetime

In an arbitrary (d+1) dimensional spacetime, the nonhomogeneous Maxwell's equation (7.32) can be written in terms of the potential as

$$\partial^2 A^\mu(x) = \frac{2\pi^{d/2}}{\Gamma(d/2)} \frac{J^\mu(x)}{c} \tag{A.1}$$

where the Lorenz gauge $\partial_\mu A^\mu$ is employed. Note that in terms of the language of the path-dependent formalism, there exists a certain set of paths, which may be called the Lorenz paths, that $\partial_\mu \mathcal{A}^\mu(\mathcal{P}) = 0$ holds.

The corresponding solution of the potential, then, can be obtained via

$$A^\mu(x) = \frac{2\pi^{d/2}}{\Gamma(d/2)c} \int d^{d+1}x' D(x, x') J^\mu(x') \tag{A.2}$$

where the current $J^\mu(x)$ of a point charge q moving on the world line $r^\mu(\tau) = \left(r^0(\tau), r^i(\tau)\right)$ can be written as

$$J^\mu(x) = qc \int d\tau \, V^\mu(\tau) \delta^{d+1}(x - r(\tau)) \tag{A.3}$$

with the velocity of the source $V(\tau)$ [2]. Furthermore, the Green's function, the propagator, $D(x, x')$ defined in Eq. (A.2) satisfies

$$\partial_x^2 D(x, x') = \delta^{d+1}(x - x') \tag{A.4}$$

with the (d+1) dimensional Dirac delta function $\delta^{d+1}(x - x')$. Then in the Fourier k-space, the transformed Green's function $\tilde{D}(k)$ yields

$$\tilde{D}(k) = -\frac{1}{k^2} \, . \tag{A.5}$$

The causal fields can be obtained via the retarded Green's function. The retarded propagator $D_r(z)$ is followed by

$$D_r(z) = -\frac{1}{(2\pi)^{d+1}} \int d^{d+1}k \, \frac{e^{-ik\cdot z}}{(k_0 + i\epsilon)^2 - \boldsymbol{k}^2} \tag{A.6}$$

with $z = x - x'$ and $\epsilon > 0$.

In a (1+1) dimensional spacetime, the field strength tensor only includes the electric field as

$$F^{\mu\nu} = \begin{pmatrix} 0 & -E \\ E & 0 \end{pmatrix}, \tag{A.7}$$

such that

$$E = F^{10} = \partial^1 A^0 - \partial^0 A^1 . \tag{A.8}$$

Then, the retarded propagator for a (1+1) dimensional spacetime reads

$$D_r(z) = \frac{\theta(z^0)}{4\pi i} \int_{-\infty}^{\infty} dk^1 \left(\frac{e^{ik^1(z^1+z^0)}}{k^1} - \frac{e^{ik^1(z^1-z^0)}}{k^1} \right). \tag{A.9}$$

Furthermore, after calculating k^1 integral for the causal vector $z^0 > |z^1|$, the retarded propagator can be written

$$D_r(z) = \frac{1}{2}\theta(z^0)\theta(z^0 - |z^1|) . \tag{A.10}$$

As a consequence, plugging the retared propagator (A.10) and the current vector (A.3) into Eq. (A.2), the causal potential

$$A^\mu = q \int d\tau \, V^\mu(\tau)\theta(x^0 - r^0(\tau))\theta\left(x^0 - r^0(\tau) - |x^1 - r^1(\tau)|\right) \tag{A.11}$$

is obtained, which is the Liénard-Wiechert potential for a (1+1) dimensional spacetime. Note that in contrast to the (3+1) case where the retardation condition appears in the vector potential, in a (1+1) dimensional world, this condition comes later with defining the causal electric field.

From Eq. (A.8), the causal electric field reads

$$\begin{aligned} E = &-q \int d\tau V^0(\tau)\theta(x^0 - r^0(\tau))\frac{\partial}{\partial x^1}\theta\left(x^0 - r^0(\tau) - \left|x^1 - r^1(\tau)\right|\right) \\ &- q \int d\tau V^1(\tau)\delta(x^0 - r^0(\tau))\theta\left(x^0 - r^0(\tau) - \left|x^1 - r^1(\tau)\right|\right) \\ &- q \int d\tau V^1(\tau)\theta(x^0 - r^0(\tau))\delta\left(x^0 - r^0(\tau) - \left|x^1 - r^1(\tau)\right|\right) . \end{aligned} \tag{A.12}$$

Since the second integral vanishes, the causal field becomes

$$E = -q \int d\tau \theta(x^0 - r^0(\tau))\delta\left(x^0 - r^0(\tau) - \left|x^1 - r^1(\tau)\right|\right)\left(V^1 \mp V^0\right) \tag{A.13}$$

where $-$ $(+)$ sign in front of V^0 is for $x^1 - r^1(\tau) > 0$ $\left(x^1 - r^1(\tau) < 0\right)$. The Dirac delta in Eq. (A.13) gives the retardation condtion

$$x^0 - r^0(\tau_0) = \left|x^1 - r^1(\tau_0)\right| . \tag{A.14}$$

Furthermore, because the velocity satisfies the condition $V^0 > \left|V^1\right|$, the causal electric field for a (1+1) dimensional world can be written as

$$E = \begin{cases} q\,\theta\left(x^1 - r^1(\tau_+\right), & x^1 - r^1(\tau) > 0, \\ \\ -q\,\theta\left(r^1(\tau_-) - x^1\right), & x^1 - r^1(\tau) < 0\,, \end{cases} \tag{A.15}$$

where the light-cone conditon is given by $x^0 - r^0(\tau_\pm) = \pm\left(x^1 - r^1(\tau_\pm)\right)$. This can be further compactified as

$$E(t,x) = q\,\left(\theta\left(x^1 - r^1(\tau_0)\right) - \theta\left(r^1(\tau_0) - x^1\right)\right)\,. \tag{A.16}$$

B. On the relativistic spin operator

The spin operator that is used in the standard relativistic quantum mechanical calculations is given by

$$S_i = \frac{\Sigma_i}{2} = \frac{1}{2}\begin{pmatrix}\sigma_i & 0\\ 0 & \sigma_i\end{pmatrix}. \tag{B.1}$$

Although it satisfies $SU(2)$ Lie algebra, there is a substantial deficiency of this operator; it does not commute with the free Dirac Hamiltonian [57]. It only commutes with the corresponding free Hamiltonian in the rest frame of a given Dirac particle. We have identified it as a deficiency, since there is no physical background of the reasoning of why it does not commute with the free Hamiltonian. On the contrary, there is neither a dynamical rotation nor a kinematic rotation on the free spin state. Namely, there is no interaction to cause any dynamical rotation and further, since one can go to an arbitrary frame from the rest frame by a single boost transformation, there cannot exist a Thomas-Wigner rotation [166, 167] on the spin state.

One way to resolve the problem is diagonalizing the free Dirac Hamiltonian via Foldy-Wouthuysen transformation. In this new representation the free Hamiltonian commutes with the spin operator (B.1) [168]. However, the rest of the formulation of the relativistic quantum mechanics should be based on the new formulation, which can be treated as a drawback.

Instead, one can construct the relativistic spin operator, which satisfies both $SU(2)$ Lie algebra and commutes with the free Hamiltonian, on the basis of the group theoretical consideration of the Poincaré transformation $x'^{\mu} = \Lambda^{\mu}{}_{\nu}x^{\nu} + a^{\mu}$. Indeed, each irreducible unitary representation of the Poincare group (combined with the discrete symmetries such as C, P, T) can be connected to the corresponding quantum state of an elementary particle [167, 169, 170]. Hence, for a Dirac particle, one should be able to construct the corresponding spin operator via the associated irreducible unitary representation.

As comprehensively described by Wigner in [167], the Poincaré group can be represented for a quantum particle on the Hilbert space of one particle states. The one particle state can be denoted with momentum $\boldsymbol{p}$ and all collective other quantum numbers σ as $|\boldsymbol{p}, \sigma\rangle = a^{\dagger}_{\boldsymbol{p},\sigma}|0\rangle$ with the vacuum state $|0\rangle$. Since $\boldsymbol{p}$ can span the entire real line, the Hilbert space of one particle state is infinite dimensional and as a consequence the associated representation can be unitary and the generators of the Poincaré group can be represented by hermitian operators [167] (see [20, 171–173] for the details). Furthermore, finding the unitary irreducible representations of the Poincaré group can reduce to finding the unitary irreducible representations of its little group [167].

The little group is the subgroup of the Poincaré group which leaves a given choice of P^μ invariant. For a massive particle, one can always defined a rest frame $P^\mu = (m, \mathbf{0})$. Trivially, mass is the first invariance, and further, the group of transformations which leaves $P^\mu = (m, 0, 0, 0)$ invariant is the group of three dimensional spatial rotations $SO(3)$. Further, for spin representation of the rotation group, one can also specify the little group as $SU(2)$ which is the double cover of $SO(3)$. It is well-known that the irreducible representations of $SU(2)$ are labeled by the spin quantum number s [115]. Thus, a massive particle can be completely characterized by two labels, mass m, and the spin s [20, 171, 172].

In fact, there is another way to see that a massive representation of the Poincaré group can be completely specified by the labels m and s. This is based on the Casimir operators. By definition, the Casimir operators are operators that commute with all the generators of the algebra, and hence, the representation on the space of the eigenstates of the Casimir operators is irreducible. Moreover, the Casimir operators can also reveal the relativistic spin operator as follows: The Poincaré group has two Casimir operators [20, 172, 174]

$$P^2 = P^\mu P_\mu \,, \tag{B.2}$$

$$W^2 = W^\mu W_\mu \,, \tag{B.3}$$

where $W^\mu = -\epsilon^{\mu\nu\rho\sigma} M_{\nu\rho} P_\sigma / 2$ is the Pauli-Lubanski vector with the generators of the homogeneous Lorentz transformations $M^{\mu\nu}$ and the translations P^μ. For a massive particle, one can go to the rest frame $P^\mu = (m, \mathbf{0})$ where the components of the Pauli-Lubanski vector yield

$$W_R^0 = 0 \,, \tag{B.4}$$

$$W_R^i = m S^i \,. \tag{B.5}$$

Here we identified the spin S^i as the value of total angular momentum J^i in the rest frame. Thus, two Casimir operators read

$$P^2 = m^2 \,, \tag{B.6}$$

$$W^2 = -m^2 \boldsymbol{S}^2 \,, \tag{B.7}$$

which leads to the facts that the representations are labeled by the mass m and by the spin s for massive particles as we promised. Further, we observe that $\boldsymbol{S}^2$ is Lorentz invariant and relativistic spin operator is related to Pauli-Lubanski vector via Eq. (B.5) as

$$\boldsymbol{S} = \frac{\boldsymbol{W_R}}{m} \,. \tag{B.8}$$

This relation can further be identified in an arbitrary frame via

$$W_R^i = L^{-1}(p)^i{}_\mu W^\mu = W^i - \frac{P^i W_0}{m + H} \tag{B.9}$$

with the inverse Lorentz transformation $L^{-1}(p)^\nu{}_\mu$ [20]. As a result, the spin operator originally defined in Eq. (B.8) yields

$$\boldsymbol{S} = \frac{\boldsymbol{W}}{m} - \frac{W_0 \boldsymbol{P}}{m(m + H)} \,, \tag{B.10}$$

and in terms of the generators of the Poincaré group, it reads

$$\boldsymbol{S} = \frac{H\boldsymbol{J}}{m} - \frac{\boldsymbol{K}\times\boldsymbol{P}}{m} - \frac{\boldsymbol{P}(\boldsymbol{P}\cdot\boldsymbol{J})}{(H+m)m}\,. \tag{B.11}$$

This form of the spin operator has been known since early days of quantum mechanics (see [175]) and later it was rederived in different context [172, 173, 176–179].

What we have proposed is the following; the spin operator (B.11) can be further elaborated in the Dirac basis via choosing the following representations for the generators of the Poincaré group [180]

$$\boldsymbol{P} = -i\nabla\,, \tag{B.12}$$

$$H = \boldsymbol{\alpha}\cdot\boldsymbol{P} + m\gamma^0\,, \tag{B.13}$$

$$\boldsymbol{J} = \boldsymbol{x}\times\boldsymbol{P} + \frac{\boldsymbol{\Sigma}}{2}\,, \tag{B.14}$$

$$\boldsymbol{K} = \frac{1}{2}\left(H\boldsymbol{x} + \boldsymbol{x}H\right)\,. \tag{B.15}$$

After plugging the representations into Eq. (B.11), it is calculated that the spin operator reads

$$\boldsymbol{S} = \frac{\gamma^0\boldsymbol{\Sigma}}{2} + \frac{\boldsymbol{P}}{2}\gamma^5\left(\gamma^0+1\right)\frac{1}{H+m}\,. \tag{B.16}$$

Finally, using the operator identity

$$\frac{1}{H+m} = \frac{\boldsymbol{\alpha}\cdot\boldsymbol{P} + m(\gamma^0+1)}{\boldsymbol{P}^2}\,, \tag{B.17}$$

we end up with the "right" relativistic spin operator

$$S_i = \frac{\gamma^0\Sigma_j}{2}\left(\delta_{ij} + (\gamma^0-1)\hat{P}_i\hat{P}_j\right)\,. \tag{B.18}$$

There are many remarkable features of this spin operator: First of all, it fulfills $SU(2)$ algebra in order to be the generator of the rotation group. Next, it commutes with the free Dirac Hamiltonian and hence the drawback that we discussed at the beginning of the appendix has been removed. Furthermore, since we constructed it via the unitary representation of the Poincaré group, it includes the γ^0 factor in itself, which identifies the Lorentz scalar as $\psi^\dagger\psi$ instead of $\overline{\psi}\psi$. Another consistent property of the relativistic spin operator (B.18) is that it yields the proper helicity operator $\boldsymbol{S}\cdot\boldsymbol{P}$ as

$$\boldsymbol{S}\cdot\boldsymbol{P} = \frac{\boldsymbol{\Sigma}\cdot\boldsymbol{P}}{2}\,. \tag{B.19}$$

Bibliography

[1] B. Zwiebach, *A First Course in String Theory* (Cambridge University Press, New York, 2004).

[2] J. D. Jackson, *Classical Electrodynamics* (Wiley, New York, 1975).

[3] J. C. Maxwell, "A dynamical theory of the electromagnetic field," Phil. Trans. R. Soc. Lond. **155**, 459–512 (1865).

[4] A. Einstein, "On the electrodynamics of moving bodies," Annalen der Physik **17**, 891–921 (1905).

[5] H. Weyl, "Quantum mechanics and group theory," Z. Phys. **46**, 1–46 (1927).

[6] S. Weinberg, *The Quantum Theory of Fields II* (Cambridge University Press, New York, 1996).

[7] L. Ryder, *Quantum Field Theory* (Cambridge University Press, New York, 1985).

[8] M. E. Peskin and D. V. Schroeder, *An Introduction to Quantum Field Theory* (Perseus Books, Reading, Massachusetts, 1995).

[9] R. Mills, Am. J. Phys. **57**, 493 (1989).

[10] C. N. Yang and R. L. Mills, "Conservation of isotopic spin and isotopic gauge invariance," Phys. Rev. **96**, 191 (1954).

[11] S. Tomonaga, "On a relativistically invariant formulation of the quantum theory of wave fields," Progress of Theoretical Physics **1**, 27–42 (1949).

[12] J. Schwinger, "On quantum-electrodynamics and the magnetic moment of the electron," Physical Review **73**, 416–417 (1948).

[13] J. Schwinger, "Quantum electrodynamics. i. a covariant formulation," Physical Review **74**, 1439–1461 (1948).

[14] R. Feynman, "Space-time approach to quantum electrodynamics," Physical Review **76**, 769–789 (1949).

[15] R. Feynman, "The theory of positrons," Physical Review **76**, 749–759 (1949).

[16] R. Feynman, "Mathematical formulation of the quantum theory of electromagnetic interaction," Physical Review **80**, 440–457 (1950).

[17] F. Dyson, "The radiation theories of tomonaga, schwinger, and feynman," Physical Review **75**, 486–502 (1949).

[18] F. Dyson, "The s matrix in quantum electrodynamics," Physical Review **75**, 1736–1755 (1949).

[19] S. Sturm, A. Wagner, B. Schabinger, J. Zatorski, Z. Harman, W. Quint, G. Werth, C. H. Keitel, and K. Blaum, Physical Review Letters **107** (2011).

[20] S. Weinberg, *The Quantum Theory of Fields I* (Cambridge University Press, New York, 1995).

[21] V. Yanovsky, V. Chvykov, G. Kalinchenko, P. Rousseau, T. Planchon, T. Matsuoka, A. Maksimchuk, J. Nees, G. Cheriaux, G. Mourou, and K. Krushelnick, "Ultra-high intensity-300-tw laser at 0.1 hz repetition rate," Opt. Express **16**, 2109–2114 (2008).

[22] A. D. Piazza, C. Müller, K. Z. Hatsagortsyan, and C. H. Keitel, "Extremely high-intensity laser interactions with fundamental quantum systems," **84**, 1177–1228 (2012).

[23] C. I. Moore, A. Ting, S. J. McNaught, J. Qiu, H. R. Burris, and P. Sprangle, "A laser-accelerator injector based on laser ionization and ponderomotive acceleration of electrons," **82**, 1688–1691 (1999).

[24] E. A. Chowdhury, C. P. J. Barty, and B. C. Walker, ""nonrelativistic" ionization of the *L*-shell states in argon by a "relativistic" 10^{19}W/cm^2 laser field," **63**, 042712 (2001).

[25] M. Dammasch, M. Dörr, U. Eichmann, E. Lenz, and W. Sandner, "Relativistic laser-field-drift suppression of nonsequential multiple ionization," **64**, 061402 (2001).

[26] K. Yamakawa, Y. Akahane, Y. Fukuda, M. Aoyama, N. Inoue, and H. Ueda, "Ionization of many-electron atoms by ultrafast laser pulses with peak intensities greater than 10^{19}w/cm^2," **68** (2003).

[27] E. Gubbini, U. Eichmann, M. Kalashnikov, and W. Sandner, "Strong laser field ionization of kr: first-order relativistic effects defeat rescattering," J. Phys. B: At., Mol. Opt. Phys. **38**, L87–L93 (2005).

[28] A. D. DiChiara, I. Ghebregziabher, R. Sauer, J. Waesche, S. Palaniyappan, B. L. Wen, and B. C. Walker, "Relativistic mev photoelectrons from the single atom response of argon to a 10^{19} W/cm^2 laser field," **101**, 173002 (2008).

[29] S. Palaniyappan, R. Mitchell, R. Sauer, I. Ghebregziabher, S. L. White, M. F. Decamp, and B. C. Walker, "Ionization of methane in strong and ultrastrong relativistic fields," **100**, 183001 (2008).

[30] A. D. DiChiara, I. Ghebregziabher, J. M. Waesche, T. Stanev, N. Ekanayake, L. R. Barclay, S. J. Wells, A. Watts, M. Videtto, C. A. Mancuso, and B. C.

Walker, "Photoionization by an ultraintense laser field: Response of atomic xenon," **81**, 043417 (2010).

[31] M. Klaiber, E. Yakaboylu, H. Bauke, K. Z. Hatsagortsyan, and C. H. Keitel, "Under-the-barrier dynamics in laser-induced relativistic tunneling," Phys. Rev. Lett. **110**, 153004 (2013).

[32] M. Razavy, *Quantum Theory of Tunneling* (World Scientic, Singapore, 2003).

[33] L. A. MacColl, "Note on the transmission and reflection of wave packets by potential barriers," **40**, 621–626 (1932).

[34] W. Pauli, *Prinzipien der Quantentheorie I / Principles of Quantum Theory I*, vol. V 1 of *Handbuch der Physik Encyclopedia of Physics* (Springer, Heidelberg, 1958).

[35] P. Carruthers and M. M. Nieto, "Phase and angle variables in quantum mechanics," **40**, 411–440 (1968).

[36] L. E. Eisenbud, Ph.D. thesis, Princeton University, Princeton (1948).

[37] E. P. Wigner, "Lower limit for the energy derivative of the scattering phase shift," **98**, 145–147 (1955).

[38] F. T. Smith, "Lifetime matrix in collision theory," Phys. Rev. **118**, 349–356 (1960).

[39] R. Landauer and T. Martin, "Barrier interaction time in tunneling," **66**, 217–228 (1994).

[40] D. Sokolovski, "Quantum traversal time, path integrals and "superluminal" tunnelling," in "Time in Quantum Mechanics," , vol. 734 of *Lecture Notes in Physics*, J. G. Muga, R. Sala Mayato, and Í. L. Egusquiza, eds. (Springer, Berlin, Heidelberg, 2007), pp. 195–233.

[41] A. M. Steinberg, "Experimental issues in quantum-mechanical time measurement," in "Time in Quantum Mechanics," , vol. 734 of *Lecture Notes in Physics*, J. G. Muga, R. Sala Mayato, and Í. L. Egusquiza, eds. (Springer, Berlin, Heidelberg, 2007), pp. 333–353.

[42] Y. Ban, E. Y. Sherman, J. G. Muga, and M. Büttiker, "Time scales of tunneling decay of a localized state," **82**, 062121 (2010).

[43] E. A. Galapon, "Only above barrier energy components contribute to barrier traversal time," **108**, 170402 (2012).

[44] H. R. Reiss, "Limits on tunneling theories of strong-field ionization," Phys. Rev. Lett. **101**, 043002 (2008).

[45] E. Yakaboylu, M. Klaiber, H. Bauke, K. Z. Hatsagortsyan, and C. H. Keitel, "Relativistic features and time delay of laser-induced tunnel-ionization," (2013).

[46] B. S. DeWitt, "Quantum theory without electromagnetic potentials," Phys. Rev. **125**, 2189 (1962).

[47] S. Mandelstam, "Quantum electrodynamics without potentials," Ann. Phys. **19**, 1 (1962).

[48] F. J. Belinfante, "Consequences of postulate of a complete commuting set of observables in quantum electrodynamics," Phys. Rev. **128**, 2832 (1962).

[49] F. Rohrlich and F. Strocchi, "Gauge independence and path independence," Phys. Rev. **139**, B476 (1965).

[50] L. V. Keldysh, Zh. Eksp. Teor. Fiz. **47**, 1945 (1964).

[51] F. H. M. Faisal, "Multiple absorption of laser photons by atoms," J. Phys. B: At., Mol. Opt. Phys. **6**, L89–L92 (1973).

[52] H. R. Reiss, "Effect of an intense electromagnetic field on a weakly bound system," **22**, 1786–1813 (1980).

[53] H. R. Reiss, "Theoretical methods in quantum optics - s-matrix and keldysh techniques for strong-field processes," Prog. Quantum Electron **16**, 1–71 (1992).

[54] F. Faisal, "Gauge-equivalent intense-field approximations in velocity and length gauges to all orders," Physical Review A **75** (2007).

[55] F. H. M. Faisal, "Gauge-invariant intense-field approximations to all orders," Journal of Physics B: Atomic, Molecular and Optical Physics **40**, F145–F155 (2007).

[56] P. Langacker, "Structure of the standard model," (2003).

[57] J. D. Bjorken and S. D. Drell, *Relativistic Quantum Mechanics* (McGraw-Hill, New York, 1964).

[58] A. Kaldun, Ph.D. thesis, Ruprecht-Karls Universität Heidelberg (2014). Referees:.

[59] L. D. Landau and E. M. Lifshitz, *The Classical Theory of Fields*, vol. 2 of *Course of Theoretical Physics* (Butterworth Heinemann, Oxford, 1975).

[60] Y. Aharonov and D. Bohm, "Significance of electromagnetic potentials in the quantum theory," Phys. Rev. **115**, 485 (1959).

[61] W. Ehrenberg and R. E. Siday, "The refractive index in electron optics and the principles of dynamics," Proc. Phys. Soc. B **62**, 8 (1949).

[62] Y. Aharonov and D. Bohm, "Further considerations on electromagnetic potentials in the quantum theory," Phys. Rev. **123**, 1511 (1961).

[63] L. Onsager, Proceedings of the International Conference on Theoretical Physics, Kyoto and Tokyo, September, 1953 (Science Council of Japan, Tokyo, 1954) p. 935 (1954).

[64] F. London, Superfluids **1**, 152 (1950).

[65] B. S. Deaver and W. M. Fairbank, "Experimental evidence for quantized flux in superconducting cylinders," Phys. Rev. Lett. **7**, 43 (1961).

[66] R. Doll and M. Nabauer, "Experimental proof of magnetic flux quantization in a superconducting ring," Phys. Rev. Lett. **7**, 51 (1961).

[67] P. A. M. Dirac, "Quantised singularities in the electromagnetic field," Proc. R. Soc. London A **133**, 60 (1931).

[68] P. A. M. Dirac, "The theory of magnetic poles," Phys. Rev. **74**, 817 (1948).

[69] E. Yakaboylu and K. Z. Hatsagortsyan, "On the quantization of the nonintegrable phase in electrodynamics," (2013).

[70] S. Weinberg, *Lectures on Quantum Mechanics* (Cambridge University Press, New York, 2013).

[71] T. T. Wu and C. N. Yang, "Concept of nonintegrable phase factors and global formulation of gauge fields," Phys. Rev. D **12**, 3845 (1975).

[72] K. G. Wilson, "Confinement of quarks," Phys. Rev. D **10**, 2445 (1974).

[73] P. G. Bergmann, "Introduction of true observables into the quantum field equations," Nuovo Cimento **3**, 1177 (1956).

[74] P. A. M. Dirac, "Gauge-invariant formulation of quantum electrodynamics," Can. J. Phys. **33**, 650 (1955).

[75] N. Cabibbo and E. Ferrari, "Quantum electrodynamics with dirac monopoles," Nuovo Cimento **23**, 1147 (1962).

[76] J. H. VanVleck, "The correspondence principle in the statistical interpretation of quantum mechanics," Proc. Nat. Acad. Sci. U.S.A. **14**, 178 (1928).

[77] C. Morette, "On the definition and approximation of feynman path integrals," Phys. Rev. **81**, 848 (1951).

[78] B. S. DeWitt, "Dynamical theory in curved spaces .1. a review of the classical and quantum action principles," Rev. Mod. Phys. **29**, 377 (1957).

[79] W. Pauli, *Lectures on Physics* (MIT Press, 1973).

[80] W. Becker, F. Grasbon, R. Kopold, D. Milošević, G. G. Paulus, and H. Walther, "Above-threshold ionization: From classical features to quantum effects," in "Advances In Atomic, Molecular, and Optical Physics," , vol. 48, B. Bederson and H. Walther, eds. (Academic Press, San Diego, 2002), pp. 35–98.

[81] S. Augst, D. Strickland, D. D. Meyerhofer, S. L. Chin, and J. H. Eberly, "Tunneling ionization of noble gases in a high-intensity laser field," **63**, 2212–2215 (1989).

[82] P. B. Corkum **71**, 1994–1997 (1993).

[83] H. R. Reiss, "Complete keldysh theory and its limiting cases," **42**, 1476–1486 (1990).

[84] H. R. Reiss, "Relativistic strong-field photoionization," J. Opt. Soc. Am. B **7**, 574–586 (1990).

[85] H. Bauke and C. H. Keitel, "Accelerating the Fourier split operator method via graphics processing units," **182**, 2454–2463 (2011).

[86] L. D. Landau and E. M. Lifshitz, *Quantum Mechanics*, vol. 3 of *Course of Theoretical Physics* (Butterworth Heinemann, Oxford, 1981).

[87] L. D. Landau and E. M. Lifshitz, *Mechanics*, vol. 1 of *Course of Theoretical Physics* (Butterworth Heinemann, Oxford, 1976).

[88] D. M. Volkov, "Über eine Klasse von Lösungen der Diracschen Gleichung," Z. Phys. **94**, 250–260 (1935).

[89] M. Klaiber, E. Yakaboylu, and K. Z. Hatsagortsyan, "Above-threshold ionization with highly charged ions in superstrong laser fields. I. Coulomb-corrected strong-field approximation," **87**, 023417 (2013).

[90] E. M. Lifshitz, L. P. Pitaevskii, and V. B. Berestetskii, *Quantum Electrodynamics*, vol. 4 of *Course of Theoretical Physics* (Butterworth Heinemann, Oxford, 1996).

[91] M. Klaiber, E. Yakaboylu, and K. Z. Hatsagortsyan, "Above-threshold ionization with highly charged ions in superstrong laser fields. II. Relativistic Coulomb-corrected strong-field approximation," **87**, 023418 (2013).

[92] C. T. L. Smeenk, L. Arissian, B. Zhou, A. Mysyrowicz, D. M. Villeneuve, A. Staudte, and P. B. Corkum, "Partitioning of the linear photon momentum in multiphoton ionization," **106**, 193002 (2011).

[93] A. S. Titi and G. W. F. Drake, "Quantum theory of longitudinal momentum transfer in above-threshold ionization," **85**, 041404 (2012).

[94] F. Bunkin, A. Kazakov, and M. Fedorov, Usp. Fiz. Nauk **107**, 559 (1972). [Sov. Phys. Usp. **15**, 416 (1973)].

[95] C. Szymanowski, V. Véniard, R. Taïeb, A. Maquet, and C. H. Keitel, "Mott scattering in strong laser fields," Phys. Rev. A **56**, 3846–3859 (1997).

[96] P. Panek, J. Z. Kamiński, and F. Ehlotzky, "Relativistic electron-atom scattering in an extremely powerful laser field: Relevance of spin effects," Phys. Rev. A **65**, 033408 (2002).

[97] P. Panek, J. Z. Kamiński, and F. Ehlotzky, "Analysis of resonances in møller scattering in a laser field of relativistic radiation power," Physical Review A **69**, 013404 (2004).

[98] M. W. Walser, C. Szymanowski, and C. H. Keitel, "Influence of spin-laser interaction on relativistic harmonic generation," **48**, 533–539 (1999).

[99] M. W. Walser and C. H. Keitel, "Spin-induced force in intense laser-electron interaction," Journal of Physics B: Atomic, Molecular and Optical Physics **33**, L221–L225 (2000).

[100] S. Ahrens, H. Bauke, C. H. Keitel, and C. Mller, "Spin dynamics in the kapitza-dirac effect," Physical Review Letters **109** (2012).

[101] A. Di Piazza, A. I. Milstein, and C. Mller, "Polarization of the electron and positron produced in combined coulomb and strong laser fields," Physical Review A **82** (2010).

[102] T.-O. Mller and C. Mller, Physics Letters B **696**, 201–206 (2011).

[103] T.-O. Mller and C. Mller, "Longitudinal spin polarization in multiphoton bethe-heitler pair production," Physical Review A **86** (2012).

[104] S. Hu and C. Keitel, "Spin signatures in intense laser-ion interaction," Physical Review Letters **83**, 4709–4712 (1999).

[105] S. Hu and C. Keitel, "Dynamics of multiply charged ions in intense laser fields," Physical Review A **63** (2001).

[106] M. Walser and C. Keitel, "Narrow high-frequency spectral features via laser-induced slow spin flips," Opt. Commun. **199**, 447–451 (2001).

[107] M. Walser, D. Urbach, K. Hatsagortsyan, S. Hu, and C. Keitel, "Spin and radiation in intense laser fields," Physical Review A **65** (2002).

[108] S. Bhattacharyya, M. Mukherjee, J. Chakrabarti, and F. H. M. Faisal, "Spin currents from helium in intense-field photo-ionization," Journal of Physics: Conference Series **80**, 012029 (2007).

[109] S. Bhattacharyya, M. Mazumder, J. Chakrabarti, and F. H. M. Faisal, "Spin dynamics in nonsequential two-photon double ionization of helium in an intense laser field," Physical Review A **83** (2011).

[110] F. H. M. Faisal, "Spin asymmetry in an intense-field ionization process," Phys. Rev. Lett. **93**, 053002 (2004).

[111] M. Klaiber, E. Yakaboylu, C. Müller, H. Bauke, G. G. Paulus, and K. Z. Hatsagortsyan, "Spin effects in relativistic ionization with highly charged ions in super-strong laser fields," (2013).

[112] H. J. W. G. B. Arfken, *Mathematical Methods for Physicists* (Elsevier, Amsterdam, 2005).

[113] G. F. Gribakin and M. Y. Kuchiev, "Multiphoton detachment of electrons from negative ions," Phys. Rev. A **55**, 3760–3771 (1997).

[114] Y. V. Vanne and A. Saenz, "Exact keldysh theory of strong-field ionization: Residue method versus saddle-point approximation," Phys. Rev. A **75**, 033403 (2007).

[115] J. J. Sakurai, *Modern Quantum Mechanics* (Addison-Wesley, Massachusetts, 1994).

[116] R. P. Feynman, "Space-time approach to non-relativistic quantum mechanics," Rev. Mod. Phys. **20**, 367 (1948).

[117] R. P. Feynman and A. R. Hibbs, *Quantum Mechanics and Path Integrals* (McGraw-Hill, New York, 1965).

[118] L. S. Schulman, *Techniques and Applications of Path Integration* (Wiley, New York, 1981).

[119] H. Kleinert, *Path Integrals in Quantum Mechanics, Statistics, Polymer Physics, and Financial Markets* (World Scientic, Singapore, 2009).

[120] H. R. Reiss and J. H. Eberly, "Green's function in intense-field electrodynamics," Phys. Rev. **151**, 1058–1066 (1966).

[121] J. H. Eberly and H. R. Reiss, "Electron self-energy in intense plane-wave field," Phys. Rev. **145**, 1035–1040 (1966).

[122] T. Boudjedaa, L. Chetouani, L. Guechi, and T. F. Hammann, "Path integral for particles of spin zero and 1/2 in the field of an electromagnetic plane-wave," Phys. Scr. A **46**, 289–294 (1992).

[123] A. Barducci and R. Giachetti, "Scalar and spinning particles in a plane-wave field," J. Phys. A: Math. Gen. **36**, 8129–8140 (2003).

[124] V. Fock, "Eigen-time in classical and quantum mechanics," Phys. Rev. **12**, 404 (1937).

[125] J. Schwinger, "On gauge invariance and vacuum polarization," Phys. Rev. **82**, 664 (1951).

[126] P. A. M. Dirac, *Lectures on Quantum Mechanics* (Yeshiva University, New York, 1964).

[127] E. S. Fradkin and D. M. Gitman, "Path-integral representation for the relativistic particle propagators and bfv quantization," Phys. Rev. D **44**, 3230–3236 (1991).

[128] L. Brink, P. D. Vecchia, and P. Howe, "lagrangian formulation of classical and quantum dynamics of spinning particles," Nucl. Phys. B **118**, 76–94 (1977).

[129] A. M. Polyakov, *Gauge Fields and Strings* (Harwood Academic, Chur, Switzerland, 1987).

[130] E. Yakaboylu, K. Z. Hatsagortsyan, and C. H. Keitel, "The propagator of a relativistic particle via the path-dependent vector potential," (2013).

[131] V. G. Bagrov and D. M. Gitman, *Exact Solutions of Relativistic Wave Equations, Sec. 16* (Kluwer Academic Publishers, Dordrecht, Boston, London, 1990).

[132] G. Nimtz, "Tunneling confronts special relativity," Foundations of Physics **41**, 1193–1199 (2011).

[133] A. I. Baz', Yad. Fiz. **4**, 252 (1966).

[134] A. Peres, "Measurement of time by quantum clocks," **48**, 552–557 (1980).

[135] P. C. W. Davies, "Quantum tunneling time," **73**, 23–27 (2005).

[136] N. Vona, G. Hinrichs, and D. Dürr, "What does one measure when one measures the arrival time of a quantum particle?" Physical Review Letters **111**, 220404 (2013).

[137] P. Eckle, M. Smolarski, P. Schlup, J. Biegert, A. Staudte, M. Schöffler, H. G. Muller, R. Dörner, and U. Keller, "Attosecond angular streaking," Nature Phys. **4**, 565–570 (2008).

[138] P. Eckle, A. N. Pfeiffer, C. Cirelli, A. Staudte, R. Dorner, H. G. Muller, M. Buttiker, and U. Keller, "Attosecond ionization and tunneling delay time measurements in helium," Science **322**, 1525–1529 (2008).

[139] A. N. Pfeiffer, C. Cirelli, M. Smolarski, D. Dimitrovski, M. Abu-samha, L. B. Madsen, and U. Keller, "Attoclock reveals natural coordinates of the laser-induced tunnelling current flow in atoms," Nature Phys. **8**, 76–80 (2012).

[140] J. Maurer, A. S. Landsman, M. Weger, R. Boge, A. Ludwig, S. Heuser, C. Cirelli, L. Gallmann, and U. Keller, "Tunneling time in ultrafast science is real and probabilistic," in "CLEO: 2013," (Optical Society of America, 2013), p. QTh1D.3.

[141] C. Cirelli, A. Pfeiffer, M. Smolarski, P. Eckle, and U. Keller, *Attosecond Physics* (Springer, Berlin Heidelberg, 2013).

[142] A. M. Perelomov and V. S. Popov, Zh. Eksp. Theor. Fiz. **50**, 1393 (1966).

[143] V. S. Popov, "Tunnel and multiphoton ionization of atoms and ions in a strong laser field (Keldysh theory)," Physics-Uspekhi **47**, 855–885 (2004).

[144] V. S. Popov, "Imaginary-time method in quantum mechanics and field theory," Phys. Atom. Nuclei **68**, 686–708 (2005).

[145] S. V. Popruzhenko, G. G. Paulus, and D. Bauer, "Coulomb-corrected quantum trajectories in strong-field ionization," **77**, 053409 (2008).

[146] S. Popruzhenko and D. Bauer, "Strong field approximation for systems with coulomb interaction," J. Mod. Opt. **55**, 2573–2589 (2008).

[147] E. Merzbacher, *Quantum Mechanics* (John Wiley, New York, 1961).

[148] M. Abramowitz and I. A. Stegun, eds., *Handbook of Mathematical Functions with Formulas, Graphs, and Mathematical Tables* (Dover Publications, Mineola, 1972).

[149] R. A. Millikan, "On the elementary electrical charge and the avogadro constant," Phys. Rev. **2**, 109–143 (1913).

[150] J. Preskill, "Magnetic monopoles," Annual Review of Nuclear and Particle Science **34**, 461–530 (1984).

[151] D. Zwanziger, "Exactly soluble nonrelativistic model of particles with both electric and magnetic charges," Phys. Rev. **176**, 1480–1488 (1968).

[152] D. Zwanziger, "Quantum field theory of particles with both electric and magnetic charges," Phys. Rev. **176**, 1489–1495 (1968).

[153] J. Schwinger, "Magnetic charge and quantum field theory," Phys. Rev. **144**, 1087–1093 (1966).

[154] J. Beringer *et al.*, "Review of particle physics," Phys. Rev. D **86**, 010001 (2012).

[155] H. Georgi and S. L. Glashow, "Unity of all elementary-particle forces," Phys. Rev. Lett. **32**, 438–441 (1974).

[156] P. Langacker, "Grand unified theories and proton decay," physics Reports-Review Section of Physics Letters **72**, 185–385 (1981).

[157] G. 't Hooft, "Magnetic monopoles in unified gauge theories," Nuclear Physics B **79**, 276–284 (1974).

[158] A. M. Polyakov, "Particle spectrum in quantum field theory," JETP Letters **20**, 194–195 (1974).

[159] C. Q. Geng and R. E. Marshak, "Uniqueness of quark and lepton representations in the standard model from the anomalies viewpoint," Phys. Rev. D **39**, 693–696 (1989).

[160] J. A. Minahan, P. Ramond, and R. C. Warner, "Comment on anomaly cancellation in the standard model," Phys. Rev. D **41**, 715–716 (1990).

[161] C. Q. Geng and R. E. Marshak, "Reply to "comment on anomaly cancellation in the standard model"," Phys. Rev. D **41**, 717–718 (1990).

[162] C. Q. Geng, "Remarks on charge quantization of fermions and bosons," Phys. Rev. D **41**, 1292–1295 (1990).

[163] K. S. Babu and R. N. Mohapatra, "Quantization of electric charge from anomaly constraints and a majorana neutrino," Phys. Rev. D **41**, 271–277 (1990).

[164] S. Rudaz, "Electric-charge quantization in the standard model," Phys. Rev. D **41**, 2619–2621 (1990).

[165] H. Bauke, S. Ahrens, C. H. Keitel, and R. Grobe, "What is the relativistic spin operator?" (2013).

[166] L. H. Thomas, "Motion of the spinning electron," Nature **117**, 514 (1926).

[167] E. Wigner, "On unitary representations of the inhomogeneous lorentz group," Ann. Math. **40**, 149–204 (1939).

[168] L. L. Foldy and S. A. Wouthuysen, "On the dirac theory of spin 1/2 particles and its non-relativistic limit," Phys. Rev. **78**, 29–36 (1950).

[169] E. P. Wigner, *Group Theory* (Academic Press Inc., New York, 1959).

[170] V. Bargmann, "Note on wigners theorem on symmetry operations," J. Math. Phys. **5**, 862 (1964).

[171] M. Maggiore, *A Modern Introduction to Quantum Field Theory* (Oxford Press, New York, 2005).

[172] Y. Ohnuki, *Unitary Representation of the Poincaré group and Relativistic Wave Equations* (World Scientic, Singapore, 1988).

[173] E. V. Stefanovich, "Relativistic quantum dynamics: A non-traditional perspective on space, time, particles, fields, and action-at-a-distance," (2013).

[174] W. I. Fushchich and A. G. Nikitin, *Symmetries of Equations of Quantum Mechanics* (Allerton Press Inc., New York, 1994).

[175] M. H. L. Pryce, "Commuting co-ordinates in the new field theory," Proc. R. Soc. London, Ser. A **150**, 0166–0172 (1935).

[176] M. H. L. Pryce, "The mass-centre in the restricted theory of relativity and its connexion with the quantum theory of elementary particles," Proc. R. Soc. London, Ser. A **195**, 62–81 (1948).

[177] F. Gürsey, "Equivalent formulations of the su_6 group for quarks," Phys. Lett. **14**, 330–331 (1965).

[178] N. N. Bogolubov, A. A. Logunov, and I. T. Todorov, *Introduction to Axiomatic Quantum Field Theory* (W. A. Benjamin, Reading, Massachusetts, 1959).

[179] L. Ryder, "Relativistic spin operator for dirac particles," Gen. Rel. Grav. **31**, 775–780 (1999).

[180] B. Thaller, *The Dirac Equation* (Springer, Berlin Heidelberg, 2010).

Acknowledgments

First of all, I would like to express my gratitude to my supervisor, Honorarprof. Dr. Christoph H. Keitel not only for accepting me as a PhD student in his theoretical group at the Max Planck Institute for Nuclear Physics but also for his outstanding supervision.

I would like to thank my supervisor, Dr. Habil. Karen Z. Hatsagortsyan for his distinguished supervision and his great help, in particular, for providing me an opportunity to discuss and follow my own ideas. I sincerely acknowledge his deep knowledge and passion.

I sincerely thank my advisor, Dr. Michael Klaiber for his excellent vision and the enjoyable collaboration.

I thank Prof. Dr. Georg Wolschin for reading my thesis and writing the second reference report and the further members of my examination committee PD. Dr. Robert Moshammer and Prof. Dr. Kurt Roth for their interest in my research topic.

I would like to express my most sincere thanks to Prof. Dr. Rainer Grobe, PD Dr. Jörg Evers, PD Dr. Antonino Di Piazza, Dr. Heiko Bauke, Sebastian Meuren and Anton Wöllert for fruitful discussions and valuable suggestions.

I would like to express my thanks to the proofreaders Dr. Felix Mackenroth, Sebastian Meuren, Anton Wöllert, and Oleg Skoromnik for their comments and help in good English language proficiency. I would like to express my special thanks and deepest gratitude to Sebastian Meuren who is always ready to help me.

I would like to thank Carsten Pinnow and Dr. Frank Köck for providing a great deal of help in technical issues.

I also owe my thanks to Ludmila Hollmach, Gesine Heinzelmann, Elisabeth Miller, and Sibel Babacan for their great help in bureaucracy aspects.

I thank my present and former office mates Dr. Michael Klaiber, Dr. Felix Mackenroth, Dr. Sven Ahrens, Dr. Wen-Te Liao for many valuable discussions and for the nice working atmosphere.

I wish to thank to my all friends for their support, especially to Amcam Bulut, Ati, Aytacım, Burak (a.k.a. Jr.), Burak (a.k.a. Kamyoncu), Duygu, Elvoş, Engin, Fıro, Güneş (a.k.a. Alp), Gürsu, Kankam Ateş, Ozan, Poypoy, Selin, Türkanım, Yiğido, Zeyno for not letting us feel all alone in Germany. I would like to thank also to my friends Anton, Bora, Güneş, Sebastian, Valentina for many enjoyable moments together. I wish to thank to my lovely cat Pisotti for the enjoyable life that we have been sharing together for seven years.

I am forever grateful to all members of my family and in particular my mother Asiye and father Kayaalp, and my brother, Onur, who have supported me throughout my life. I am sincerely grateful to my beloved grandfather Mehmet Kartal who passed away when I was doing my Ph.D. I also owe my gratitude to my parents-in-law.

Finally and above all, this work is specially dedicated to my one and only love Özge for her endless support and patience, in good times and bad times.

It is for you to find a way, my friends,
To help good men arrive at happy ends.
You write the happy ending to the play!
There must, there must, there's got to be a way!

***Bertolt Brecht**, The Good Person of Szechwan*

In Memory of

Ahmet Atakan
Mehmet Ayvalıtaş
Abdullah Cömert
Ali İsmail Korkmaz
Ethem Sarısülük
Medeni Yıldırım